

**EFFECT OF WASTEWATER COLLOIDS ON
MEMBRANE REMOVAL OF MICROCONSTITUENT
ANTIBIOTIC RESISTANCE GENES**

By

Maria Virginia Riquelme Breazeal

Thesis submitted to the faculty of the Virginia Polytechnic Institute and State University in
partial fulfillment of the requirements for the degree of

Master of Science

In

Environmental Engineering

Amy J. Pruden-Bagchi, Chair

John T. Novak

Peter J. Vikesland

August 5, 2011

Blacksburg, Virginia

Keywords: Antibiotic resistance genes, ARGs, wastewater, colloids, microfiltration, MF,
ultrafiltration, UF, nanofiltration, NF.

EFFECT OF WASTEWATER COLLOIDS ON MEMBRANE REMOVAL OF MICROCONSTITUENT ANTIBIOTIC RESISTANCE GENES

Maria Virginia Riquelme Breazeal

ABSTRACT

Anthropogenically generated antibiotic resistance genes (ARGs) are considered emerging contaminants, as they are associated with a critical human health challenge, are persistent independent of a bacterial host, are subject to transfer between bacteria, and are present at amplified levels in human-impacted environments. Given the gravity of the problem, there is growing interest in advancing water treatment processes capable of limiting ARG dissemination. This study examined the potential for membrane treatment of microconstituent ARGs, and the effect of wastewater colloids on their removal. Native and spiked extracellular *vanA* (vancomycin resistance) and *bla*_{TEM} (β -lactam resistance) ARGs were tracked by quantitative polymerase chain reaction through a cascade of membrane filtration steps. To gain insight into potential associations occurring between ARGs and colloidal material, the wastewater colloids were characterized by scanning electron microscopy, as well as in their protein, polysaccharide, and total organic carbon content. The results suggest that extracellular DNA (eDNA) containing ARGs interacts with wastewater colloids, and can both be protected against degradation and be removed more efficiently in the presence of wastewater colloidal material. Thus, ARG removal may be achievable in sustainable water reuse scenarios using lower cost membranes than would have been selected based on molecular size alone. As membranes are likely to play a vital role in water sustainability, the results of this study enable consideration of ARG removal as part of a comprehensive strategy to manage emerging contaminants and to minimize overall public health risks.

ACKNOWLEDGEMENTS

I express my most sincere gratitude to Dr. Amy Pruden, my primary advisor, for her never-ending support, guidance, and undying patience. I also thank Dr. John Novak and Dr. Peter Vikesland, both committee members, for their invaluable time and support during the duration of this project. I have learned a lot from all of you and cannot thank you enough for taking me as your advisee.

I convey my heartfelt appreciation to Julie Petruska for sharing her presence and vast knowledge, and for kindly offering her useful support, usually on short call. I sincerely thank Brian Sinclair, Paramjeet Pati, and Jody Smiley for their help during experimental setup and sample analyses. I express my warmest gratitude to all members of the Pruden lab for their technical support, friendship, and many laughs. I hope to have many more.

My deepest appreciation and love to my family. To my husband, Cirano, and to my son, Nicolas, for their marvelous (and entertaining) presence, love, and support. Thank you for reminding me of what the most important things in life really are. To my mother, Miriam, for her caring support and for being an inspiration in my life. To my brother, Robinson, for his “moral support” and countless laughs. To the rest of my family, whom I know that even from far away are still with me in thought and spirit. I love you all.

Financial support for this project was provided by the Water Environment Research Foundation (WERF), and by the NSF CBET CAREER award #0547342.

TABLE OF CONTENTS

1. ANTIBIOTIC RESISTANCE GENES IN WASTEWATER: BACKGROUND AND LITERATURE REVIEW	1
1.1. ANTIBIOTIC RESISTANCE	3
1.1.1. <i>Antibiotic resistance mechanisms</i>	5
1.1.2. <i>Antibiotic resistance genes</i>	7
1.1.3. <i>Horizontal gene transfer</i>	9
1.1.4. <i>Occurrence and selection in water and wastewater treatment</i>	10
1.2. EXTRACELLULAR DNA OCCURRENCE	11
1.3. DNA-COLLOID INTERACTIONS	12
1.4. FILTRATION	15
1.4.1. <i>Microfiltration (MF) and ultrafiltration (UF)</i>	17
1.5. GOAL AND OBJECTIVES	18
1.6. HYPOTHESES	18
2. DNA EXTRACTION FROM DILUTE WATER SAMPLES: METHOD DEVELOPMENT	19
2.1. INTRODUCTION	19
2.1.1. <i>Intracellular and extracellular DNA extraction from dilute water samples</i>	20
2.2. MATERIALS AND METHODS	21
2.2.1. <i>WWTP effluent collection</i>	21
2.2.2. <i>Preparation of solutions and silica suspension</i>	21
2.2.3. <i>Plasmid preparation</i>	22
2.2.4. <i>E. coli growth curve and preparation of cell suspension</i>	23
2.2.5. <i>Experimental setup</i>	24
2.2.6. <i>Extracellular DNA concentration by silica binding</i>	25
2.2.7. <i>Intracellular DNA concentration by microfiltration</i>	26
2.2.8. <i>Total DNA concentration by silica binding and microfiltration</i>	26
2.2.9. <i>Total DNA concentration by freeze drying</i>	27
2.2.10. <i>DNA extraction, purification, and resuspension</i>	27

2.2.11. <i>DNA quantification</i>	27
2.3. RESULTS	28
2.3.1. <i>Plasmid extraction</i>	29
2.3.2. <i>DNA degradation</i>	30
2.3.3. <i>Intracellular and extracellular DNA extraction</i>	32
2.3.4. <i>Comparison of total DNA concentration methods</i>	34
2.3.5. <i>Comparison of DNA isolation methods: Extraction, purification, and resuspension</i>	36
2.4. DISCUSSION	37
2.4.1. <i>DNA degradation</i>	38
2.4.2. <i>Extracellular DNA</i>	38
2.4.3. <i>Intracellular DNA</i>	40
2.4.4. <i>Comparison of total DNA concentration methods</i>	41
2.4.5. <i>Comparison of DNA isolation methods: Extraction, purification, and resuspension</i>	42
2.5. CONCLUSIONS	44
3. MATERIALS AND METHODS	45
3.1. PLASMID PREPARATION	45
3.2. WWTP EFFLUENT COLLECTION AND INITIAL FILTRATION	46
3.3. EXPERIMENTAL SETUP	46
3.4. MICROFILTRATION AND ULTRAFILTRATION	47
3.5. DNA CONCENTRATION, EXTRACTION, AND QUANTIFICATION	48
3.6. COLLOID CHARACTERIZATION	49
3.6.1. <i>Non-purgeable organic carbon, proteins, and polysaccharides</i>	49
3.6.2. <i>Scanning electron microscopy</i>	50
3.7. STATISTICAL ANALYSES	50
4. EFFECT OF WASTEWATER COLLOIDS ON MEMBRANE REMOVAL OF MICROCONSTITUENT ARGs: RESULTS	51
4.1. DNA DEGRADATION	51
4.1.1. <i>WWTP A (1st trial)</i>	51
4.1.2. <i>WWTP A (2nd trial)</i>	53
4.1.3. <i>WWTP B</i>	55
4.1.4. <i>WWTP C</i>	57

4.2. POST-FILTRATION DNA QUANTIFICATION	59
4.2.1. <i>WWTP A (1st trial)</i>	61
4.2.2. <i>WWTP A (2nd trial)</i>	63
4.2.3. <i>WWTP B</i>	65
4.2.4. <i>WWTP C</i>	67
4.3. COLLOID CHARACTERIZATION	69
4.3.1. <i>Total Organic Carbon (TOC)</i>	69
4.3.2. <i>Proteins and polysaccharides</i>	71
4.3.4. <i>Scanning Electron Microscopy (SEM)</i>	75
4.4. COMPARISON BETWEEN PVDF AND ALUMINA MEMBRANES	84
5. EFFECT OF WASTEWATER COLLOIDS ON MEMBRANE REMOVAL OF MICROCONSTITUENT ARGs:	87
DISCUSSION AND CONCLUSIONS	87
5.1. DNA DEGRADATION	88
5.2. POST-FILTRATION DNA QUANTIFICATION	89
5.3. COLLOID CHARACTERIZATION AND CORRELATION ANALYSES	91
5.4. COMPARISON BETWEEN PVDF AND ALUMINA MEMBRANES	92
5.5. SUMMARY AND CONCLUSIONS.....	93
5.6. UNANSWERED QUESTIONS.....	94
REFERENCES.....	95
APPENDIX A	100

LIST OF FIGURES

Figure 1.1. Genetic reactors in antibiotic resistance. Human or animal-associated microorganisms (black circles) combine with environmental bacteria (white circles) generating a potential node for gene exchange and the reintroduction (back arrows) of existing and novel resistance mechanisms into human and animal microbiota (7).	2
Figure 1.2. Rise of antibiotic resistance among bacterial strains. MRSA: Methicillin-resistant <i>Staphylococcus aureus</i> , VRE: Vancomycin-resistant <i>Enterococcus</i> , FQRP: Fluoroquinolone-resistant <i>Pseudomonas aeruginosa</i> (57).	4
Figure 1.3. New antibacterial agents approved by the FDA in the U.S. from 1983 to present (57). Used under fair use, 2011.	5
Figure 1.4. Mechanisms of antibiotic resistance (46). Image obtained from the Science Creative Quarterly website (http://www.scq.ubc.ca) on June, 2011. Used under fair use, 2011.	6
Figure 1.5. Relationship between type of filtration system and contaminant removal (34, 65)...	16
Figure 2.1. Map of pCR [®] 4-TOPO [®] plasmid map indicating <i>vanA</i> gene insertion site (Invitrogen, Carlsbad, CA). Used under fair use, 2011.	23
Figure 2.2. Diagram of experimental setup described in Section 2.2.5.	25
Figure 2.3. qPCR quantified <i>bla</i> _{TEM} , <i>vanA</i> , and 16S rRNA gene concentrations in plasmid extraction products. Mini: Plasmids extracted using the Qiagen Plasmid Mini kit (Qiagen, Valencia, CA). Mega: Plasmids extracted using the Qiagen Plasmid Mega Kit (Qiagen, Valencia, CA). Numerical values provided in Appendix A, Table A 1.	30
Figure 2.4. Degradation test of plasmid and genomic DNA suspended in PBS, monitored by qPCR. Test points represent average of triplicate qPCR measurements. Numerical values are given in Appendix A, Table A 2.	31
Figure 2.5. Degradation test of DNA in a PBS solution containing <i>E. coli</i> cells, monitored by qPCR. Test points represent average of triplicate qPCR measurements. Numerical values are given in Appendix A, Table A 2.	31

Figure 2.6. Degradation of DNA in a filtered WWTP effluent sample, monitored by qPCR. Test points represent average of triplicate qPCR measurements. Numerical values are given in Appendix A, Table A 2..... 32

Figure 2.7. qPCR quantification of eDNA isolated by silica sorption. eDNA was spiked into corresponding treatments in the form of a plasmid carrying the *bla*_{TEM} and *vanA* ARGs. Circles, squares, and diamonds indicate theoretical 100% yield of *bla*_{TEM}, *vanA*, and 16S rRNA gene concentrations in spiked samples, respectively. Numerical values provided in Appendix A, Table A 3..... 33

Figure 2.8. qPCR quantification of DNA isolated by filtration and washing of membrane to remove eDNA. eDNA was spiked into corresponding treatments in the form of a plasmid carrying the *bla*_{TEM} and *vanA* ARGs. Circles indicate theoretical 100% yield of *bla*_{TEM} and *vanA* genes. Diamond indicates theoretical 100% yield of intracellular 16S rRNA genes from spiked *E. coli* cells. Numerical values are provided in Appendix A, Table A 3. 34

Figure 2.9. qPCR quantification of the *bla*_{TEM} gene extracted from a variety of aqueous samples after concentration by silica sorption+filtration versus freeze drying. Circles indicate theoretical 100% *bla*_{TEM} gene concentration in spiked samples. Numerical values are given in Appendix A, Table A 3..... 35

Figure 2.10. qPCR quantification of the *vanA* gene extracted from a variety of aqueous samples after concentration by silica sorption+filtration versus freeze drying. Circles indicate theoretical 100% *vanA* gene concentration. Numerical values are given in Appendix A, Table A 3..... 35

Figure 2.11. qPCR quantification of the 16S rRNA gene extracted from a variety of aqueous samples after concentration by silica sorption+filtration versus freeze drying. Circles indicate theoretical 16S rRNA gene concentration in spiked samples. Numerical values are given in Appendix A, Table A 3..... 36

Figure 2.12. Relative concentrations obtained after DNA extraction, purification, and resuspension of freeze-dried DNA from WWTP effluent or buffer. Horizontal line indicates spiked *bla*_{TEM} gene concentration. Numerical values provided in Appendix A, Table A 4..... 37

Figure 3.1. Diagram of experimental setup and method sequence..... 47

Figure 4.1. DNA degradation test results obtained for WWTP A (1st trial) *bla*_{TEM} genes. *bla*_{TEM} genes in samples collected for each time step during 4 hours were quantified in qPCR triplicate reactions. 52

Figure 4.2. DNA degradation test results obtained for WWTP A (1st trial) *vanA* genes. *vanA* genes in samples collected for each time step during 4 hours were quantified in qPCR triplicate reactions. 52

Figure 4.3. DNA degradation test results obtained for WWTP A (1st trial) 16S rRNA genes. 16S rRNA genes in samples collected for each time step during 4 hours were quantified in qPCR triplicate reactions. 53

Figure 4.4. DNA degradation test results obtained for WWTP A (2nd trial) *bla*_{TEM} genes. *bla*_{TEM} genes in samples collected for each time step during 4 hours were quantified in qPCR triplicate reactions. 54

Figure 4.5. DNA degradation test results obtained for WWTP A (2nd trial) *vanA* genes. *vanA* genes in samples collected for each time step during 4 hours were quantified in qPCR triplicate reactions. 54

Figure 4.6. DNA degradation test results obtained for WWTP A (2nd trial) 16S rRNA genes. 16S rRNA genes in samples collected for each time step during 4 hours were quantified in qPCR triplicate reactions. 55

Figure 4.7. DNA degradation test results obtained for WWTP B *bla*_{TEM} genes. *bla*_{TEM} genes in samples collected for each time step during 5 hours were quantified in qPCR triplicate reactions. 56

Figure 4.8. DNA degradation test results obtained for WWTP B *vanA* genes. *vanA* genes in samples collected for each time step during 5 hours were quantified in qPCR triplicate reactions. 56

Figure 4.9. DNA degradation test results obtained for WWTP B 16S rRNA genes. 16S rRNA genes in samples collected for each time step during 5 hours were quantified in qPCR triplicate reactions. 57

Figure 4.10. DNA degradation test results obtained for WWTP C *bla*_{TEM} genes. *bla*_{TEM} genes in samples collected for each time step during 4.5 hours were quantified in qPCR triplicate reactions. 58

Figure 4.11. DNA degradation test results obtained for WWTP C *vanA* genes. *vanA* genes in samples collected for each time step during 4.5 hours were quantified in qPCR triplicate reactions. 58

Figure 4.12. DNA degradation test results obtained for WWTP C 16S rRNA genes. 16S rRNA genes in samples collected for each time step during 4.5 hours were quantified in qPCR triplicate reactions. 59

Figure 4.13. Gene concentrations in unspiked WWTP A (1st trial) filtrates. Samples were qPCR quantified in triplicate reactions. Error bars represent analytical error and are larger than measurement where absent. 60

Figure 4.14. Gene concentrations in unspiked WWTP B filtrates. Samples were qPCR quantified in triplicate reactions. Error bars represent analytical error and are larger than measurement where absent. 60

Figure 4.15. *bla*_{TEM} gene fraction in spiked buffer and WWTP A (1st trial) filtrates. Numerical values provided in Appendix A, Table A 9. 61

Figure 4.16. *vanA* gene fraction in spiked buffer and WWTP A (1st trial) filtrates. Numerical values provided in Appendix A, Table A 9. 62

Figure 4.17. 16S rRNA gene fraction in spiked buffer and WWTP A (1st trial) filtrates. Numerical values provided in Appendix A, Table A 9. 62

Figure 4.18. *bla*_{TEM} gene fraction in spiked buffer and WWTP A (2nd trial) filtrates. Numerical values provided in Appendix A, Table A 9. 63

Figure 4.19. *vanA* gene fraction in spiked buffer and WWTP A (2nd trial) filtrates. Numerical values provided in Appendix A, Table A 9. 64

Figure 4.20. 16S rRNA gene fraction in spiked buffer and WWTP A (2 nd trial) filtrates. Numerical values provided in Appendix A, Table A 9.	64
Figure 4.21. <i>bla</i> _{TEM} gene fraction in spiked buffer and WWTP B filtrates. Numerical values provided in Appendix A, Table A 9.....	65
Figure 4.22. <i>vanA</i> gene fraction in spiked buffer and WWTP B filtrates. Numerical values provided in Appendix A, Table A 9.....	66
Figure 4.23. 16S rRNA gene fraction in spiked buffer and WWTP B filtrates. Numerical values provided in Appendix A, Table A 9.....	66
Figure 4.24. <i>bla</i> _{TEM} gene fraction in spiked buffer and WWTP C filtrates. Numerical values provided in Appendix A, Table A 9.....	67
Figure 4.25. <i>vanA</i> gene fraction in spiked buffer and WWTP C filtrates. Numerical values provided in Appendix A, Table A 9.....	68
Figure 4.26. 16S rRNA gene fraction in spiked buffer and WWTP C filtrates. Numerical values provided in Appendix A, Table A 9.....	68
Figure 4.27. TOC concentrations in serially filtered unspiked WWTP A (1 st trial) samples.	69
Figure 4.28. Correlation between membrane removal of <i>bla</i> _{TEM} genes and TOC. One-sided Pearson correlation coefficient, <i>r</i> , is 0.62 (<i>p</i> < 0.01).	70
Figure 4.29. Correlation between membrane removal of <i>vanA</i> genes and TOC. One-sided Pearson correlation coefficient, <i>r</i> , is 0.62 (<i>p</i> < 0.01).	70
Figure 4.30. Protein concentrations in serially filtered unspiked WWTP A (1 st trial) samples. ..	71
Figure 4.31. Correlation between membrane removal of <i>bla</i> _{TEM} genes and proteins. One-sided Pearson correlation coefficient, <i>r</i> , is 0.80 (<i>p</i> < 0.01).	72
Figure 4.32. Correlation between membrane removal of <i>vanA</i> genes and proteins. One-sided Pearson correlation coefficient, <i>r</i> , is 0.83 (<i>p</i> < 0.01).	72

Figure 4.33. Polysaccharide concentrations in serially filtered unspiked WWTP A (1 st trial) samples.....	73
Figure 4.34. Correlation between membrane removal of <i>bla</i> _{TEM} genes and polysaccharides. One-sided Pearson correlation coefficient, <i>r</i> , is 0.60 (<i>p</i> < 0.01).....	73
Figure 4.35. Correlation between membrane removal of <i>vanA</i> genes and polysaccharides. One-sided Pearson correlation coefficient, <i>r</i> , is 0.62 (<i>p</i> < 0.01).....	74
Figure 4.36. Correlation between membrane removal of <i>bla</i> _{TEM} genes and the added protein and polysaccharide concentrations. One-sided Pearson correlation coefficient, <i>r</i> , is 0.82 (<i>p</i> < 0.01). 74	74
Figure 4.37. Correlation between membrane removal of <i>vanA</i> genes and the added protein and polysaccharide concentrations. One-sided Pearson correlation coefficient, <i>r</i> , is 0.83 (<i>p</i> < 0.01). 75	75
Figure 4.38. SEM image of freeze-dried WWTP A effluent filtered through a 100 kDa-pore size membrane. Reference bar = 1 μm. Magnification = 20,000 X.....	76
Figure 4.39. SEM image of freeze-dried WWTP A effluent filtered through a 100 kDa-pore size membrane. Reference bar = 200 nm. Magnification = 80,000 X.....	76
Figure 4.40. SEM image of freeze-dried WWTP A effluent filtered through a 100 kDa-pore size membrane. Reference bar = 2 μm. Magnification = 25,000 X.....	77
Figure 4.41. SEM image of freeze-dried WWTP A effluent filtered through a 1 kDa-pore size membrane. Reference bar = 2 μm. Magnification = 8,000 X.....	77
Figure 4.42. SEM image of freeze-dried WWTP C effluent filtered through a 1.2 μm-pore size membrane. Reference bar = 200 μm. Magnification = 100 X.....	78
Figure 4.43. SEM image of freeze-dried WWTP C effluent filtered through a 1.2 μm-pore size membrane. Reference bar = 10 μm. Magnification = 1,500 X.....	78
Figure 4.44. SEM image of freeze-dried WWTP C effluent filtered through a 0.1 μm-pore size membrane. Reference bar = 10 μm. Magnification = 2,000 X.....	79

Figure 4.45. SEM image of freeze-dried WWTP C effluent filtered through a 0.1 μm -pore size membrane. Reference bar = 2 μm . Magnification = 6,000 X.	79
Figure 4.46. SEM image of freeze-dried WWTP C effluent filtered through a 0.1 μm -pore size membrane. Reference bar = 2 μm . Magnification = 10,000 X.	80
Figure 4.47. SEM image of freeze-dried WWTP C effluent filtered through a 0.1 μm -pore size membrane. Reference bar = 1 μm . Magnification = 20,000 X.	80
Figure 4.48. SEM image of freeze-dried WWTP C effluent filtered through a 0.1 μm -pore size membrane. Reference bar = 1 μm . Magnification = 5,000 X.	81
Figure 4.49. SEM image of freeze-dried WWTP C effluent filtered through a 0.1 μm -pore size membrane. Reference bar = 1 μm . Magnification = 17,000 X.	81
Figure 4.50. SEM image of freeze-dried WWTP C effluent filtered through a 100 kDa-pore size membrane. Reference bar = 2 μm . Magnification = 3,000 X.	82
Figure 4.51. SEM image of freeze-dried WWTP C effluent filtered through a 100 kDa-pore size membrane. Reference bar = 2 μm . Magnification = 9,000 X.	82
Figure 4.52. SEM image of freeze-dried WWTP C effluent filtered through a 100 kDa-pore size membrane. Reference bar = 200 nm. Magnification = 30,000 X.	83
Figure 4.53. SEM image of freeze-dried WWTP C effluent filtered through a 1 kDa-pore size membrane. Reference bar = 10 μm . Magnification = 500 X.	83
Figure 4.54. SEM image of freeze-dried WWTP C effluent filtered through a 1 kDa-pore size membrane. Reference bar = 200 nm. Magnification = 30,000 X.	84
Figure 4.55. Comparison between 0.1 μm pore size PVDF and alumina membranes for the removal of <i>bla</i> _{TEM} genes. Numerical values provided in Appendix A, Table A 15.	85
Figure 4.56. Comparison between 0.1 μm pore size PVDF and alumina membranes for the removal of <i>vanA</i> genes. Numerical values provided in Appendix A, Table A 15.	85

Figure 4.57. Comparison between 0.1 μm pore size PVDF and alumina membranes for the removal of 16S rRNA genes. Numerical values provided in Appendix A, Table A 15..... 86

Figure 4.58. Filtrate fraction of spiked buffer after 0.1 μm PVDF or Alumina membrane filtration. Measurements obtained from spiked control buffer during the four filtration experiments were compiled and averaged. Numerical values are provided in Table A 16..... 86

Figure 5.1. Graphical representation of DNA-colloid interactions in wastewater. Blue circles represent colloidal material in the wastewater. Red lines represent eDNA in a stable sorbed state. WWTP clarifier image obtained from the St. Peters, MO website on August 2011 and used under fair use, 2011 (<http://www.stpetersmo.net/wastewater.aspx>) (16). 94

Figure A 1. *E. coli* growth curve..... 100

LIST OF TABLES

Table 1.1. Common antibiotics, their mode of action, and major mechanisms of resistance (25).	7
Table 1.2. Genetic elements involved ARG dissemination (55).	8
Table 1.3. Summary of materials observed to interact with and/or protect DNA against enzymatic degradation, and transformation ability of sorbed DNA.	13
Table 1.4. General characteristics of membranes (65).	17
Table 2.1. DNA isolation methods tested in this study.	21
Table 2.2. Limit of quantification for the <i>bla</i> _{TEM} , <i>vanA</i> , and 16S rRNA genes.	29
Table 2.3. Relative DNA yield obtained from each DNA isolation method.	42
Table 3.1. General characteristics and sampling dates associated with each WWTP.	45
Table 3.2. General characteristics of membranes used in this study.	48
Table 4.1. Pearson correlation coefficients and their corresponding p-values associated with the correlation between colloidal component- and gene-membrane removal.	75
Table A 1. Gene concentrations reported in Figure 2.3.	100
Table A 2. Degradation values reported in Figure 2.4 - Figure 2.6.	101
Table A 3. Numerical values used to create Figure 2.7 - Figure 2.11.	101
Table A 4. qPCR quantification results shown in Figure 2.12.	102
Table A 5. qPCR quantification results shown in Figure 4.1 - Figure 4.3.	102
Table A 6. qPCR quantification results shown in Figure 4.4 - Figure 4.6.	103
Table A 7. qPCR quantification results shown in Figure 4.7 - Figure 4.9.	103
Table A 8. qPCR quantification results shown in Figure 4.10 - Figure 4.12.	104
Table A 9. qPCR results and calculated values shown in Figure 4.15 - Figure 4.26.	105

Table A 10. qPCR quantified post-filtration gene concentrations in spiked and unspiked WWTPA (1 st trial) and buffer samples.	107
Table A 11. qPCR quantified post-filtration gene concentrations in spiked and unspiked WWTPA (2 nd trial) and buffer samples.	107
Table A 12. qPCR quantified post-filtration gene concentrations in spiked and unspiked WWTP B and buffer samples.	108
Table A 13. qPCR quantified post-filtration gene concentrations in spiked and unspiked WWTP C and buffer samples.	108
Table A 14. Total non-purgeable organic carbon, protein, and polysaccharide values graphed in Sections 4.3.1 – 4.3.3.	109
Table A 15. Gene and colloidal component fractions used to compare PVDF and alumina membranes in Figure 4.55 - Figure 4.57 (Section 4.4).	109
Table A 16. Spiked buffer filtrate fractions associated with the 0.1 μm pore size PVDF and Alumina membranes compared in Figure 4.58.	110

LIST OF ABBREVIATIONS

- ARB:** Antibiotic resistant bacteria
- ARGs:** Antibiotic resistance genes
- BSA:** Bovine serum albumin
- eDNA:** Extracellular DNA
- EDTA:** Ethylenediaminetetraacetic acid
- EPS:** Extracellular polymeric substances
- HGT:** Horizontal gene transfer
- iDNA:** Intracellular DNA
- MDR:** Multidrug resistance
- MF:** Microfiltration
- MRSA:** Methicillin-resistant *Staphylococcus aureus*
- MWCO:** Molecular weight cutoff
- NOM:** Natural organic matter
- RO:** Reverse osmosis
- rRNA:** Ribosomal RNA
- tDNA:** Total DNA
- UF:** Ultrafiltration
- VRSA:** Vancomycin-resistant *Staphylococcus aureus*
- WWTP:** Wastewater treatment plant

1. ANTIBIOTIC RESISTANCE GENES IN WASTEWATER: BACKGROUND AND LITERATURE REVIEW

Antibiotic resistance and, particularly, multidrug resistance (MDR), are an increasingly critical problem affecting human health. Nosocomial (i.e., hospital-acquired) infections caused by antibiotic resistant bacteria (ARB) are not only a leading cause of rising mortality and morbidity among human patients, but are also the cause of increased treatment costs (43). The increased use of antibiotics in human and veterinary medicine, as well as in agriculture, has played a significant role in the emergence, dissemination, and selection of ARB. In medicine, antibiotics are mainly used for prophylactic and therapeutic purposes; and in agriculture, antibiotics are used as therapeutic, prophylactic, metaphylactic (short-term disease control), and growth enhancing agents (35, 63). ARB from each of these sources can interact with environmental bacteria as shown in Figure 1.1 (7), contributing to the dissemination and emergence of antibiotic resistance in human-impacted environments. Thus, anthropogenically generated antibiotic resistance could be said to disseminate into the environment via two main pathways: wastewater effluent and agricultural runoff (7, 58). This study focuses on the first source.

Antibiotic resistance is encoded in segments of DNA called antibiotic resistance genes (ARGs), several of which can be carried on bacterial plasmids or other transmissible elements as clusters, rather than as single genes. ARGs can be transferred inter- or intra-species through horizontal gene transfer (HGT) processes such as conjugation, transformation and transduction, and subsequently persist by remaining a part of the bacterial chromosome or as a mobile genetic element. Through increased fitness, then, ARB may be preferentially selected as they live and reproduce in the antibiotic-laden niches that were previously colonized by their sensitive counterparts. For this reason, overuse, misuse, and disposal of antibiotics are of particular concern for contributing to the antibiotic resistance problem, since these practices all have the potential to expose bacteria unnecessarily to antibiotic residues, thus enhancing the selection of ARB.

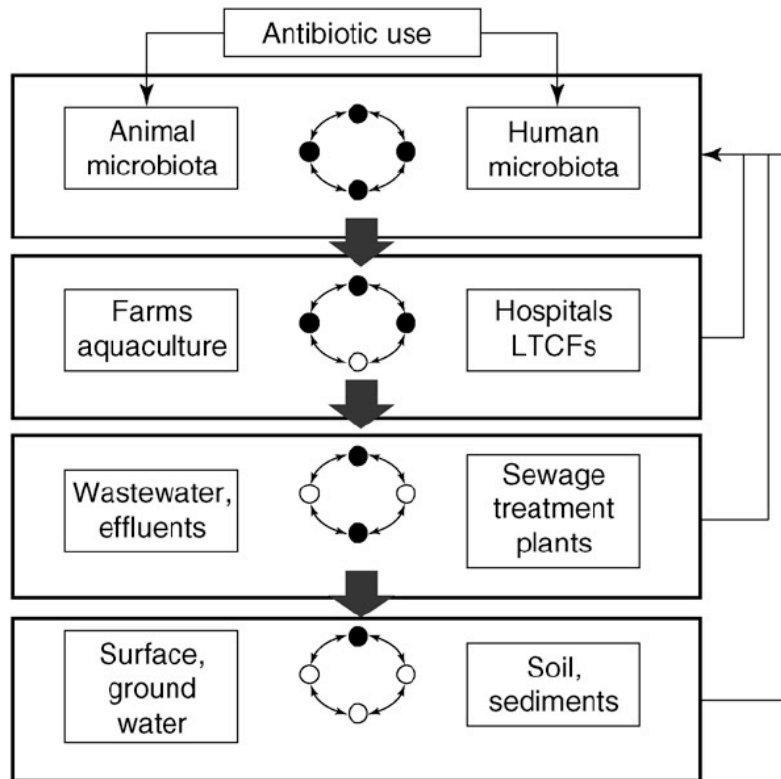


Figure 1.1. Genetic reactors in antibiotic resistance. Human or animal-associated microorganisms (black circles) combine with environmental bacteria (white circles) generating a potential node for gene exchange and the reintroduction (back arrows) of existing and novel resistance mechanisms into human and animal microbiota (7).

Because of the ability of ARGs to transcend their bacterial host, ARGs themselves, rather than ARB, are considered to be the primary contaminants of concern in this research (49). Due to our centralized water infrastructure, the presence of low levels of antibiotics, ARB and ARGs in wastewater is inevitable, and represents a potentially important node both for spreading antibiotic resistance and for alleviating the problem. Ideally, wastewater treatment plants (WWTP) could serve as a means of removing or destroying anthropogenically derived ARGs prior to water discharge, reuse or other applications; however, WWTP disinfection systems are currently designed to kill or inactivate ARB rather than eliminate ARGs, and thus the treatment potential for ARGs is largely unknown. A more detailed description concerning antibiotic resistance mechanisms, genes, spread, and occurrence is provided later in this chapter.

Given the mechanisms of persistence and dissemination of ARGs within drinking water sources, it would be ideal to minimize the concentrations of these emerging contaminants prior to release of treated wastewater. However, little is known about the potential for wastewater treatment to destroy or remove DNA. In particular, membrane filtration processes are commonly used for the removal of a wide variety of contaminants, but most would not be expected to have much effect on DNA based purely on its molecular weight. For this reason, we explored the potential for DNA to interact with wastewater colloidal particles in order to increase ARG removal efficiency through membrane/filtration processes.

DNA is well known to interact with clay minerals and various soil colloidal particles (14, 15, 18, 39, 40, 50). Considering that significant amounts of suspended colloidal particles are present in wastewaters, these interactions represent a promising and unexploited approach for the removal of ARGs from contaminated wastewater. However, most of the available studies concerning DNA-colloid interactions have been carried out in simplified artificial systems; thus, there is a need for studies that emphasize the behavior and fate of DNA *in situ*. In addition, the relationship between the removal of ARG-colloid complexes and membrane pore size has not been investigated in natural systems. A review of relevant studies discussing DNA-colloid interactions is provided in Section 1.3. A discussion regarding membrane filtration is provided in Section 1.4.

1.1. ANTIBIOTIC RESISTANCE

Over the course of the past 60 years, antibiotic resistance has been escalating in relation to the increased development, production, and use of antibiotics (1, 2). As some antibiotics become ineffective due to the rise of resistant pathogens, new and improved antibiotics are developed to take their place. However, resistance to the new drugs soon arises by evolutionary adaptation and natural selection; and these new antibiotics, too, are bound to become ineffective. Figure 1.2 shows the rise of antibiotic resistance among three common bacterial pathogens. In the end, multidrug resistant microorganisms or “superbugs” characterized by resistance to multiple antibiotic agents dominate the previously antibiotic sensitive niches, and the methods by which MDR infections can be treated become limited. This limitation is shown in Figure 1.3, where the number of antibiotics approved by the FDA between 1983 and the present is shown.

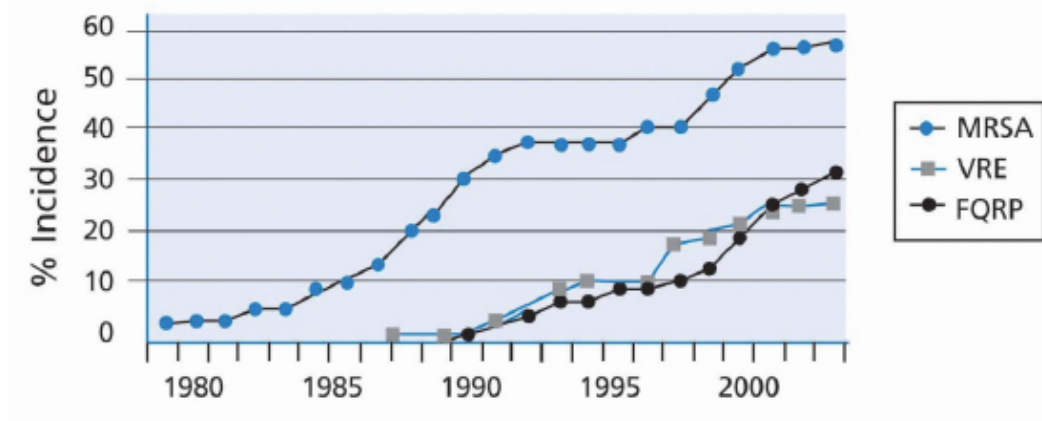


Figure 1.2. Rise of antibiotic resistance among bacterial strains. MRSA: Methicillin-resistant *Staphylococcus aureus*, VRE: Vancomycin-resistant *Enterococcus*, FQRP: Fluoroquinolone-resistant *Pseudomonas aeruginosa* (57).

Antibiotic resistance can be acquired through a mutation, genetic recombination or HGT. Mutations are permanent or heritable changes in DNA sequences; and, by definition, become amplified and carried on as bacteria replicate. Genetic recombination is the process through which two pieces of DNA can break and rejoin causing a DNA crossover event. ARGs are often carried in transposons, which also encode the transposase enzyme required for their transposition (a type of non-homologous recombination) from one place in the genome (i.e., a plasmid) to another (i.e., the chromosome). In this way, ARGs obtained via a HGT event through a plasmid, for example, have the potential to become a part of the bacterial chromosome and vice versa. The process of HGT will be explained in detail in Section 1.1.3.

Examples of medically relevant antibiotic resistant pathogens include nosocomial related bacteria such as methicillin resistant *Staphylococcus aureus* (MRSA), vancomycin resistant *Staphylococcus aureus* (VRSA), multidrug resistant *Enterococcus faecalis* and *E. faecium*; opportunistic bacteria such as multidrug resistant *Pseudomonas aeruginosa*; and food borne bacteria such as multidrug resistant *Salmonella* and *E. coli*, among many others. These bacteria pose a threat to human health, as it has been shown that the length of illness and patient mortality significantly increases when the pathogen is antibiotic resistant. For example, in a five-year study reported in 2008, Sostarich et al. (56) showed that patients with bloodstream infections of

Gram-negative multiresistant bacteria had significantly higher mortality rates than the control group, which was comprised of patients that had been infected with antibiotic-sensitive Gram-negative bacteria.

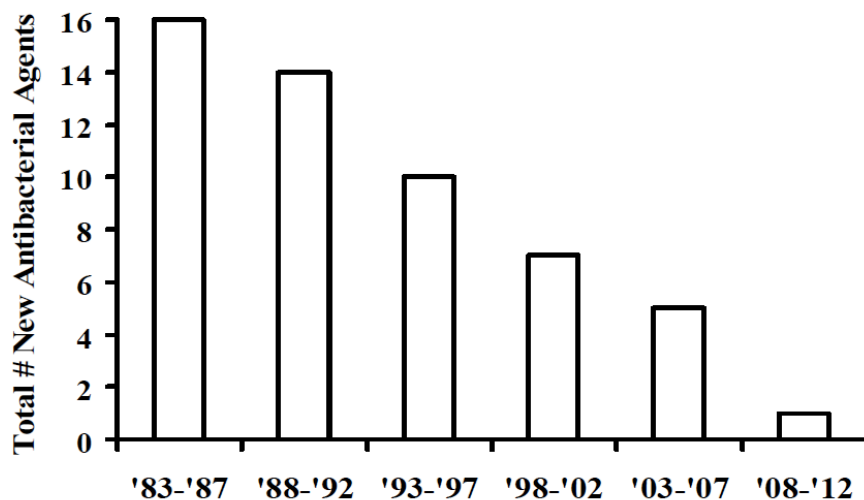


Figure 1.3. New antibacterial agents approved by the FDA in the U.S. from 1983 to present (57). Used under fair use, 2011.

Overall, multidrug resistant pathogens are a growing concern in the medical setting, as antibiotic resistance is the cause of an increased mortality rate among human patients and of greater medical and research costs. Because it is unrealistic and highly unlikely that anthropogenic ARGs and ARB will become completely eradicated, study efforts that focus on limiting the dissemination of these contaminants are needed and represent the heart of this project.

1.1.1. ANTIBIOTIC RESISTANCE MECHANISMS

Bacteria can quickly develop mechanisms of resistance to antibiotics, whereby they become unaffected by exposure to these agents. Antibiotics can either be bacteriostatic by inhibiting bacterial cell growth, or bactericidal by killing the microorganism. In a recent study, Huang et al. (24) reported the 18 most commonly used antibiotics for human therapy to be six β -

lactams (amoxicillin, cephalixin, penicillin, cefprozil, cefuroxime, and loracarbef), three macrolides (azithromycin, clarithromycin, and erythromycin), two fluoroquinolones (ciprofloxacin and levofloxacin), two aminoglycosides (neomycin and tobramycin), one sulfonamide (sulfamethoxazole), one tetracycline (tetracycline), and three others. Bacterial resistance mechanisms to all of these antibiotics have been observed.

Mechanisms of antibiotic resistance include the synthesis of enzymes that break down the antimicrobial drug, chemical modification of the drug, uptake inhibition, efflux pumps, target overproduction, metabolic bypass, and, most commonly, modification of the drug target site (22, 25). These mechanisms are highlighted in Figure 1.4. After acquisition of antibiotic resistance through a mutation or HGT, selective pressure is all that is needed for ARB to amplify and disseminate ARGs.

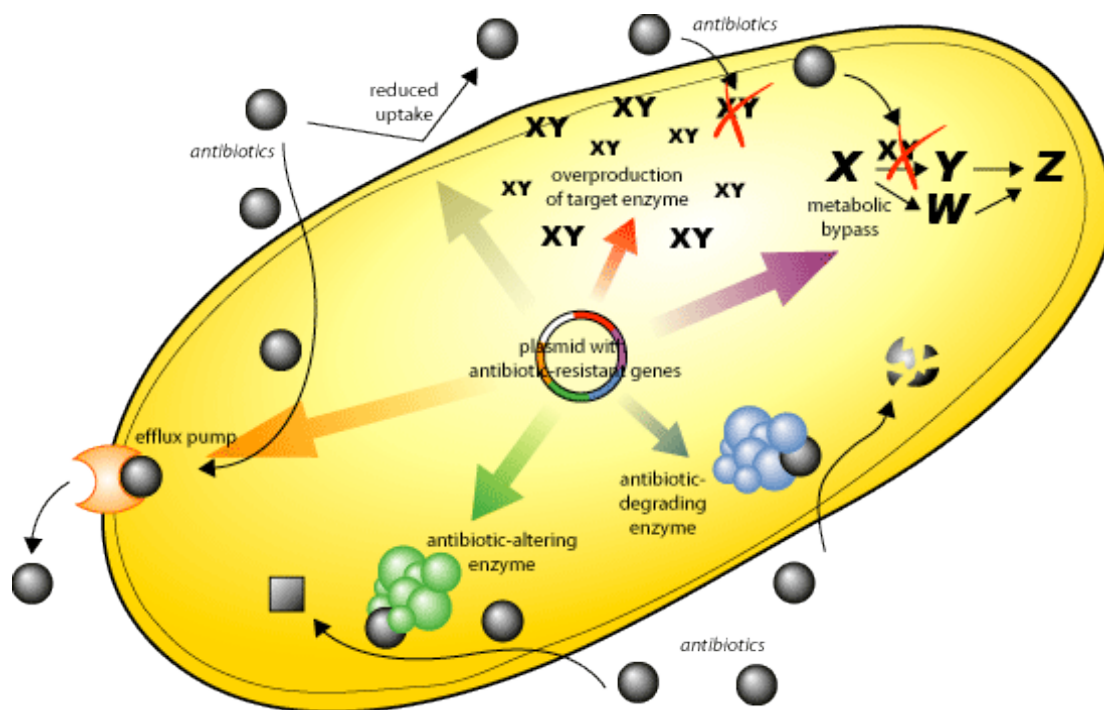


Figure 1.4. Mechanisms of antibiotic resistance (46). Image obtained from the Science Creative Quarterly website (<http://www.scq.ubc.ca>) on June, 2011. Used under fair use, 2011.

In his review of the basic mechanisms of antibiotic resistance, Jayaraman et al. (25) presented examples of mechanisms through which bacteria can become resistant to antibiotics,

and discussed possible reasons leading to the evolution of antibiotic resistance. Common examples of the antibacterial mechanisms discussed are described in Table 1.1, and include influx-efflux systems (common in tetracycline resistance), chemical alteration of antibiotics (such is the action of β -lactamases), alteration of antibiotic target (such as the target for Vancomycin); although other non-heritable mechanisms have been observed, such as the formation of slow- or non-growing persistent cells, the formation of biofilms whose inner cells are protected against toxic substances, and the formation of revertant swarming cells that are able to repopulate their environment after antibiotic treatment is finished (25). Interestingly, there is growing evidence that at low levels, antibiotics could have an activity other than acting as antibacterial compounds; and that their bactericidal activity may not be their original ecological function (25).

Table 1.1. Common antibiotics, their mode of action, and major mechanisms of resistance (25).

Category	Some members	Mode of action	Major mechanisms of resistance
β -Lactams	Penicillins, Cephalosporins, Cefotaximes, Carbapenems	Inhibition of cell-wall synthesis	Cleavage by β -lactamases, ESBLs, CTX-mases, Carbapenemases, altered PBPs
Aminoglycosides	Streptomycin, Gentamycin, Tobramycin, Amikacin	Inhibition of protein synthesis	Enzymatic modification, efflux, ribosomal mutations, 16S rRNA methylation
Quinolones	Ciprofloxacin, Ofloxacin, Norfloxacin	Inhibition of DNA replication	Efflux, modification, target mutations
Glycopeptides	Vancomycin	Inhibition of cell-wall synthesis	Altered cell walls, efflux
Tetracyclines	Tetracycline	Inhibition of translation	Mainly efflux
Rifamycins	Rifampin (Rifampicin)	Inhibition of transcription	Altered β -subunit of RNA polymerase
Streptogramins	Virginiamycins, Quinupristin, Dalfopristin	Inhibition of cell-wall synthesis	Enzymatic cleavage, modification, efflux
Oxazolidinones	Linezolid	Inhibition of formation of 70S ribosomal complex	Mutations in 23S rRNA genes followed by gene conversion
Macrolides	Erythromycin, Clarithromycin, Roxithromycin	Inhibition of protein synthesis	23S rRNA post-transcriptional methylation

1.1.2. ANTIBIOTIC RESISTANCE GENES

ARGs are DNA segments that encode proteins necessary to impart resistance to a particular antibiotic or antibiotic class through the mechanisms previously mentioned (see

Section 1.1.1). Most ARGs can be found in self-transmissible or mobilizable genetic elements such as integrons, transposons, and plasmids. Many ARGs are found in gene cassettes that form part of the chromosome or a plasmid, or that have become part of integrons over time. Integrons are genetic elements that recruit gene cassettes from elsewhere in the genome and integrate them into their own genetic material. In this regard, genetic linkage of ARGs for different classes of antibiotics is a growing cause of resistance to multiple antibiotics; accordingly, when one antibiotic is administered, resistant bacteria to multiple antibiotics are potentially selected (59).

Transposons are DNA elements that can “transpose” or jump from one place to another in the bacterial genome, and which reside either in the bacterial chromosome or in extrachromosomal genetic elements such as plasmids. Plasmids are not only self-replicating genetic elements, but some of them also encode their own transfer into plasmid-free bacteria through the HGT process of conjugation. Horizontal transfer, described in the following section, can be induced by selective pressure such as exposure to antibiotics (59). Table 1.2, adapted from Snyder and Champness (55), describes the roles and characteristics of the genetic elements that are involved in the transfer of ARGs.

Table 1.2. Genetic elements involved ARG dissemination (55).

Genetic element	Characteristics	Role in spread of resistance genes
Self-transmissible plasmid	Circular, autonomously replicating element; carries genes needed for conjugal DNA transfer	Transfers resistance genes; mobilizes other elements that carry resistance genes
Conjugative transposon	Integrated element that can excise to form a nonreplicating circular transfer intermediate; carries genes needed for conjugal DNA transfer	Same as self-transmissible plasmid; highly promiscuous, transferring between Gram-positive and Gram-negative genera and species
Mobilizable plasmid	Circular, autonomously replicating element; carries site and genes that allow it to use the conjugal apparatus provided by a self-transmissible plasmid	Transfer of resistance genes
Transposon	Moves from one DNA segment to another within the same cell	Carries resistance genes from chromosome to plasmid or vice versa
Gene cassette	Circular, nonreplicating DNA segment containing only open reading frames; integrates into integrons	Carries resistance genes
Integron	Integrated DNA segment that contains an integrase, a promoter, and an integration site for gene cassettes	Forms clusters of resistance genes that are transcribed under control of the integron promoter

In addition to ARGs, plasmids are also known to carry resistance genes for heavy metals, genes that expand the metabolic capabilities of the cell, virulence determinants, and DNA repair enhancement genes (8). Because HGT can be induced by selective pressure, transfer of any of the genes carried by the plasmid will inevitably mean the transfer of ARGs and other DNA contaminants present in it. Even in the absence of mobile plasmids, it is only necessary to add a short DNA sequence called the origin of transfer to a replicative element to render it mobilizable by conjugation (53).

1.1.3. HORIZONTAL GENE TRANSFER

HGT is an important mechanism shaping prokaryotic and eukaryotic evolution (12, 30). Based on the extensive interactions observed among all living species, Seveno et al. (53) highlighted the potential for gene transfer within different environmental niches including plants, soil and agricultural settings, aquatic environments, animals, and humans. In addition, the significance of inter-domain and inter-species HGT, especially among prokaryotes, is strongly supported by others (12). It has been estimated that between 1.6% and 32.6% of prokaryotic genes are the product of HGT events (28). In agreement with this wide estimate, Ochman et al. (42) showed that 16.6% of the *Synechocystis* PCC6803 genome and 12.8% of the *E. coli* K12 genome are products of HGT.

HGT can occur in one of three ways: conjugation, transformation, and transduction. Conjugation refers to the transfer of genetic material from one bacterial cell to another by direct cell contact. This method usually involves a plasmid-encoded “sex pilus”, which holds the cells together while genetic transfer occurs through a channel that directly connects the two cells. Transformation, on the other hand, results from the incorporation and expression of exogenous DNA by a competent cell. Transduction is the process through which genetic material is transferred from one bacterium to another via bacterial viruses called bacteriophages.

Although there are three known methods through which HGT can occur, it is widely thought that conjugation is the most important pathway of ARG transfer (23, 44, 53). Nevertheless, ARGs that are horizontally transferred by transformation and transduction have the potential to further spread through the process of conjugation, if insertion into a mobile element

occurs. In this regard, the membrane filtration processes investigated in this study could also eliminate potential DNA donors capable of conjugation.

1.1.4. OCCURRENCE AND SELECTION IN WATER AND WASTEWATER TREATMENT

The presence and prevalence of ARGs has been reported in drinking water sources and treated drinking water (49, 52, 67). In addition, an increase in ARG concentration in tap water as compared to treated drinking water and source water has been reported (67), suggesting ARB growth and/or horizontal transfer within drinking water distribution lines. Furthermore, several studies have previously shown that water disinfection processes such as chlorination can select for ARB (4, 38, 54). The potential for ARB selection is especially a concern as we as a society strive for water reuse and sustainability, which inevitably entails a tightening of the water cycle.

Among aquatic environments, special importance should be given to environments that are rich in nutrients such as eutrophic water bodies and WWTPs, as these are environments that contain high concentrations of suspended organic matter that can not only act as substrates for biofilm formation, but also as rich sources of nutrients to sustain bacterial proliferation (53). These rich biofilms can be the source of both extracellular ARGs and of live ARG donors. For this reason, it is ideal to eliminate both live cells and extracellular DNA (eDNA) from wastewater prior to release into the environment.

Common water and wastewater disinfection methods include chlorination, ozone treatment, and ultraviolet (UV) treatment, although residual chlorine or chloramine is usually required to keep microbial counts low throughout drinking water distribution lines. Given that the prevalence of ARB in WWTP has been established (5, 69), the likelihood is high that ARGs exit the wastewater treatment process undamaged and undetected, persist in the environment, contaminate drinking water sources and are potentially transferred to pathogenic bacteria. A recent study showed that disinfection processes such as chlorination and UV disinfection do not significantly contribute to the removal of ARB and ARGs from wastewater effluent, and that although high removal rates can be achieved, high concentrations of ARB and ARGs are released into the environment after conventional treatment (37). A different study highlighted the prevalence of MRSA in wastewaters; and showed that wastewater treatment processes may

reduce the number and diversity of MRSA strains, but can also select for strains with increased resistance (11).

1.2. EXTRACELLULAR DNA OCCURRENCE

It has been widely observed that eDNA constitutes a large fraction of the total DNA (tDNA) pool in the environment (17, 66). This free or colloid-sorbed eDNA can represent a potential source of ARG contamination that could be assimilated by naturally competent bacteria (27). Coranildesi et al (17) noted that the presence and persistence of large amounts of eDNA, due to biofilm formation or to sorption onto colloids, might have important implications for bacterial metabolism, providing a source of nitrogen and phosphorous and/or exogenous nucleotides, and may also contribute to HGT through natural transformation.

DNA is released into the environment during cell lysis and through active secretion mechanisms involved in the formation and development of biofilms (19). Biofilms are held together by extracellular polymeric substances (EPS) such as polysaccharides, proteins and eDNA. When sorbed to colloids or to other polymeric substances, eDNA becomes protected against environmental damage and enzymatic degradation, and can persist for long periods of time while remaining a potential source for transformation of naturally competent bacterial (47).

Recently, Das et al. (19) investigated the effect of eDNA on the initial adhesion and aggregation of several Gram positive bacteria on hydrophobic and hydrophilic surfaces. They found that, in general, bacterial adhesion and aggregation is mediated by attractive forces, electrostatic and acid-base interactions, and by protein interactions; although adhesion to hydrophobic surfaces lacks the acid-base interactions and results in weaker biofilms (19). In both cases, however, their experiments showed that eDNA plays a significant role in the bacterial adhesion and aggregation events that lead to biofilm formation (19).

Tetz et al. (61) investigated the effect of DNase I on the characteristic of early biofilm formation of two unrelated Gram negative and Gram positive bacteria: *Escherichia coli* and *Staphylococcus aureus*. Their results showed that although the biomass of bacterial biofilms was significantly reduced if grown in the presence of DNase I, these biofilms still contained eDNA of

about 30 kbp (61). Because total degradation of eDNA was observed in a cell free EPS matrix, the authors concluded that DNA is constantly released from the cells (61); however, the option that the eDNA may be protected by the presence of cells and their EPS was not considered. The results of this experiment also supported the idea that eDNA is an important component in the formation of biofilms, viability of the cells within the biofilm, and resistance of the bacteria against environmental and antimicrobial damage (61). Consequently eDNA should be expected to be found in significant quantities throughout the environment.

In a review of the origin, behavior and fate for eDNA in water soil and sediment, Pietramellara et al. (47) supported the idea that eDNA can represent a significant fraction of the tDNA pool in soil and sediment because sorption onto soil and sediment particles increases its stability and decreases its susceptibility to enzymatic degradation (47). Protection against enzymatic degradation could be due to proteases degrading nucleases, or to sorption of the enzyme to soil components, which causes its inactivation (47). As mentioned previously, this eDNA represents a potential source of ARG contamination if the bacteria from which it was released had somehow become resistant to a single or multiple antibiotics due to HGT or to selective pressure. In this regard, membrane filtration as a polishing wastewater treatment step would not only have the advantage of removing ARG contamination associated with colloids, but would also remove potential carriers and transmitters of antibiotic resistance. The removal of other contaminants such as virulence genes, antibiotics and other pharmaceuticals could also be achieved.

1.3. DNA-COLLOID INTERACTIONS

DNA has been extensively observed to sorbed to a variety of inorganic and, to a lesser extent, organic materials. Experiments exploring the behavior of DNA under different conditions (i.e., ionic strength, pH, temperature, and cations) have been performed using a variety of substrates such as soils, clays, silica and natural organic matter (NOM) (14, 36, 39, 40, 51). Remarkably, sorbed DNA has not only been shown to be increasingly stable and protected against enzymatic degradation (13, 15, 50, 61), but it has also been shown to retain or even have an increased ability to transform competent bacteria (13, 18, 27). This increased availability could be due to the solid surface providing a stable substrate where undisrupted interactions

between bacterial cells and DNA can take place. Table 1.3 summarizes the DNA interactions discussed in this section.

Lorenz et al. (31) modeled the sorption potential, protection against DNase degradation, and fate of eDNA in a flow through system of sand filled columns under different conditions of ionic strength, temperature, cations, and pH. DNA sorption was found to increase at higher ionic strengths and at lower pH, indicating that DNA sorption is a charge dependent process; but no correlation was found between temperature and extent of sorption in this study (31). It was also concluded that the DNA-sand complex is a stable association that protects DNA against enzymatic degradation by DNase I enzyme (31). In addition, it was proposed that the sorption of DNA to sand particles occurred by cation bridging (supported by numerous later findings), and desorption is enhanced by ethylenediaminetetraacetic acid (EDTA) (31). Furthermore, after washing-EDTA eluted sand with detergents and accomplishing no DNA desorption, it was concluded that hydrophobic interactions between DNA and sand play only a minor role, if any, on DNA sorption (31).

Table 1.3. Summary of materials observed to interact with and/or protect DNA against enzymatic degradation, and transformation ability of sorbed DNA.

Material	Sorption	Protection against DNase degradation	Transformation ability	References
Organic and inorganic clays	+	+	+	(13-15, 27)
Soil colloids and particles	+	+	+	(13-15, 51)
Silica/sand	+	+	*	(31, 36, 39, 41, 50)
Charcoal	+	*	*	(36)
Humic acids	+	+	+	(18)
NOM	+	*	*	(39)

* Data not available.

Mitra et al. (36) investigated the mechanistic aspect of DNA sorption at different solid-liquid interfaces as a function of DNA concentration, pH, ionic strength and temperature. They found that in all cases the initial rate of sorption is controlled by diffusion, and that sorption

steady state is reached after nearly six hours (36). In addition, the rate of sorption was found to be of first order with two kinetic constants (36). The presence of two kinetic constants was explained by the initial attachment of the DNA molecules to the solid surface (first constant). When the surface becomes crowded with DNA molecules, polymer-polymer interactions occur causing the DNA molecules to rearrange and allow access of additional molecules to the surface (second constant) (36).

Nguyen et al. (41) found that that diffusion coefficients for plasmid DNA increase with increasing ionic strength, and that increasing Ca^{2+} concentrations lead to increasing diffusion coefficients, suggesting the presence of smaller plasmid DNA molecules. The plasmid DNA molecules are highly negatively charged at pH 6 and 8 due to their phosphate backbone; and in high ionic strength solutions, the intramolecular electrostatic repulsion among negatively charged subsections of the DNA macromolecule is screened by the ions in solution; thus reducing intramolecular electrostatic repulsion and leading to a more compact conformation or smaller size of DNA with higher diffusion coefficients (41). Because at the studied pH conditions both the silica surface and the plasmid DNA are negatively charged, increasing ionic strength containing monovalent or divalent cations causes shielding of the negative charges, thus substantially decreasing the repulsive electrostatic forces and facilitating DNA sorption to silica (41). This effect is especially enhanced in the presence of divalent cations such as Ca^{2+} (41), and was later found to be even stronger in the presence of transition metal divalent cations such as Cu^{2+} (39). Divalent cations, especially Ca^{2+} and Cu^{2+} , can also significantly reduce the charge of silica surface by binding to silanol groups present on the surface of the silica particles, thus resulting in reduced electrostatic repulsion between the DNA and the silica surface (39, 41). The combination of the DNA and silica charge neutralization by calcium ions, and the increase in the DNA diffusion coefficient lead to an increase in the sorption rate of the plasmid molecules to the silica surface; moreover, this sorption was shown to be irreversible when rinsing with solutions containing lower ionic strength (41). It was suggested that DNA sorption to silica surfaces involves two steps: reaction of metal cations with silica surfaces to reduce the negative charge on the silica and subsequent sorption of plasmid DNA on the silica surfaces.

More related to our research are the interactions between DNA and organic colloids from wastewater. Nguyen et al. (40), found that at low ionic strength there was no detectable circular plasmid DNA sorption, and little sorption of linear DNA onto the NOM layer. At higher ionic

strengths, however, the sorption rates were comparable between circular and linear DNA (40). This effect was attributed to electrostatic double layer repulsion between the DNA and the NOM layer (40). Both DNA and NOM are negatively charged at ambient temperature; thus increasing the ionic strength also increases the shielding effects and diminishes repulsive conditions, allowing interactions to occur (40). Because no DNA detachment was detected when the sorbed DNA was rinsed with solutions of low ionic strength, it was suggested that eDNA can sorbed onto NOM or NOM-covered solid surfaces, and will not be released during rain or other events when the ionic strength of the water decreases rapidly (40).

1.4. FILTRATION

Anthropogenically propagated ARB and ARGs can be released into the environment via two main pathways: wastewater effluent and agricultural runoff; with the potential to re-expose humans via treated water used for consumption, bathing, and recreation. Accordingly, membrane filtration can provide a barrier for transmittance of ARGs and ARB through the water-wastewater cycle both by preventing the human medicine-related resistance elements from exiting WWTP and entering the environment, and by preventing the human acquisition of agriculturally derived ARGs and ARB. However, because disinfection of treated wastewater serves the primary purpose of only inactivating ARB and not necessarily impacting the genetic material, ARG removal represents the main focus of this research.

Several types of membrane filters are available for water treatment, ranging from the semi-permeable membranes used for reverse osmosis (RO), to membrane filtration media with $\geq 1 \mu\text{m}$ pore size used in membrane cartridge filtration (MCF) systems (62). Nanofiltration (NF) membranes and RO are most often used for the removal of dissolved contaminants, while microfiltration (MF) membranes and ultrafiltration (UF) membranes are generally used for the removal of suspended or colloidal particulate matter (34, 62). As the pore size of a particular membrane type becomes smaller, the membrane is said to become “tighter”; similarly, as the pore size of that membrane type becomes larger, the membrane is said to become “looser” (34). Consequently, a loose ultrafiltration membrane may be able to remove similarly sized particles as a tight MF membrane. A brief comparison between membrane pore size and the size of common water contaminants is shown in Figure 1.5.

Approx. MWCO (kDa)	1		100		1000		
Approx. effective pore size (µm)	0.0001	0.001	0.01	0.1	1	10	100
Separation Process	Reverse Osmosis						
	Nanofiltration						
	Ultrafiltration						
	Microfiltration						
					Conventional media filtration		
Common water contaminants	Aqueous salts						
	Metal ions						
	Amino acids						
	Oligonucleotides						
	Sugars						
	Humic Acids						
	Antibiotics						
	Proteins						
	Colloids						
	Viruses						
	Clays						
	Bacteria						
	Silt						
Sand							
Approx. operating Pressure (kPa)	7000	1000	300	100	10		

Figure 1.5. Relationship between type of filtration system and contaminant removal (34, 65).

For this project, several membrane pore sizes in the MF and UF range were used. Because our focus was on colloidal particles, or particles ranging between 1 nm and 1 µm in size, the largest MF membrane used had a 1.2 µm pore size. Similarly, because we were only interested in removing DNA and not smaller molecules such as sugars or salts, the tightest UF membrane used had a molecular weight cut off (MWCO) of 1 kDa. It is important to note that as removal efficiency of smaller particles/molecules increases, so does energy demand (See Table 1.4). Therefore, the ideal strategy is to select the minimum pore size that meets the requirements to remove the contaminants of concern. Understanding the relationship between DNA and colloids may effectively help to significantly reduce the required pore size for removal.

Table 1.4. General characteristics of membranes (65).

Membrane operation	Driving force	Mechanism of separation	MWCO range (Da)	Pore size range (μm)	Operating pressure (psi)
Microfiltration (MF)	Pressure or vacuum	Size exclusion	>100000	0.1-10	1-30
Ultrafiltration (UF)	Pressure	Size exclusion	>2000-100000	0.01-0.1	3-80
Nanofiltration (NF)	Pressure	Size exclusion	300-1000	0.001-0.01	70-220
Reverse Osmosis (RO)	Pressure	Solution diffusion + charge and size exclusion	100-200	<0.001	800-1200

1.4.1. MICROFILTRATION (MF) AND ULTRAFILTRATION (UF)

MF and UF membranes are used to remove particles, larger molecules, and other particulate organic and inorganic matter from water through a pressure-driven sieving mechanism. The difference between MF and UF lies in the pore size distribution of the membrane (68), and unlike nanofiltration or RO, MF and UF membranes are not capable of removing dissolved constituents (6). MF/UF membrane pore sizes range from 0.001 μm (1 nm) for the tightest UF membranes to about 10 μm for the loosest MF membranes (68). MF membrane pore sizes typically range from 0.1 to 10 μm in diameter, and are designed to remove microorganisms and particles in the micron size range. Although highly misleading, UF membranes are generally characterized based on a MWCO rather than on size, which is the dominant factor controlling UF rejection (68). MWCO refers to the molecular weight of the smallest retained molecules; however, because of molecule conformation, the effective size and radius of gyration of these molecules can differ significantly.

Membrane chemistry determines properties such as hydrophobicity or hydrophilicity, presence or absence of ionic charges, chemical and thermal resistance, binding affinity for solute particles, biocompatibility, etc. (68). Because we desired to test ARG removal based on membrane pore size rather than on interactions with the membrane itself, we chose hydrophilic membranes that had low sorption potential for biomolecules such as proteins and DNA.

1.5. GOAL AND OBJECTIVES

The overall goal of this project was to investigate the effect of wastewater colloids on the removal of ARGs by membrane filtration. To achieve this goal, the following objectives were specified:

- 1) Quantify the removal of ARGs following membrane filtration through a tightening cascade of MF and UF membranes and determine whether ARG removal in the presence of colloids significantly differed from ARG removal in the absence of colloids.
- 2) Characterize the colloidal composition in terms of organic carbon, proteins, and polysaccharides and explore potential relationships in the removal of each of these components and the removal of ARGs.

1.6. HYPOTHESES

The following two hypotheses were tested:

- 1) There is a difference between the membrane removal of ARGs in the presence of colloids when compared to the removal of ARGs in the absence of colloids.
- 2) There is a positive correlation between the removal of ARGs and the removal of colloidal components within the tightening membrane cascade.

2. DNA EXTRACTION FROM DILUTE WATER SAMPLES: METHOD DEVELOPMENT

2.1. INTRODUCTION

As mentioned in the previous chapter, intracellular DNA (iDNA) is not the only significant component of the tDNA pool in the environment. eDNA also forms part of this total pool, and in some cases it has even more significance than the intracellular fraction (See section 1.2). However, DNA extraction methods generally focus on isolating genomic DNA from cell cultures, tissue samples, solid environmental samples, and other solid-phase samples; and generally overlook the importance of free or sorbed DNA from environmental sources. Thus, there is a need to develop improved eDNA extraction techniques in order to better assess DNA removal technologies.

There are three main steps associated with the extraction of iDNA: (1) Cell lysis, or breaking open the cells to obtain the DNA lodged within them; (2) DNA washing and removal of cell debris and proteins; and (3) DNA elution or resuspension. Additional steps can be performed to remove additional contaminants that may interfere with or inhibit subsequent analytical steps. Commercial kits specializing in the extraction and purification of DNA from a variety of sources are widely available.

When dealing with environmental water samples, extracting iDNA is regarded as a relatively simple procedure that only requires filtering a predetermined volume of the sample and then isolating the DNA from the filter membrane by conventional methods. This technique; however, is faulty in that it may not accurately portray the iDNA composition of the sample due to potential contamination by a portion of the eDNA fraction. A few studies have incorporated eDNA extraction techniques. eDNA can be either free or associated with other matter. The latter fraction can either be associated with organic or inorganic surfaces such as colloids, or can be part of biological aggregates such as biofilms. In either case, extracting the tDNA pool from an environmental water sample can be achieved by concentrating the sample without causing damage to the DNA, and then applying a conventional DNA extraction method. Pote et al. (48)

recently applied this technique for the extraction of tDNA by concentrating groundwater and drinking water fountain samples 200 times using a lyophilizer or freeze-dryer.

The purpose of the experiments described in this chapter was to (1) compare different methods for extracting the tDNA pool from dilute water samples; (2) test the effectiveness of membrane filtration for the extraction of pure iDNA; (3) test additional methodologies for the separate extraction of extracellular and intracellular DNA from water samples; and (4) compare the yields of DNA extraction and DNA purification from wastewater samples versus DNA extraction, purification, and resuspension from buffer samples. The results obtained from these experiments will be used to determine the methodology to be applied in the overall project.

2.1.1. INTRACELLULAR AND EXTRACELLULAR DNA EXTRACTION FROM DILUTE WATER SAMPLES

Separate extraction of eDNA and iDNA from sediment and biofilm samples has been previously attempted (17, 66) and is an important requirement for characterizing the size, composition, relative contribution, and fate of each fraction within a variety of solid- and liquid-phase environmental samples. However, separate extraction of the two fractions from a dilute water sample has remained an unsolved challenge, as even extraction of the tDNA pool from such samples remains free of a standardized or commercial protocol.

Corinaldesi et al. (17) achieved the simultaneous recovery of extracellular and intracellular DNA from sediment samples, and reported that the eDNA fraction was 10 to 70 times higher than the intracellular fraction. According to the authors, the most difficult tasks for isolation of eDNA in sediment are avoiding eDNA contamination with iDNA, separating the two types of DNA, and obtaining pure DNA suitable for subsequent molecular analyses. Other factors affecting the recovery of DNA include DNA sorption to sediment colloids, coextraction of enzymatic inhibitors, and degradation and shearing of DNA (17).

Wu and Xi (66) compared several chemical and enzymatic methods for the isolation of eDNA from biofilm samples. The extractants tested included cation removers (cation-exchange resin (CER) and EDTA), strong denaturants (sodium dodecyl sulfate (SDS) and NaOH), and enzymes (*N*-glycanase, Dispersin B, Proteinase K) (66). It was concluded that enzymatic

methods aimed at releasing EPS-bound eDNA were more effective in preventing cell lysis than chemical methods; thus, enzymatic methods may be more accurately applied for the extraction of both free and biofilm-associated eDNA (66).

2.2. MATERIALS AND METHODS

The DNA isolation methods tested in this study are described in Table 2.1. Two methods were tested for the concentration and subsequent extraction of the tDNA pool from dilute water samples. Distinct extracellular and intracellular DNA extraction was also attempted. The methodology is described below.

Table 2.1. DNA isolation methods tested in this study.

Method	Purpose	DNA extraction required?	Target DNA fraction
Silica sorption	DNA isolation	No	Extracellular
Filtration	DNA concentration	Yes	Intracellular
Silica sorption + filtration	DNA concentration	Yes	Total
Freeze drying	DNA concentration	Yes	Total

2.2.1. WWTP EFFLUENT COLLECTION

The WWTP effluent was collected during cold winter or early spring active weekdays between Tuesdays and Fridays, avoiding rain or snow events occurring in the last 24 hours. The effluent was immediately transported to the lab and subjected to experimental manipulations. All experiments were carried out at room temperature except where noted otherwise.

2.2.2. PREPARATION OF SOLUTIONS AND SILICA SUSPENSION

DNA wash solutions 1 and 2 contained 50 mM NaCl, 10 mM tris (hydroxymethyl) aminomethane (Tris) buffer pH 7.5 (pH adjusted using HCl), 50% v/v ethanol, and 1.5 mM (solution 1) or no (solution 2) EDTA, respectively. The solutions were prepared and autoclaved prior to ethanol addition.

Silica suspension: 10 g of 99% silicon dioxide particles (0.5 - 10 μm diameter, 80% with 1 - 5 μm diameter; Sigma-Aldrich, St. Louis, MO) were washed three times with nanopure water in 50 ml conical centrifuge tubes by centrifugation at $6000 \times g$ for 1.5 min per wash step. The silica was then resuspended in 100 ml of 2 mM CuCl_2 , 44 mM NaCl solution and subsequently autoclaved.

Phosphate buffered solution (PBS): Each of the components (137 mM NaCl, 2.7 mM KCl, 10 mM Na_2HPO_4 , 1.76 mM KH_2PO_4) was dissolved in nanopure water, after which the pH was adjusted to 7.4 using NaOH or HCl, if necessary, and the solution was autoclaved.

2.2.3. PLASMID PREPARATION

Genomic DNA from vancomycin-resistant *Enterococcus* (VRE) was used as template for the amplification of a 732 bp portion of the *vanA* gene, using the primers previously described by Dutka-Malen et al. (21). The 25 μl reaction contained 1X Master Taq reaction buffer (5 Prime, Gaithersburg, MD), 1X Taq Master PCR enhancer (5 Prime, Gaithersburg, MD), 1.5 mM Mg^{2+} solution (5 Prime, Gaithersburg, MD), 0.05 mM of each deoxynucleoside triphosphate (Promega, Madison, WI), 0.2 μM of each primer, 1.75 U Taq DNA polymerase (5 Prime, Gaithersburg, MD), 1 μl template DNA, and autoclaved nanopure water to a final volume of 25 μl . The thermal component of the reaction consisted of an initial 3 min denaturing step at 95 $^\circ\text{C}$; followed by 50 cycles of a 30 s denaturing step at 95 $^\circ\text{C}$, a 30 s annealing step at 54 $^\circ\text{C}$, and a 30 s extension step at 72 $^\circ\text{C}$; and a 7 min final extension step at 72 $^\circ\text{C}$. The *vanA* PCR product was cloned using the TOPO TA cloning kit (Invitrogen, Carlsbad, CA), following the manufacturer's instructions. A map of the 4,688-bp resulting plasmid is shown in Figure 2.1. The plasmids were then extracted using the Qiagen Plasmid Mini Kit (Qiagen, Valencia, CA), according to manufacturer's instructions.

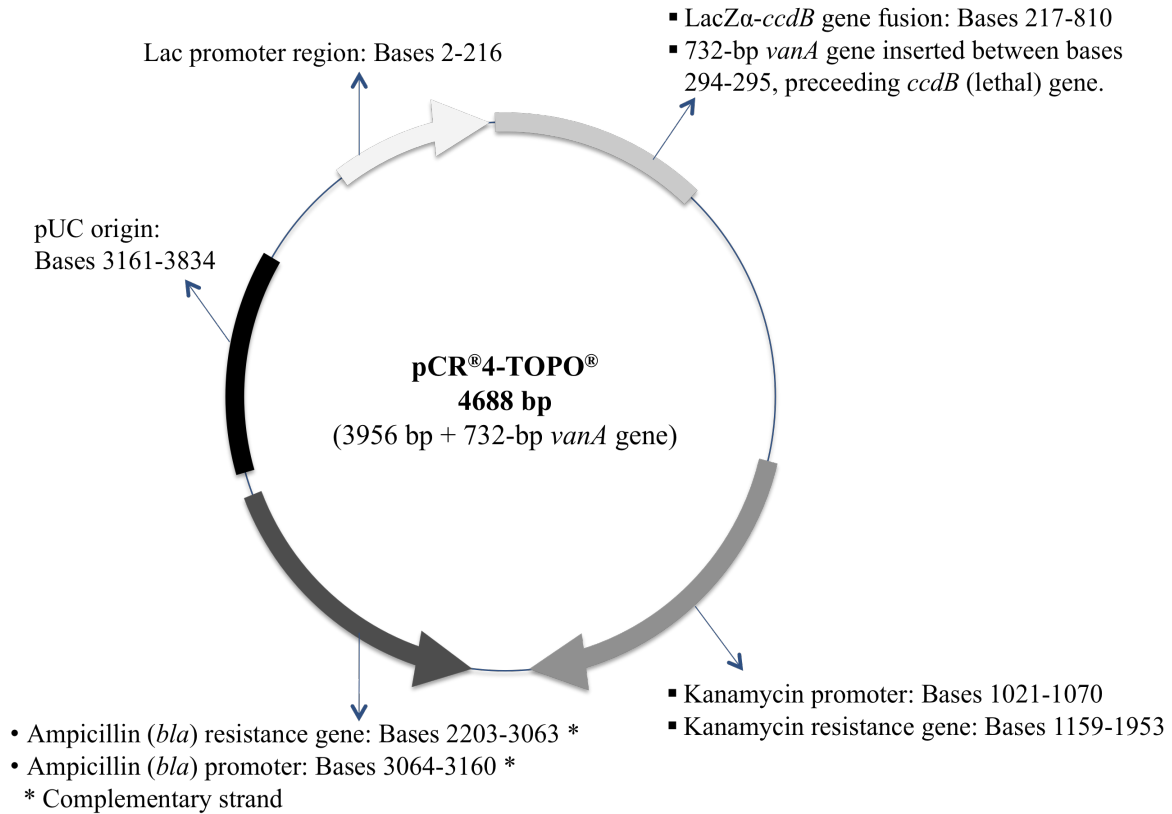


Figure 2.1. Map of pCR[®]4-TOPO[®] plasmid map indicating *vanA* gene insertion site (Invitrogen, Carlsbad, CA). Used under fair use, 2011.

2.2.4. *E. COLI* GROWTH CURVE AND PREPARATION OF CELL SUSPENSION

A growth curve showing the lag, exponential, and stationary phases of *E. coli* growth was needed in order to grow the cells to the middle of the exponential phase. At this phase in growth, metabolism is most active; and because there is little cell death and lysis, there is also little DNA release.

To build a growth curve, a premade 1 ml freezer stock of *E. coli* cells was transferred to 100 ml LB broth and grown in a shaking incubator set to 37 °C and 200 rpm. The cell density was monitored using a Spectronic 20 Spectrophotometer (Milton Roy Company, Ivyland, PA) set to 580 nm, and taking absorbance readings every 15 to 30 min until the cell density reached the stationary phase. A different vial of the same *E. coli* freezer stock was grown on 100 ml LB broth under the same conditions (37 °C and 200 rpm) to the middle of the exponential phase, according to the previously generated growth curve. The cells were centrifuged at 5,000×g for 20

min, and resuspended three times in PBS to wash and eliminate eDNA and excess medium. A fraction of the final cell suspension was diluted and plated onto LB agar in order to estimate the cell concentration.

2.2.5. EXPERIMENTAL SETUP

In order to determine the efficiency of eDNA, iDNA, and tDNA extraction by the methods described in the following sections (Sections 2.2.6 – 2.2.10) five flasks were set up as follows (See Figure 2.2): (1) Phosphate buffered solution (PBS) only blank; (2) PBS solution + $\sim 1 \times 10^7$ plasmid copies/ μl ; (3) PBS solution + $\sim 1 \times 10^5$ *E. coli* cells/ml + $\sim 1 \times 10^7$ plasmid copies/ μl ; (4) WWTP B effluent only; and (5) WWTP B effluent + $\sim 1 \times 10^7$ plasmid copies/ μl . All flasks contained 300 ml of buffer or wastewater, and were kept at room temperature throughout the experiment. Spiked samples were placed on a shaker at a low speed for 4 hours in order to allow interactions between the eDNA and the colloidal material. A minimum interaction time of 4 hours was chosen based on typical WWTP retention times and on DNA sorption times reported in the literature (36). Samples were also collected at 1 and 2.5 hours to test for DNA degradation. After 4 hours, 10 ml of each sample was subjected to DNA concentration and subsequent extraction using the methods described in the following sections (Section 2.2.6 – Section 2.2.10).

An additional experiment was setup with the purpose of comparing DNA extraction, purification, and resuspension methods for the isolation of DNA in future experiments. DNA extraction is a process designed to disrupt cells and extract iDNA. A purification step is typically done with the purpose of eliminating additional cell debris and contaminants that could cause interferences in downstream analyses. In DNA purification, the DNA is washed and impurities that may interfere with subsequent analytical steps are removed from the sample; however, this process is not designed to extract iDNA or to remove high contaminant concentrations. The purpose of DNA resuspension is only to re-dissolve concentrated DNA that is already free of contaminants. Four flasks were filled with 600 ml of unspiked Tris buffer (10 mM Tris pH adjusted to 8 using HCl), spiked Tris buffer, unspiked WWTP A effluent (initially filtered through 1.2 μm filter), and spiked WWTP A effluent (initially filtered through 1.2 μm filter). Spiked samples were spiked with the previously prepared *bla*_{TEM} and *vanA* gene-containing

plasmids (see Section 2.2.3) to a final concentration of 10^6 plasmid copies/ μl . DNA extraction, purification, and resuspension techniques were tested and compared for freeze-dry concentrated buffer samples, and only the first two were compared for freeze-dry concentrated WWTP effluent samples, as PCR inhibiting contaminants are known to be present in WWTP effluents.

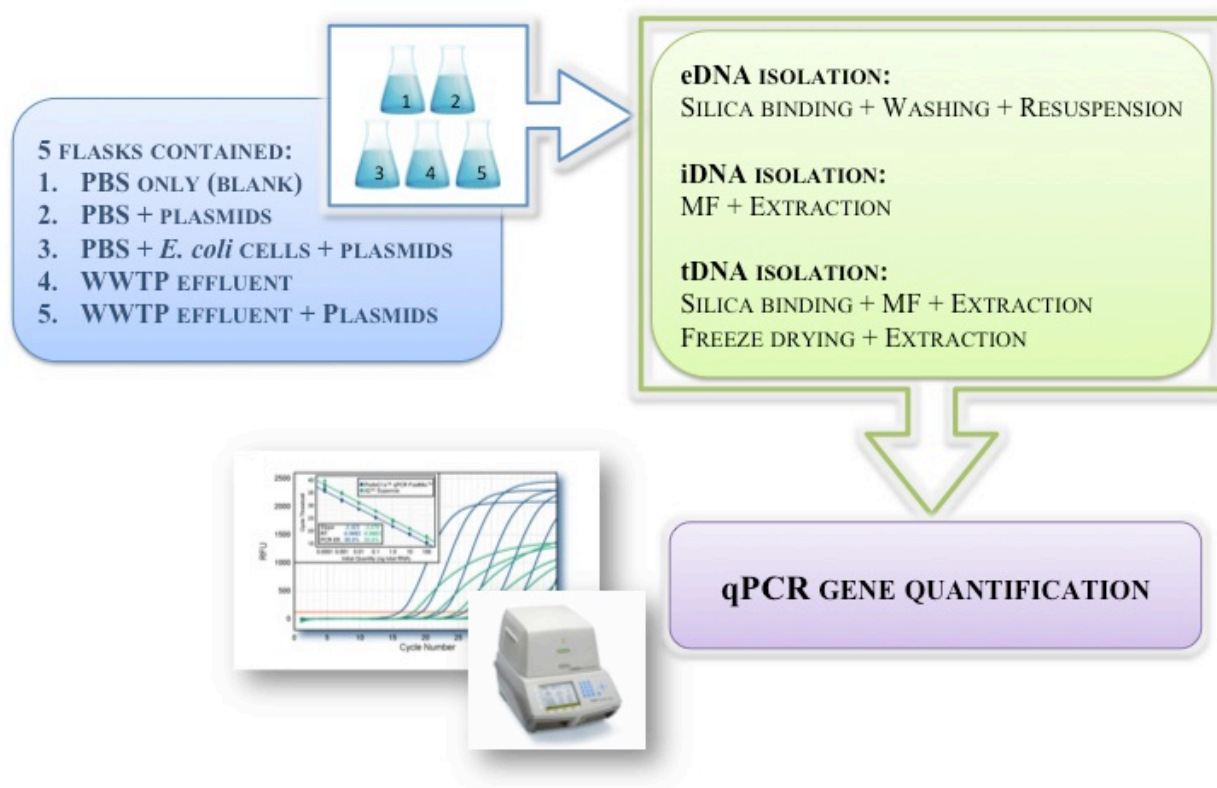


Figure 2.2. Diagram of experimental setup described in Section 2.2.5.

2.2.6. EXTRACELLULAR DNA CONCENTRATION BY SILICA BINDING

The purpose of applying this eDNA extraction method was to concentrate, wash, and resuspend eDNA present in wastewater and control buffer samples while excluding iDNA in the undisturbed whole cells. The concentration step was hoped to work by preferentially binding the eDNA to the silica particles in the presence of a high Cu^{2+} concentration. Washing would then be achieved in conditions of high salt concentration and the presence of the chelating agent EDTA. These conditions would maintain the DNA sorbed onto the silica particles while chelating Cu^{2+}

ions and washing away impurities. Finally, the eDNA would be collected by running ion-free nanopure water through the silica, thus allowing the DNA to desorb and redissolve in an iDNA-free medium.

Ten-milliliter samples were collected from each of the flasks (See section 2.2.5) and mixed with 10 ml of silica suspension in sterile 50 ml conical centrifuge tubes. The contents of the tube were mixed for 15 minutes to allow sorption of DNA to the silica particles. After 15 min, the tubes were centrifuged at $6000\times g$ for 1 min and the supernatant was decanted. The silica pellet was resuspended in 10 ml of DNA wash solution 1 (containing EDTA), transferred to a 0.2 μm Maxi-Spin filter tube (Chromtech, Apple Valley, MN), and centrifuged at $6000\times g$ for 5 min. The silica was then resuspended in 10 ml of DNA wash solution 2, and centrifuged again at $6000\times g$ for 5 min. Additional centrifugation was sometimes required if all of the liquid did not pass through the membrane the first time, which is likely when the presence of large amounts of silica clogs the membrane. After washing, the silica was allowed to air-dry for 10 min, after which the DNA was eluted with 1 ml of autoclaved nanopure water.

2.2.7. INTRACELLULAR DNA CONCENTRATION BY MICROFILTRATION

Ten-milliliter samples collected from each of the flasks (Section 2.2.5) were filtered through a 0.22 μm membrane (Millipore, Billerica, MA), using a Nalgene[®] polysulfone filter holder (Thermo Fisher Scientific, Rochester, NY). The membranes were washed with 50 ml of PBS, collected in sterile Petri dishes, and refrigerated until the next morning when DNA extraction was done as described below.

2.2.8. TOTAL DNA CONCENTRATION BY SILICA BINDING AND MICROFILTRATION

Ten-milliliter samples were collected from each of the flasks (Section 2.2.5) and mixed for 15 min with 10 ml of silica suspension in a 50 ml conical centrifuge tube. The mixture was then filtered through a 0.22 μm membrane (Millipore, Billerica, MA), using a Nalgene[®] polysulfone filter holder (Thermo Fisher Scientific, Rochester, NY). The membranes were collected and refrigerated in sterile Petri dishes until the next morning when DNA extraction was carried out as described below.

2.2.9. TOTAL DNA CONCENTRATION BY FREEZE DRYING

Ten-milliliter samples (Section 2.2.5) were preserved at -80°C prior to freeze-drying in a FreeZone Plus 2.5 Liter Benchtop Freeze Dry System (Labconco, Kansas City, Missouri). The powder remaining after freeze-drying was directly subjected to DNA extraction as described below.

2.2.10. DNA EXTRACTION, PURIFICATION, AND RESUSPENSION

DNA was extracted from the membranes and the freeze-dried powder using the FastDNA Spin Kit for Soil, Catalog # 6560-200 (MP Biomedicals, Solon, OH), according to the manufacturer's protocol. A reduced homogenization step was applied during DNA extraction using a speed setting of 4 for 20 sec in the FastPrep[®] instrument (MP Biomedicals, Solon, OH). For extracting DNA from the filtered samples, the membranes were initially cut up into small pieces using flame-sterilized tweezers, and inserted in the lysing matrix tubes. In the case of the filtered silica, however, it was necessary to divide the membranes into two lysing matrix tubes as there was insufficient volume available in only one tube. For extraction of the freeze dried material, the initial addition of Sodium Phosphate Buffer and MT buffer was done in the same glass container where the wastewater or buffer sample had been freeze dried. This aided in minimizing transfer losses and reduced the possibility of contamination by bacteria or particles suspended in the air. After thoroughly mixing, the suspension was transferred to the lysing matrix tube, where the DNA extraction was carried out as recommended in the DNA extraction manual. DNA purification was done using the PowerClean DNA Cleanup Kit (MoBio Laboratories, Carlsbad, CA). DNA resuspension was only performed on freeze-dried buffer samples by dissolving the freeze-dried material in 500 µl of autoclaved nanopure water.

2.2.11. DNA QUANTIFICATION

Quantification of the vancomycin resistance *vanA* gene, the β-lactamase *bla*_{TEM} gene, and the 16S rRNA gene was done by real time quantitative polymerase chain reaction (qPCR), using the CFX96 Touch[™] Real-Time PCR Detection System (Bio-Rad, Hercules, CA). Reactions containing 40 nM of each primer, 1X SsoFast[™] EvaGreen[®] Supermix (Bio-Rad, Hercules, CA),

1 μ l template DNA, and sterile nanopure to a final volume of 10 μ l, were setup in triplicates for all samples. The primers used for amplification of the 16S rRNA gene (1369F & 1492R) were previously described by Suzuki et al. (60); those used for amplification of the *vanA* gene were vanAstF, described by Bockelmann et al. (10), and *vana3RP*, described by Volkmann et al. (64); and those used for the amplification of the *bla*_{TEM} gene were described by Bibbal et al. (9). The temperature programs consisted of a 95 °C initial denaturing step for 30 sec; 40 cycles of denaturing at 95 °C for 5 sec, annealing and extension at 60 °C (*vanA* and *bla*_{TEM}), and 55.3°C (16S), for 5 sec, and an additional extension step at 72°C for 5 sec for *vanA* amplifications only. A melt curve was also built at the end of every reaction to verify specificity by ramping the temperature from 65 °C to 95 °C by 0.5 °C for 5 sec. A calibration curve was constructed for each set of reactions using at least five standards. A limit of quantification (LOQ) was calculated for each gene by averaging gene concentrations in 10 reaction blanks and multiplying that value by 3. The standards were prepared by serially diluting an M13 PCR product of known concentration, obtained after cloning a PCR product of each gene of interest (16S rRNA, *vanA*, or *bla*_{TEM}) using the TOPO TA cloning kit (Invitrogen, Carlsbad, CA), PCR amplifying them and their flanking sequences using the M13 primers provided with the cloning kit, quantifying the PCR product by gel imaging, and calculating the concentration of gene copies using the relationship described by Pei et al. (45).

2.3. RESULTS

Several DNA extraction methods were compared with the purpose of identifying the most efficient and effective methods for the extraction of iDNA, eDNA, and tDNA from dilute water samples. A DNA degradation test was simultaneously carried out as a way to account for potential DNA losses during the experiments. Five flasks were set up as described in the experimental section and as shown in Figure 2.2. The unspiked PBS was used as experimental blank in order to confirm the absence of contamination and the validity of the results. Plasmid+*E. coli* cell spiked PBS was used to explore the extent of contamination, if any, of one DNA fraction (i.e., eDNA or iDNA) when extracting the converse fraction. Unspiked WWTP effluent was tested in order to estimate the actual eDNA and iDNA concentrations present in the WWTP effluent; while spiked WWTP effluent was included as a means to test the efficiency of

eDNA recovery from the complex aqueous matrix. Finally, the eDNA extraction efficiency in the presence of cells or of WWTP effluent was compared to the efficiency in the absence of colloidal material or cells (i.e., in spiked PBS) in order to test for colloid or cell interference during extraction. Triplicate qPCR reactions were setup for each concentration measurement. The results obtained from this experiment are described in this section. The LOQ, shown in Table 2.2, was calculated to be 1.1×10^2 for the *bla*_{TEM} gene, 0.8 for the *vanA* gene, and 5.0×10^2 for the 16S rRNA gene. The *E. coli* growth curve used to determine the range of the exponential phase of the cells used for intracellular DNA spiked experiments is provided in Appendix A, Figure A 1.

Table 2.2. Limit of quantification for the *bla*_{TEM}, *vanA*, and 16S rRNA genes.

Gene	Average blank concentration (ABC) (gene copies/μl)	LOQ (ABC × 3) (gene copies/μl)
<i>bla</i> _{TEM} gene	36.6	1.1×10^2
<i>vanA</i> gene	0.3	0.8
16S rRNA gene	166.1	5.0×10^2

2.3.1. PLASMID EXTRACTION

The plasmid extraction was repeated on several occasions, yielding the general product characteristics shown in Figure 2.3. Two main characteristics of the plasmid extracts were noted: (1) Distinct *bla*_{TEM} and *vanA* concentrations, where the *vanA* gene concentration was up to 73% lower than the *bla*_{TEM} gene concentration; and (2) the presence of genomic DNA contamination was usually between 2 and 5 orders of magnitude lower than the *bla*_{TEM} gene concentration. The *bla*_{TEM} gene concentration generally ranged between 2×10^{10} and 1×10^{12} gene copies/μl, with the *vanA* gene concentrations lagging by less than 1 order of magnitude. The genomic DNA concentration, quantified through the 16S rRNA gene, was between 2 and 5 orders of magnitude below the *bla*_{TEM} gene concentration. Background genomic DNA contamination is typical and difficult to eliminate due to its ubiquitous nature, and for our experimental purposes the existing concentration difference between the genomic and plasmid DNA should be sufficient not to influence the plasmid behavior in downstream experiments. Although the plasmid extraction was repeated in an attempt to obtain less contaminated product, the extraction results remained

consistent. Switching to the Plasmid Mega kit (Qiagen, Valencia, CA), which provides larger yields, produced similar results.

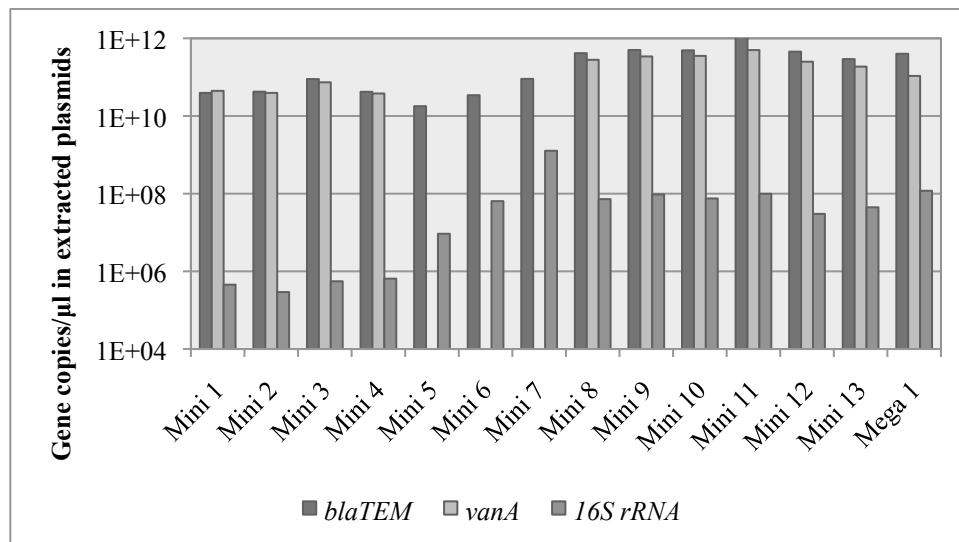


Figure 2.3. qPCR quantified *bla*_{TEM}, *vanA*, and 16S rRNA gene concentrations in plasmid extraction products. Mini: Plasmids extracted using the Qiagen Plasmid Mini kit (Qiagen, Valencia, CA). Mega: Plasmids extracted using the Qiagen Plasmid Mega Kit (Qiagen, Valencia, CA). Numerical values provided in Appendix A, **Table A 1**.

2.3.2. DNA DEGRADATION

Based on the *bla*_{TEM} gene quantification of the plasmid extraction product, a final concentration of 10^7 plasmids/μl was spiked. Negligible degradation was observed in the buffer and wastewater samples during the 4-hour time allotted for DNA degradation. Although all of the samples were spiked to the same final plasmid concentration, the sample consisting of an *E. coli* cell suspension in PBS resulted in higher plasmid concentrations than the rest of the samples, with *bla*_{TEM}, *vanA*, and 16S rRNA gene concentrations of 4.7×10^7 , 8.8×10^6 , and 1.2×10^7 gene copies/μl, respectively, at 4 hours. Figure 2.4 - Figure 2.6 illustrate the quantification results of the degradation tests.

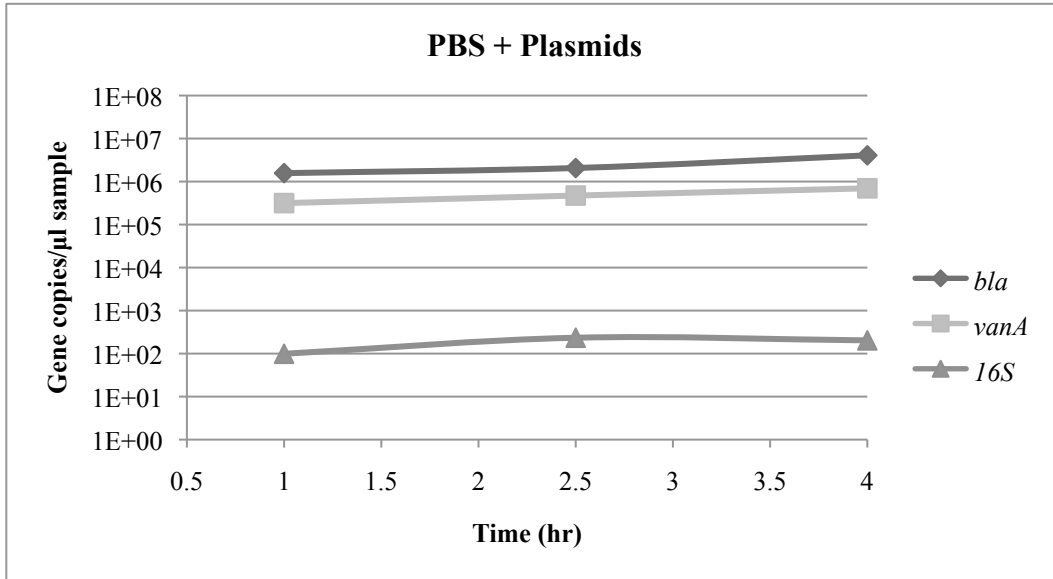


Figure 2.4. Degradation test of plasmid and genomic DNA suspended in PBS, monitored by qPCR. Test points represent average of triplicate qPCR measurements. Numerical values are given in Appendix A, **Table A 2.**

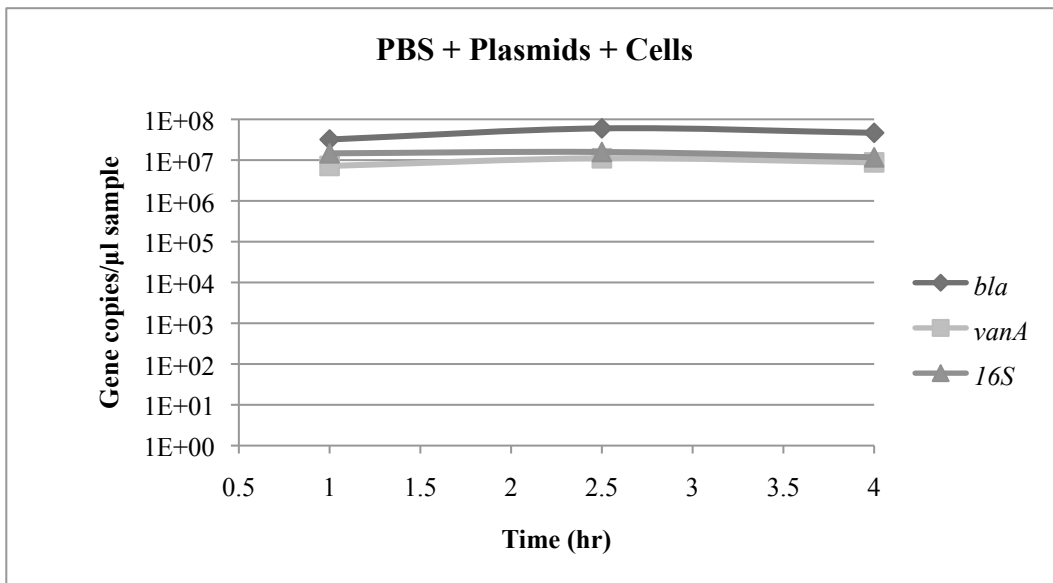


Figure 2.5. Degradation test of DNA in a PBS solution containing *E. coli* cells, monitored by qPCR. Test points represent average of triplicate qPCR measurements. Numerical values are given in Appendix A, **Table A 2.**

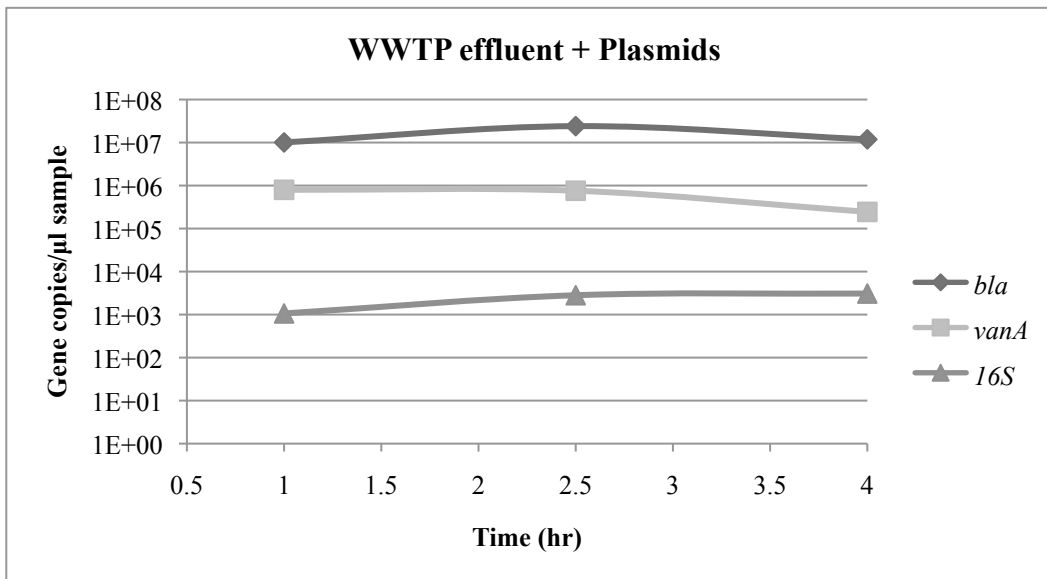


Figure 2.6. Degradation of DNA in a filtered WWTP effluent sample, monitored by qPCR. Test points represent average of triplicate qPCR measurements. Numerical values are given in Appendix A, **Table A 2**.

2.3.3. INTRACELLULAR AND EXTRACELLULAR DNA EXTRACTION

Attempts were made to extract extracellular and intracellular DNA from water samples using the silica sorption and microfiltration methods described in Sections 2.2.6 and 2.2.7, respectively. The results are shown in Figure 2.7 and Figure 2.8, respectively.

The gene concentrations measured in extracts obtained from the PBS+plasmid samples by silica sorption (expected to provide eDNA only) were over 4 orders of magnitude lower than the spiked extracellular concentration of 1×10^7 plasmids/ μl , which were known to be extracellular. The concentrations measured in the PBS+cells+plasmid and WWTP effluent+plasmid extracts obtained by silica sorption were slightly higher than the concentrations measured in the PBS+plasmid sample, but still over 2 orders of magnitude lower than the spiked value of 1×10^7 gene copies/ μl . The 16S rRNA gene concentration in the PBS+cells+plasmid was 9.8×10^3 gene copies/ μl , which is high relative to the initial proportions of the three spiked genes.

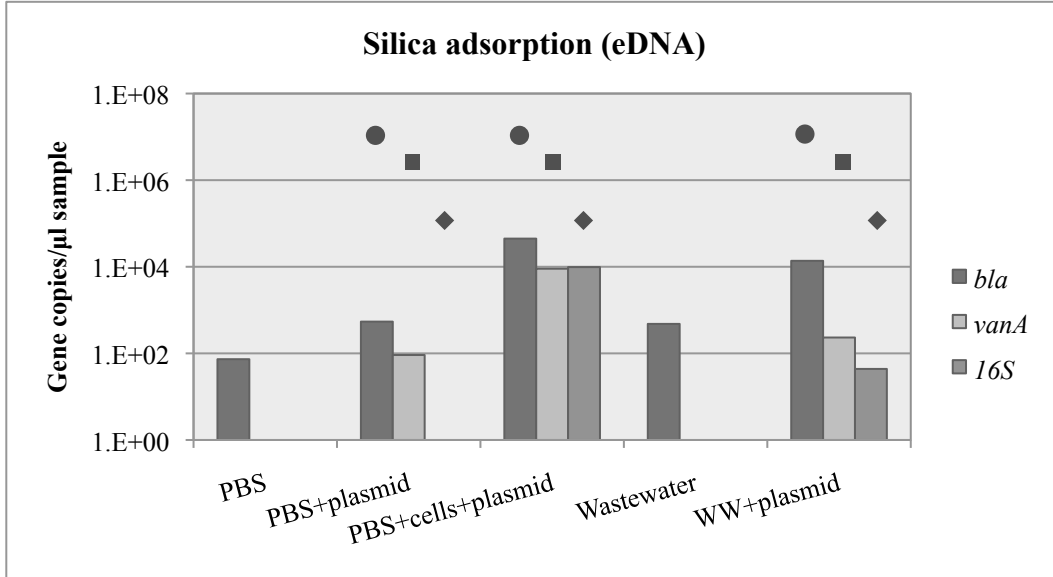


Figure 2.7. qPCR quantification of eDNA isolated by silica sorption. eDNA was spiked into corresponding treatments in the form of a plasmid carrying the *bla*_{TEM} and *vanA* ARGs. Circles, squares, and diamonds indicate theoretical 100% yield of *bla*_{TEM}, *vanA*, and 16S rRNA gene concentrations in spiked samples, respectively. Numerical values provided in Appendix A, **Table A 3**.

Filtration of water through a 0.22 μm membrane is the general approach taken to isolate iDNA from a water sample. For this experiment, a 0.22 μm membrane was used to filter 10 ml of WWTP effluent or buffer. The membrane was then rinsed to reduce carryover of eDNA, and subjected to direct DNA extraction. Spiked eDNA was recovered by this method even from samples lacking colloidal material or cells, indicating the direct retention of some eDNA by microfiltration membranes. The extracellular *bla*_{TEM} and *vanA* gene concentrations were measured to be even higher than the concentrations measured in the extract obtained by silica sorption, a method expected to be more effective for the extraction of eDNA. *bla*_{TEM} and *vanA* gene concentrations were 4.0 × 10⁴ and 8.9 × 10³, 1.4 × 10⁵ and 3.4 × 10⁴, and 1.6 × 10⁴ and 1.1 × 10³ gene copies/μl for the PBS+plasmid, PBS+cells+plasmids, and WWTP effluent+plasmids samples, respectively. 16S rRNA genes were only detected in the PBS+cells+plasmids and WWTP effluent+plasmid samples, at 9.9 × 10⁵ and 2.1 × 10² gene copies/μl, respectively.

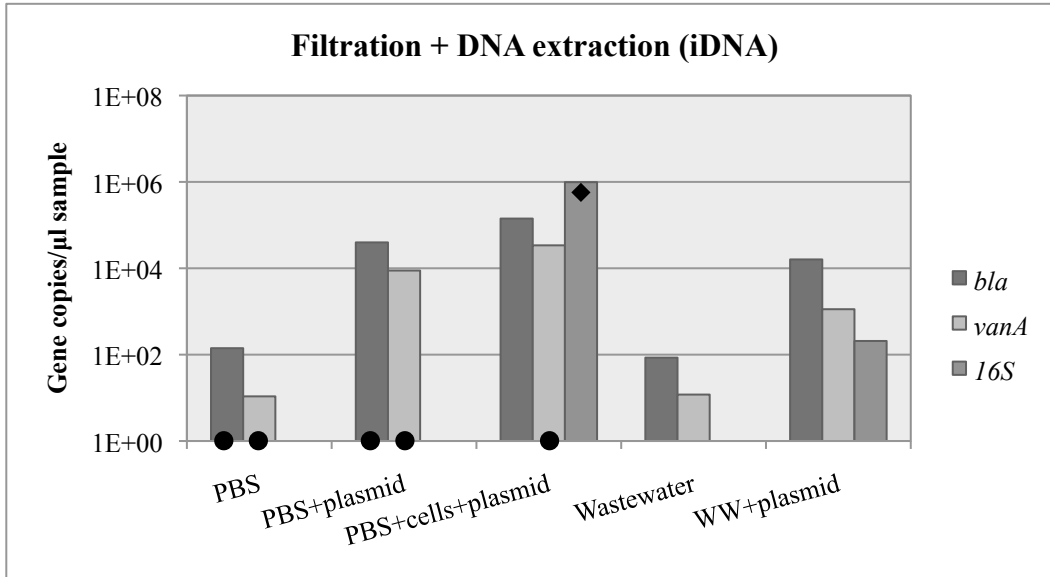


Figure 2.8. qPCR quantification of DNA isolated by filtration and washing of membrane to remove eDNA. eDNA was spiked into corresponding treatments in the form of a plasmid carrying the *bla*_{TEM} and *vanA* ARGs. Circles indicate theoretical 100% yield of *bla*_{TEM} and *vanA* genes. Diamond indicates theoretical 100% yield of intracellular 16S rRNA genes from spiked *E. coli* cells. Numerical values are provided in Appendix A, **Table A 3**.

2.3.4. COMPARISON OF TOTAL DNA CONCENTRATION METHODS

Freeze-drying and silica sorption+filtration DNA isolation methods are compared in this section. For almost all genes and sample types, freeze-drying was the isolation method that provided the greatest yields; usually 0.5 to 2 orders of magnitude higher concentrations than the silica sorption+filtration method. Again, the PBS+cells+plasmid samples appeared to contain a higher plasmid concentration (4.7×10^7 gene copies/ μ l) than was originally spiked (1×10^7 gene copies/ μ l). The gene quantification results comparing both tDNA isolation methods are shown in Figure 2.9, Figure 2.10, and Figure 2.11 for the *bla*_{TEM}, *vanA*, and 16S rRNA genes, respectively.

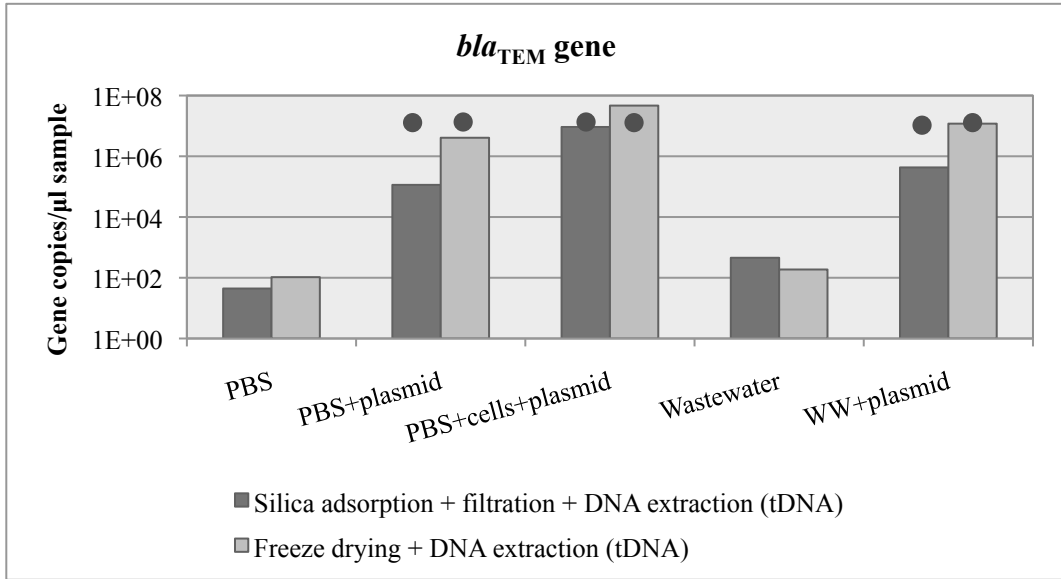


Figure 2.9. qPCR quantification of the *bla*_{TEM} gene extracted from a variety of aqueous samples after concentration by silica sorption+filtration versus freeze drying. Circles indicate theoretical 100% *bla*_{TEM} gene concentration in spiked samples. Numerical values are given in Appendix A, **Table A 3**.

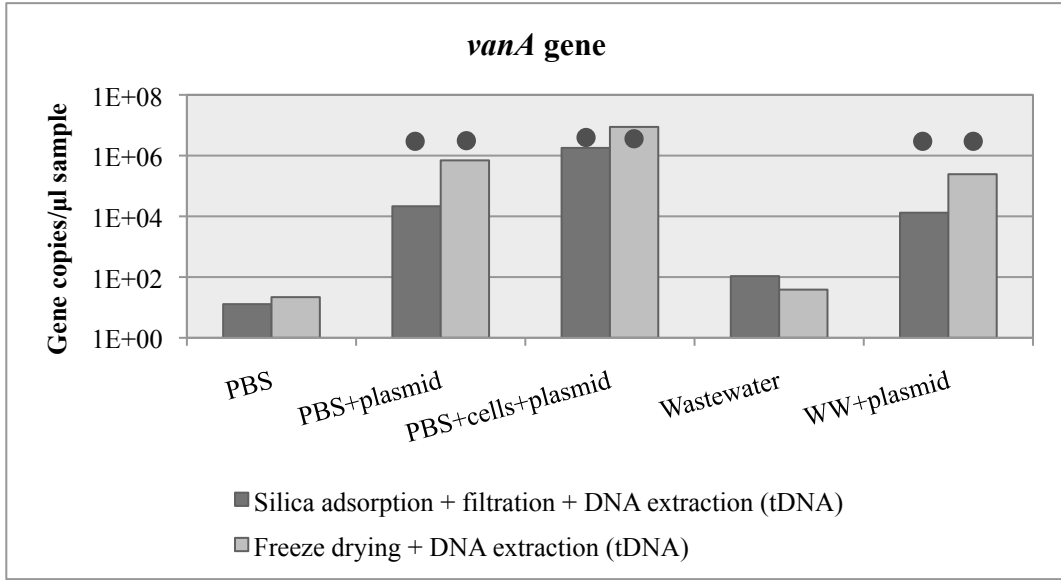


Figure 2.10. qPCR quantification of the *vanA* gene extracted from a variety of aqueous samples after concentration by silica sorption+filtration versus freeze drying. Circles indicate theoretical 100% *vanA* gene concentration. Numerical values are given in Appendix A, **Table A 3**.

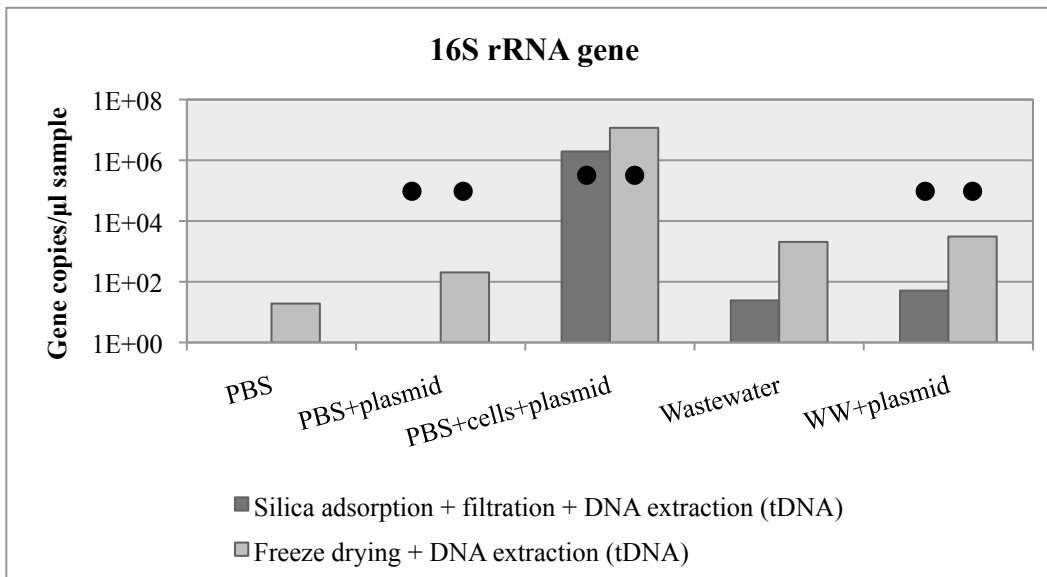


Figure 2.11. qPCR quantification of the 16S rRNA gene extracted from a variety of aqueous samples after concentration by silica sorption+filtration versus freeze drying. Circles indicate theoretical 16S rRNA gene concentration in spiked samples. Numerical values are given in Appendix A, **Table A 3**.

2.3.5. COMPARISON OF DNA ISOLATION METHODS: EXTRACTION, PURIFICATION, AND RESUSPENSION

DNA extraction and purification were compared for freeze-dry concentrated buffer and WWTP effluent samples as described in Section 2.2.5. In addition, resuspension of freeze-dried WWTP effluent was compared to extraction and purification for no-colloid buffer samples. The DNA resuspension method is not applicable to WWTP effluent samples due to the presence of colloids, humic acids, and other PCR inhibiting materials in such samples that can interfere with molecular analysis. Triplicate qPCR reactions were setup for each sample concentration measurement. An example of the results typically obtained is shown in Figure 2.12. Additional results showed similar relative extraction efficiencies; however, these are not shown because they were carried out after microfiltration and can include minimal DNA losses due to filtration.

In no-colloid buffer samples, DNA extraction was compared to DNA resuspension. DNA extraction was less effective in all cases, yielding only 0.4 – 4.2% of the DNA concentrations yielded by resuspension. DNA purification from buffer samples was also less effective than DNA resuspension, although more effective than extraction, yielding 30-42% of the

resuspension values. Interestingly, the opposite case was observed when isolating DNA from WWTP effluent samples, where DNA purification was less effective than DNA extraction, yielding 0.8 – 3.8% of the DNA yielded by DNA extraction.

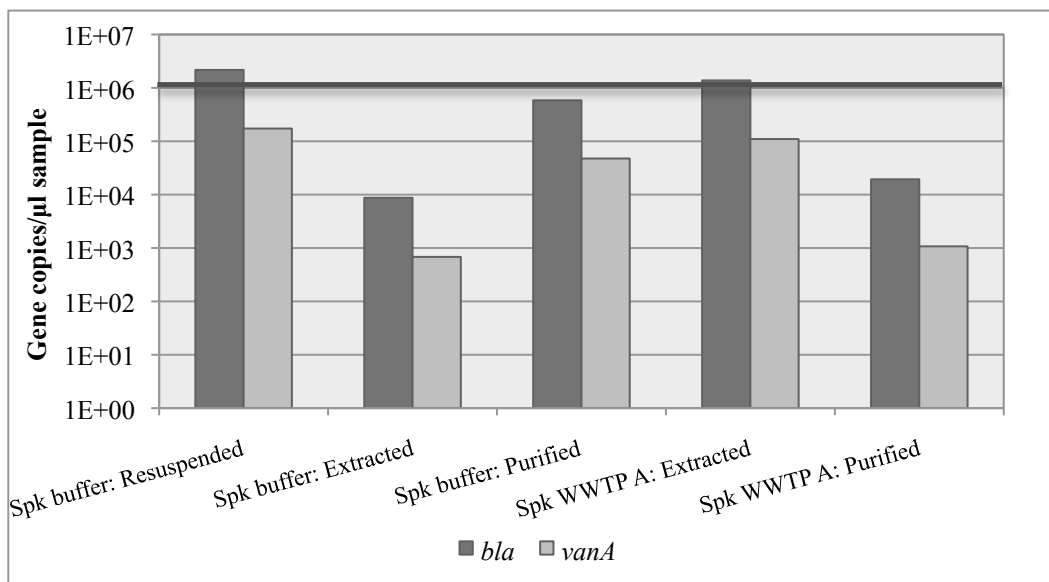


Figure 2.12. Relative concentrations obtained after DNA extraction, purification, and resuspension of freeze-dried DNA from WWTP effluent or buffer. Horizontal line indicates spiked *bla*_{TEM} gene concentration. Numerical values provided in Appendix A, **Table A 4**.

Optimal DNA isolation methods from buffer versus WWTP effluent were found to differ. DNA resuspension was found to be the most effective DNA isolation method from buffer samples, while DNA extraction was found to be the most effective DNA isolation method from WWTP effluents. DNA extraction from WWTP effluent yielded 64-66% of the DNA yielded by resuspension of a freeze-dried buffer sample of the same original concentration.

2.4. DISCUSSION

The purpose of this study was to identify the methodology that would be most applicable, effective, and efficient for the isolation of DNA from wastewater effluent and control buffer samples for application in subsequent experiments. Four different methods were tested for the

isolation of extracellular, intracellular, and total DNA from dilute water samples: Filtration through 0.22 μm pore-size membrane (iDNA), silica sorption (eDNA), freeze drying (tDNA), and silica sorption coupled with filtration through 0.22 μm pore-size membrane (tDNA). Two DNA isolation methods (DNA extraction and DNA purification) were also compared in terms of DNA yield, as well as simple DNA resuspension from buffer samples. Because wastewater contains nucleases and PCR inhibitors, however, DNA resuspension was not attempted as an isolation method for WWTP effluent samples. A degradation test was performed simultaneously in order to track the rate of DNA degradation and be able to account for potential biotic of DNA loss. A discussion of the results shown in section 2.3 of this chapter is provided in this section.

2.4.1. DNA DEGRADATION

As shown in the results section, little degradation of the spiked DNA was observed throughout the four hours allotted for DNA interactions with colloids. Although there seems to be a slight fluctuation among the different gene concentrations with time, the initial and final concentrations are comparable for all samples. For this reason, any significant DNA losses were assumed to be attributed to the DNA isolation method.

Based on the degradation results, it was also evident that more eDNA was recovered from the PBS+cells+plasmids samples than originally spiked. This phenomenon could be due to interactions between the DNA and *E. coli* cells, causing aggregations that appeared to amplify the plasmid DNA concentrations. It is worth noting that at the end of the four-hour period allotted for DNA-colloid interactions to occur, strings and clumps of aggregated cells were observed for the PBS+cells+plasmids sample. It is possible that the plasmid DNA interacted with these cell aggregations or even contributed to their formation.

2.4.2. EXTRACELLULAR DNA

A method involving the sorption of DNA onto silica particles in the presence of Cu^{2+} was attempted as a way to isolate and wash eDNA from a water sample. Silica sorption is generally used as a step during conventional DNA extraction; however, its use has never, to our knowledge, been attempted as a method to isolate eDNA from a water sample. Nguyen et al. (39,

41) reported that DNA binds strongly to silica in the presence of divalent and transition metal cations such as Ca^{2+} , Mg^{2+} , Cu^{2+} , Co^{2+} and Zn^{2+} . This was explained by the high binding affinity of the cations towards both the phosphate backbone of DNA and the silanol groups on the surface of silica particles (39, 41). In the presence of transition metal cations the diffusion coefficients are highest due to the specific binding of the cations to the phosphate backbone causing charge screening and a more compact conformation of the DNA molecules (39). Because Cu^{2+} was found to be the best sorption facilitator in the mentioned studies, this cation was chosen to prepare the silica suspension in this study.

Because EDTA is a stronger chelating agent than DNA molecules, addition of this chemical causes Cu^{2+} to preferentially bind to the EDTA, causing the DNA layer on the silica to become less viscous and thicker due to hydration, and allowing detachment of the DNA from the silica surface (39). For this reason, the first DNA wash solution contained EDTA, as well as the less binding Na^+ , and the DNA precipitating ethanol. Because EDTA is a PCR inhibitor by chelates the Mg^{2+} required by the DNA polymerase as a cofactor, the second DNA wash solution was used as a means to maintain the DNA precipitated, and washing away the EDTA- Cu^{2+} complexes simultaneously.

Wastewater contains live cells, cell debris such as proteins, enzymes (nucleases), lipids, polysaccharides and DNA, humic acids, and to a lesser extent inorganic material. It was hoped that DNA would preferentially bind to the silica particles in the presence of a transition metal cations due to its negatively charged nature; however, it is possible that other materials could have competitively bound to the silica particles, thus inhibiting the access of DNA to the silica surface. It is also possible that the DNA did interact with the silica and that it was extracted, but that its PCR amplification was inhibited by the presence of other materials which may have also sorbed to the silica.

In addition to a low yield of eDNA, a higher proportion of genomic DNA than initially spiked was recovered from the PBS+cells+plasmid sample. Several possibilities are discussed: (1) The method somehow disrupted the *E. coli* cells, likely during the centrifugation steps, thus releasing genomic DNA into the extraction product; (2) there was a higher binding affinity for linear genomic DNA than for circular plasmid DNA to the silica matrix, and thus the genomic DNA was preferentially bound and isolated over the plasmid DNA; and (3) a combination of

these two phenomena. In any case, the silica sorption method in its initial step was not effective in either reliably recovering eDNA or in excluding iDNA from the extracted DNA pool. For this reason, this method was not selected for further application in this study, though future improvements are possible. One possible approach may be to complement a freeze-drying procedure for the concentration of tDNA with the application of enzymatic and chelating agents such as the ones discussed by Wu and Xi (66) for the release and isolation of eDNA from a complex EPS- and colloid-containing matrix.

2.4.3. INTRACELLULAR DNA

Filtration is conventionally done to extract iDNA from water samples; however, it was found that this method does not truly distinguish extracellular from intracellular DNA. Retention of eDNA was observed in this study even in cases where there were no colloids or cellular material available for DNA interaction (See Figure 2.8). This suggests that DNA can directly interact with membranes even when they are designed to have low binding affinity. The fact that MF membranes can retain eDNA, either free or sorbed to colloids, is an important finding that has implications for the interpretation of environmental data obtained by this method. It has been generally assumed that membranes retain only intact cells, whereas this study demonstrates that this is not the case. Because eDNA can remain stable and protected when in the sorbed form (15, 47, 50), DNA analyses performed using this method can provide misleading data regarding the bacterial composition of the water environment being tested.

An additional experiment was done to test whether DNase treatment could be used as a way to degrade eDNA with the purpose of isolating the intracellular fraction in the absence of any eDNA contamination. However, this method was abandoned for several reasons: (1) The amount of DNase that would be needed for a large dilute water sample would be too high to make this method feasible for widespread use. (2) The conditions needed for DNase treatment and subsequent enzyme inactivation, including high temperature (65 °C) and chemical addition (20 mM ethylene glycol tetraacetic acid (EGTA)), could cause cell damage and the subsequent loss of some of the iDNA fraction, as well as serve as inhibitors to downstream PCR. (3) Sorption of eDNA to colloids has been shown to protect DNA against enzymatic degradation (15, 50); thus, complete degradation of eDNA is unlikely. Although DNase treatment can be and

has been successfully applied for the degradation of eDNA of pure cultures or biofilm samples, it is not a feasible method in the case of water samples containing colloids and other DNA protective materials.

2.4.4. COMPARISON OF TOTAL DNA CONCENTRATION METHODS

Two methods were attempted and compared for concentrating the tDNA pool from a WWTP effluent sample: Freeze-drying and silica sorption coupled with filtration through a 0.22 µm pore size membrane. Freeze-drying has been previously used for the concentration of DNA in dilute water samples (48). The DNA yields obtained by DNA extraction of freeze-dried material were consistently higher than those obtained from the silica sorption+filtration method.

DNA extraction of the buffer+cells+plasmids sample after freeze-dry concentration yielded a higher concentration of DNA than originally spiked. This phenomenon was previously discussed as considered to be product of DNA-cell interactions occurring during the formation of bacterial aggregates. Bacterial aggregates were not visible during the initial cell spike; instead, the PBS medium became noticeably turbid upon addition of the cells. After the 4-hr stabilization time, however, the PBS medium became clear, and clumps and strings of cells were observed instead. It is hypothesized that the spiked eDNA interacted with the cells and it is possible that it may have also played a role in the formation of cell aggregates. This would not be surprising, as DNA has been shown to play a role as a structural scaffold in biofilm formation (19, 61).

Freeze-dry concentration was the most successful of the attempted methods in that it was relatively straightforward, and yielded the highest DNA concentrations. Thus, it could be said to be generally gentle on DNA unlike other methods requiring additional handling such as sorption or centrifugation. Although freeze-drying was the most successful method, the fact that it requires the use of a freeze-dryer makes it both expensive and time consuming. The process of freeze-drying itself is not a very labor-intensive procedure; however, it requires a relatively long waiting period (1 day/L water at optimal conditions), and the use of appropriate glassware that can handle extreme temperatures.

The method for concentrating tDNA by silica sorption+filtration did yield higher concentrations of eDNA than filtration alone, indicating that some eDNA does sorbed to the

silica particles. For this reason, this method may still have potential to be improved and may have benefits for the concentration and extraction of tDNA from dilute water samples in the absence of a freeze dryer, and in the need of a faster method. The lower DNA yield obtained from the sorption+filtration method in comparison to the freeze-drying technique could be due to DNA damage during sample handling, incomplete DNA sorption to the silica, or incomplete DNA desorption and recovery from the silica.

2.4.5. COMPARISON OF DNA ISOLATION METHODS: EXTRACTION, PURIFICATION, AND RESUSPENSION

DNA extraction, purification, and resuspension methods were tested and their yields compared as described in Table 2.3. The yields obtained from the application of the different methods varied depending on the sample type. For example, DNA extraction yielded the highest DNA quantities for WWTP effluent samples, but the lowest quantities from spiked buffer samples. Similarly, DNA purification yielded high DNA quantities from buffer samples, but very low quantities from WWTP effluent samples. DNA resuspension yielded the highest values among the methods tested for DNA isolation from buffer samples. This was expected as resuspension involves less manipulation steps during which DNA degradation, damage, or contamination could occur.

Table 2.3. Relative DNA yield obtained from each DNA isolation method.

DNA isolation method	Filtered WWTP effluent	Spiked buffer
DNA extraction	+++ (1.25)	+ (0.01)
DNA purification	+ (0.03)	++ (0.42)
DNA resuspension	N/A	+++ (1.36)

+ Symbol represents the total-DNA yield obtained from applying each method: Highest yield (+++), intermediate yield (++), and lowest yield (+). A tentative C/C_0 *bla*_{TEM} gene concentration is shown in parenthesis for averaged measurements; however, some of the measurements were taken after filtration through 0.45 and 0.1 μ m pore-size membranes and can include minimal DNA losses due to filtration. N/A: Not applicable.

As noted previously, DNA purification differs from DNA extraction in that the earlier method is not meant to disrupt cellular material in order to extract iDNA. Purification is only designed to remove relatively small concentrations of potential contaminants that could inhibit

downstream analyses requiring PCR. DNA extraction, on the other hand, not only disrupts cells to isolate their DNA, but also purifies the DNA from cellular debris and other potential contaminants (e.g. soil particles, proteins, humic acids, etc.). When dealing with environmental samples, it is sometimes necessary to further purify the DNA after extraction in order to prevent interferences during analyses.

Possible reasons explaining the differences observed in the DNA purification yields between the different sample types are:

- Incomplete DNA recovery from WWTP effluent samples due to exclusion of colloid-sorbed DNA. One of the initial steps in DNA purification involves the addition of reagents that precipitate non-DNA materials. These potential inhibitors are then separated from the suspended DNA by centrifugation. It is likely that during this centrifugation step DNA-colloid complexes remain associated and become excluded along with other contaminants.
- Incomplete elimination of PCR inhibitors, such as humic acids, if these were present in higher concentrations in the WWTP effluent than could be handled by the purification kit. This, however, would only affect the measurement of the DNA concentration, and would not necessarily mean that the DNA is not present in the purified sample. It is usually sufficient to dilute PCR inhibitors prior to analysis, but this would not be possible in a case where DNA concentrations are inherently low, and inhibitor removal would be necessary.

Differences in the DNA extraction yields from the different sample types could be due to one or more of the following reasons:

- Protection of eDNA in the presence of colloidal material (yielding more DNA for WWTP effluent samples)
- The corresponding damage of eDNA in the absence of colloidal material (yielding less DNA for buffer samples)
- Stronger sorption of buffer DNA onto the binding matrix in the absence of colloidal material (yielding less DNA for buffer samples).

Ideally, DNA analysis results should be directly comparable in terms of gene concentrations; however, the results obtained from this experiment indicate that no single DNA isolation method is optimal for all sample types. For this reason the results obtained from subsequent experiments should not be directly compared in terms of concentrations, but relatively compared in terms of DNA fraction in filtrate. Furthermore, in order to obtain the highest possible yields from such dilute samples, DNA extraction and resuspension will be the methods used when isolating DNA from WWTP effluent and buffer samples, respectively.

2.5. CONCLUSIONS

The following conclusions were drawn from the experiments comparing various eDNA, iDNA, and tDNA isolation techniques on WWTP effluent and control buffer samples:

- Negligible DNA degradation was observed over the duration of the experiment. DNA degradation tests will continue to be incorporated in all experiments in the case that WWTP effluent variability contributes to biodegradation in some cases.
- Discrete extraction of intracellular and extracellular DNA from complex and dilute samples was only partially successful in this study. Additional refinement is recommended in future studies.
- DNA concentration by freeze-drying provided the greatest yield among the methods tested and will be the total-DNA isolation pretreatment method applied in subsequent experiments.
- DNA extraction and resuspension were found to provide the greatest yield when isolating DNA from WWTP effluent and buffer samples, respectively. Therefore, DNA extraction will be applied to WWTP effluent samples and resuspension will be applied to buffer samples in subsequent experiments.
 - Because recoveries differed among the different eDNA and tDNA extraction methods, absolute comparisons will be avoided across experimental conditions. Instead, comparisons will focus on relative removal fractions.

3. MATERIALS AND METHODS

Four experiments were setup in which a cascade of MF and UF steps was used to compare the removal of ARGs from colloid-containing versus colloid-lacking aqueous samples. Effluent from three representative WWTPs was applied as colloid-containing material in order to test the occurrence of DNA-colloid interactions in a complex environmental matrix, as well as the reproducibility of the results. In addition, the experiment was repeated for one of the WWTPs in order to explore how robust any effects of wastewater colloids were with time in a given WWTP. Tris buffer (pH 8) was used as colloid-free material in order to better preserve the DNA throughout the experiment, as low salt concentrations could cause DNA degradation, while high salt concentrations could promote the sorption of the genetic material to the glass containers used to hold the samples. The key characteristics of the WWTPs selected for this study are shown on Table 3.1.

Table 3.1. General characteristics and sampling dates associated with each WWTP.

WWTP effluent source	Capacity	Influent composition	Key processes	Collection date
WWTP A	6 MGD	Residential, industrial	Conventional treatment, UV disinfection	3/25/11 (1st trial) 4/21/11 (2nd trial)
WWTP B	9 MGD	Residential, hospital, industrial	Conventional treatment, chlorination/dechlorination	3/1/11
WWTP C	6 MGD	Residential, hospital, high Na ₂ SO ₄ industrial	Conventional treatment, nitrification, chlorination/dechlorination	4/7/11

Conventional treatment: Primary clarification, aeration, secondary clarification, and disinfection.

3.1. PLASMID PREPARATION

The amplification and extraction of plasmids was done as described in the methods section of chapter 2. However, the larger capacity and higher yield Plasmid Mega kit (Qiagen, Valencia, CA) was used instead of the Mini kit in order to obtain larger volumes of concentrated plasmids. The β -lactam (*bla*_{TEM}) resistance gene is an ubiquitous ARG, and because it was already built into the plasmid, it represented a convenient way to quantify the plasmid concentration in the samples.

The vancomycin resistance *vanA* gene was chosen as the gene insert in the preparation of the plasmids because of its relevance in the problem of antibiotic resistance, and as a way to support plasmid quantifications. Vancomycin is currently used as a last resort life-saving drug, and recent emergence of vancomycin-resistant bacteria, such as vancomycin-resistant *Enterococci* (VRE) (22), supports the importance of this project and the urgent need for solutions.

3.2. WWTP EFFLUENT COLLECTION AND INITIAL FILTRATION

Final WWTP effluent was collected from each of the wastewater treatment facilities at most 6 hours before the experiment was carried out. Effluent collection occurred during cold working weekdays between Tuesday and Friday, avoiding rain or snow events taking place during the past 24 hours. The effluent was immediately transported to the lab where it was kept at 4 °C prior to use. As pretreatment to eliminate particles outside the colloid size range, the effluent was vacuum-filtered through a 1.2 µm pore-size mixed cellulose ester membrane (Millipore, Billerica, MA), using a sterilized Nalgene® polysulfone filter holder (Thermo Fisher Scientific, Rochester, NY).

3.3. EXPERIMENTAL SETUP

The experiment was set up and carried out as illustrated in Figure 3.1. Four 1000-ml flasks were filled with 600 ml of (1) 10 mM Tris buffer pH 8 (blank), (2) 10 mM Tris pH 8 spiked with *vanA* gene-containing plasmids to a final concentration of 1×10^7 or 1×10^8 plasmid copies/µl based on *bla*_{TEM} gene concentrations (no-colloid control), (3) filtered WWTP effluent, and (4) filtered WWTP effluent spiked with *vanA* gene-containing plasmids to a final concentration of 1×10^7 or 1×10^8 plasmid copies/µl based on *bla*_{TEM} gene concentrations. The flasks were lightly agitated for 4 hours using a Burrell wrist action shaker (Burrell Scientific, Pittsburg, PA) to allow DNA interactions with wastewater colloids. 10-ml subsamples were taken from each of the four flasks throughout the duration of the experiment to test for DNA degradation.

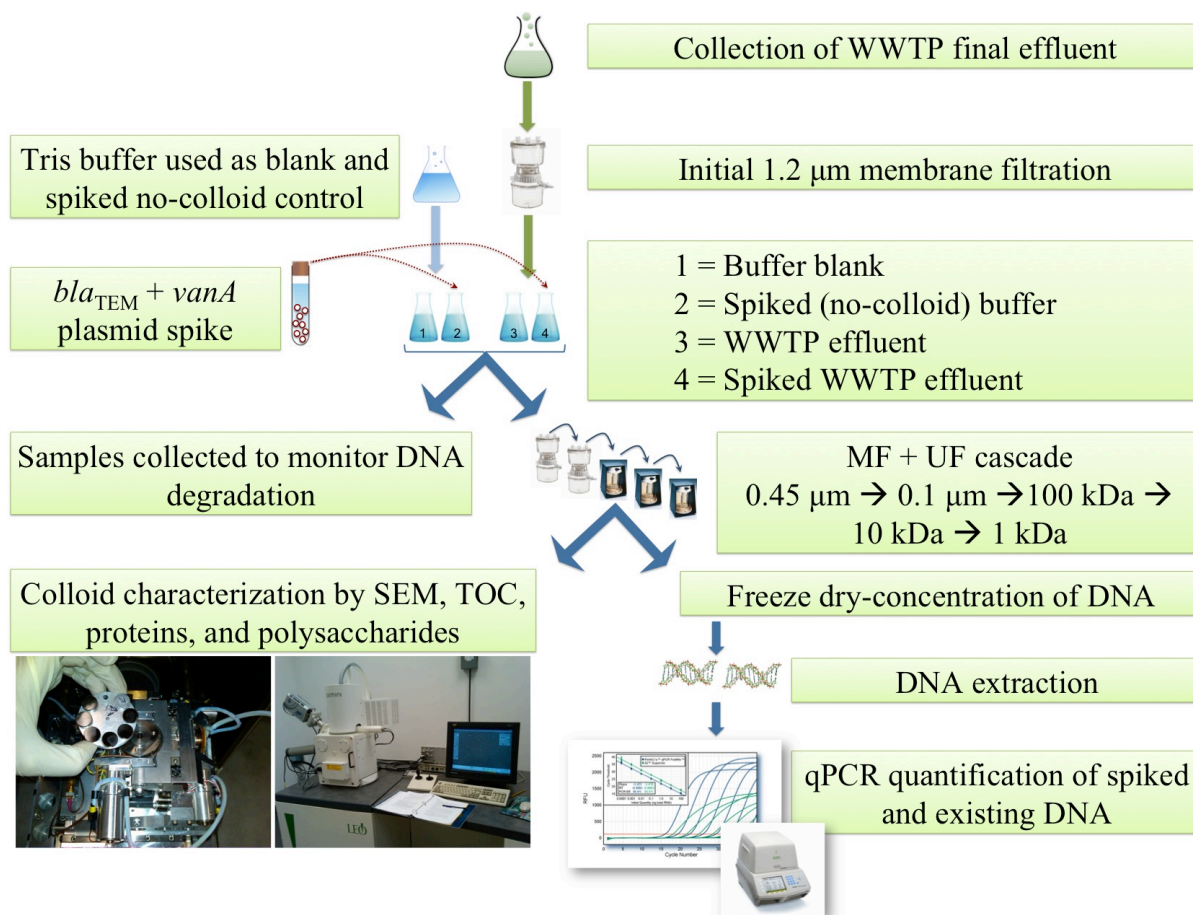


Figure 3.1. Diagram of experimental setup and method sequence.

3.4. MICROFILTRATION AND ULTRAFILTRATION

Sequential filtration steps were carried out for each of the flask contents as follows: First, 500 ml of the flask contents were filtered through the membrane with the largest pore size (0.45 μm -pore size membrane). Next, ten-milliliter samples were pipetted into previously baked 30 ml Qorpak clear graduated glass bottles (Qorpak, Bridgeville, PA). Other samples were also collected for colloid characterization and SEM imaging. The remaining water/buffer was then filtered through the following membrane (0.1 μm -pore size membrane). The process was repeated for each of the filtrates and applying the membranes in decreasing pore size: 0.45 μm \rightarrow 0.1 μm \rightarrow 100 kDa \rightarrow 10 kDa \rightarrow 1 kDa. The flask contents were processed in the following order: (1) Buffer blank, (2) unspiked wastewater, (3) spiked buffer, (4) spiked wastewater. The later of the sample conditions was analyzed after the four-hour period allotted for DNA-colloid interactions to occur.

MF was carried out using a 0.45 µm- and a 0.1 µm-pore size, durapore hydrophilic polyvinylidene fluoride (PVDF) membrane (Millipore, Billerica, MA), and a Nalgene® polysulfone filter holder (Thermo Fisher Scientific, Rochester, NY). MF filtrates were kept in the bottom part of the filter holder container. In addition, the efficiency of an inorganic alumina 0.1 µm pore size membrane, Anodisc 47 (Whatman GmbH, Germany), was compared to that of the Durapore membrane of the same pore size. Ultrafiltration was done using 100 kDa-, 10 kDa-, and 1 kDa-MWCO Ultracel regenerated cellulose membranes (Millipore, Billerica, MA); and a 8200 Ultrafiltration Stirred Cell (Millipore, Billerica, MA). UF filtrates flowed into baked glass flasks kept covered by baked aluminum foil. Because the UF membranes were reusable, they were cleansed between usages using DNA Away (Molecular Bio Products, San Diego, CA) followed by a thorough rinsing step that included filtering water through the membrane for at least 10 min. A list of the membrane types and pore sizes is provided in Table 3.2.

Table 3.2. General characteristics of membranes used in this study.

Membrane pore size	Membrane material	Manufacturer
1.2 µm	Mixed cellulose esters	Millipore
0.45 µm	PVDF	Millipore
0.1 µm	PVDF	Millipore
0.1 µm	Alumina	Whatman
100 kDa	Regenerated cellulose	Millipore
10 kDa	Regenerated cellulose	Millipore
1 kDa	Regenerated cellulose	Millipore

3.5. DNA CONCENTRATION, EXTRACTION, AND QUANTIFICATION

After collection, the 10-ml samples were immediately frozen and stored at -80 °C prior to freeze-drying, which was done using the FreeZone Plus 2.5 Liter Benchtop Freeze Dry System (Labconco, Kansas City, Missouri). Extraction of DNA from the freeze-dry-concentrated samples was carried out as described in Chapter 2 using the FastDNA Spin Kit for Soil, Catalog # 6560-200 (MP Biomedicals, Solon, OH). Briefly, the Sodium Phosphate and MT buffers were added directly to the concentrated sample, mixed, and transferred to the lysing matrix tube where the remaining of the DNA extraction steps were carried out as recommended in the kit's manual. qPCR DNA quantification was carried out on triplicates of 1:10 diluted samples in a CFX96

Touch™ Real-Time PCR Detection System (Bio-Rad, Hercules, CA), as described in Chapter 2. The background gene concentrations detected on each analytical blank were subtracted from the measured sample concentration. Each individual measurement was then multiplied by the dilution factor (10), multiplied by the extraction volume, and divided by the volume of each sample in microliters ($1 \times 10^4 \mu\text{l}$) to obtain the final concentration in gene copies/ μl of each sample. The three measurements per sample were then averaged and reported for each sample.

3.6. COLLOID CHARACTERIZATION

The colloid characterization was done both chemically by measuring organic carbon, proteins, and polysaccharides; and microscopically using scanning electron microscopy.

3.6.1. NON-PURGEABLE ORGANIC CARBON, PROTEINS, AND POLYSACCHARIDES

Non-purgeable organic carbon concentrations were measured using the Shimadzu TOC-VCSN analyzer (Shimadzu Scientific Instruments, Columbia, MD), using potassium hydrogen phthalate (KHP) as the standard. Polysaccharide concentrations were measured by the phenol-sulfuric acid method described by Dubois (20) using dextrose as standard.

Protein concentrations were measured by the Lowry method (32) using bovine serum albumin (BSA) as a standard. Briefly, Reagents 1-3 were used to prepare Reagents 4-5 as specified below. Next, 1.4 ml of Reagent 4 were added to 1 ml of sample and mixed thoroughly. 0.2 ml of Reagent 5 were mixed in. The mix was incubated for 45 min at room temperature and the absorbance read at 750 nm. The reagent recipes are outlined below:

- *Reagent 1* = 143 mM NaOH, 270 mM Na_2CO_3
- *Reagent 2* = 57 mM CuSO_4
- *Reagent 3* = 124 mM Na-tartrate
- *Reagent 4* = Reagent 1:Reagent 2:Reagent 3 = 100:1:1 (made daily)
- *Reagent 5* = Folin Ciocalteus reagent diluted 5:6 with distilled water

3.6.2. SCANNING ELECTRON MICROSCOPY

Scanning electron microscopy was done using a Leo 1550 Field Emission Scanning Electron Microscope (SEM) (Carl Zeiss Nano Technology systems, International). For preparation, ~25 μl of each sample was spread thinly on a SEM stud, frozen at -80°C , and freeze-dried using the FreeZone Plus 2.5 Liter Benchtop Freeze Dry System (Labconco, Kansas City, Missouri). Before imaging, the freeze-dried material was coated with gold and palladium using a Cressington 208HR high-resolution sputter-coater.

3.7. STATISTICAL ANALYSES

Statistical analyses were performed using the R statistics software. Statistical differences between the membrane removal of ARGs in the presence versus the absence of colloids were calculated using a two-way analysis of variance (ANOVA) test. The test was applied to the log of the filtrate gene fraction from spiked WWTP effluent or spiked buffer as the dependent variable. The presence/absence of colloids and the membrane pore sizes were the independent terms in the tests. The tests were repeated for each of the genes monitored separately. A significance value $\alpha = 0.05$ (i.e. $p < 0.05$) was considered significant. A correlation test between the filtrate fraction of each of the colloidal components and the logarithm of the filtrate gene fraction was also done in R, applying a one-sided Pearson correlation test.

4. EFFECT OF WASTEWATER COLLOIDS ON MEMBRANE REMOVAL OF MICROCONSTITUENT ARGs: RESULTS

4.1. DNA DEGRADATION

The DNA degradation test results for all WWTPs are described in Sections 4.1.1 – 4.1.4 (Numerical values provided in Appendix A, Table A 5 - Table A 8). Negligible degradation was observed in the spiked buffer or WWTP effluent samples, suggesting that any observed DNA removal after subsequent filtration should be attributable to retention by the membranes either by size exclusion of the DNA itself, exclusion of DNA-colloid complexes, or interaction with the membrane material. The gene concentrations measured in the unspiked buffer blank were used to determine the absence of contamination during the experiment. Gene concentrations in WWTP effluent samples were followed in order to monitor existing ARG and genomic DNA concentrations; and, if possible, to characterize the behavior of native sorbed DNA. All gene concentrations are reported in Appendix A, Table A 5 - Table A 8.

4.1.1. WWTP A (1ST TRIAL)

DNA degradation results for *bla*_{TEM}, *vanA*, and 16S rRNA genes are shown in Figure 4.1 - Figure 4.3. Negligible degradation was observed in the spiked samples. A higher concentration of native DNA was detected in this WWTP effluent than in all WWTP effluents subsequently used. The 1.2 µm pore size membrane WWTP effluent filtrates contained an average of 2.2×10^3 , 3.1×10^2 , and 1.2×10^4 *bla*_{TEM}, *vanA*, and 16S rRNA gene copies/µl, respectively. The average concentrations detected in the experimental blank were 3.4×10^2 , 0, and 4.6 *bla*_{TEM}, *vanA*, and 16S rRNA gene copies/µl, respectively.

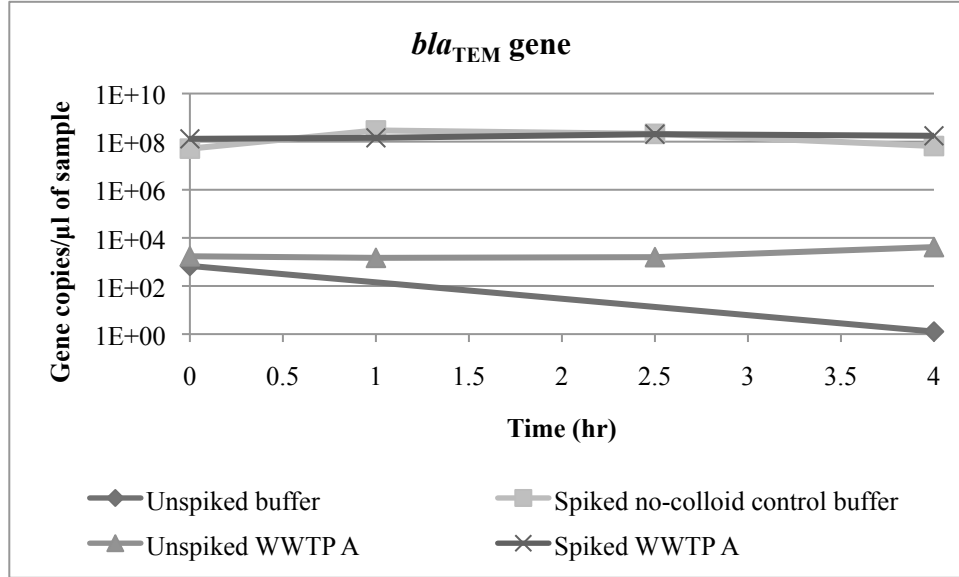


Figure 4.1. DNA degradation test results obtained for WWTP A (1st trial) *bla*_{TEM} genes. *bla*_{TEM} genes in samples collected for each time step during 4 hours were quantified in qPCR triplicate reactions.

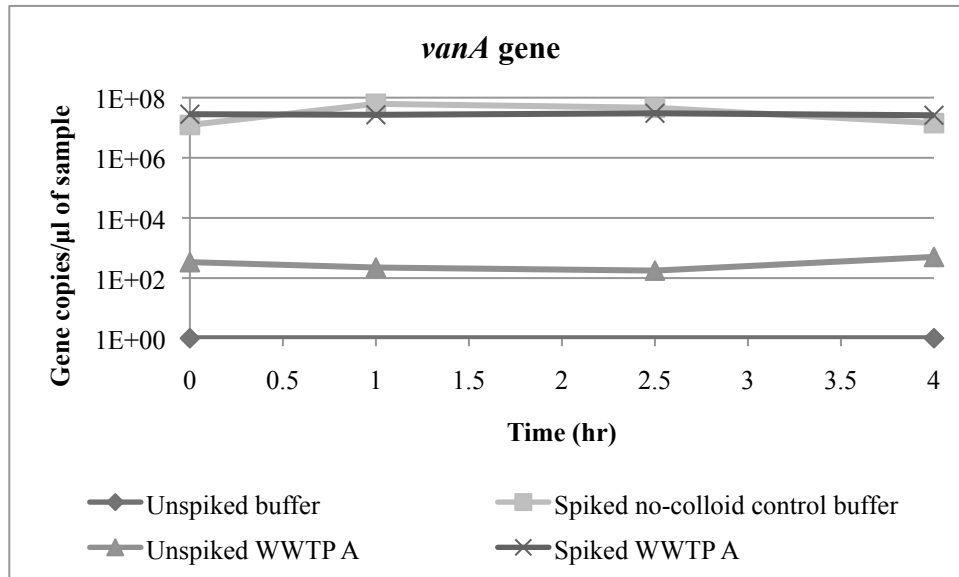


Figure 4.2. DNA degradation test results obtained for WWTP A (1st trial) *vanA* genes. *vanA* genes in samples collected for each time step during 4 hours were quantified in qPCR triplicate reactions.

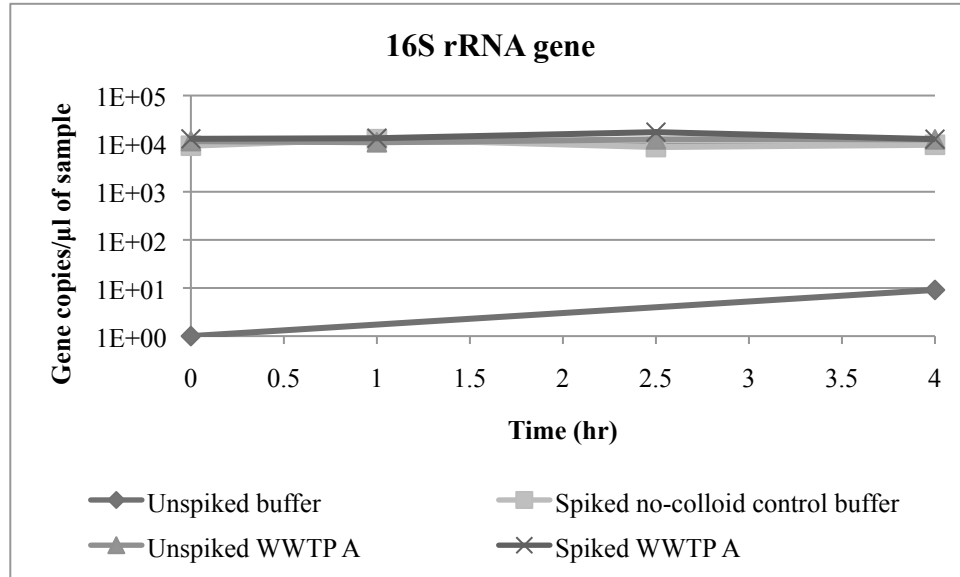


Figure 4.3. DNA degradation test results obtained for WWTP A (1st trial) 16S rRNA genes. 16S rRNA genes in samples collected for each time step during 4 hours were quantified in qPCR triplicate reactions.

4.1.2. WWTP A (2ND TRIAL)

DNA degradation results for *bla*_{TEM}, *vanA*, and 16S rRNA genes are shown in Figure 4.4 - Figure 4.6. Negligible degradation was observed in the spiked samples.

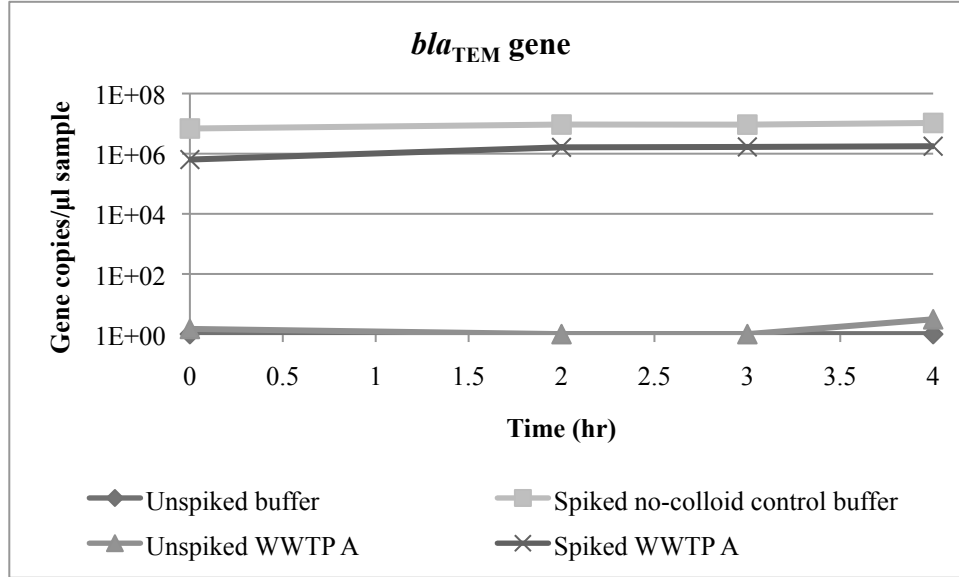


Figure 4.4. DNA degradation test results obtained for WWTP A (2nd trial) *bla*_{TEM} genes. *bla*_{TEM} genes in samples collected for each time step during 4 hours were quantified in qPCR triplicate reactions.

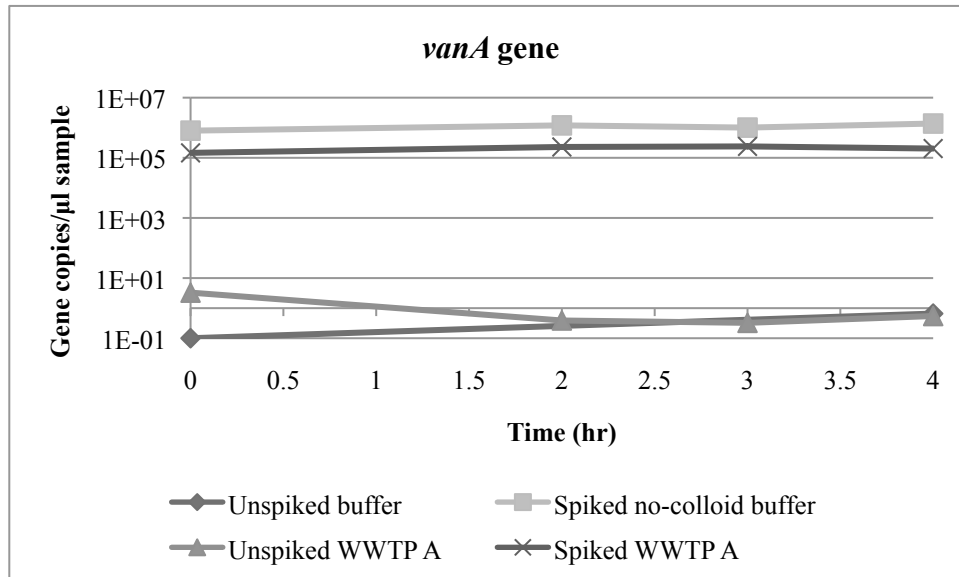


Figure 4.5. DNA degradation test results obtained for WWTP A (2nd trial) *vanA* genes. *vanA* genes in samples collected for each time step during 4 hours were quantified in qPCR triplicate reactions.

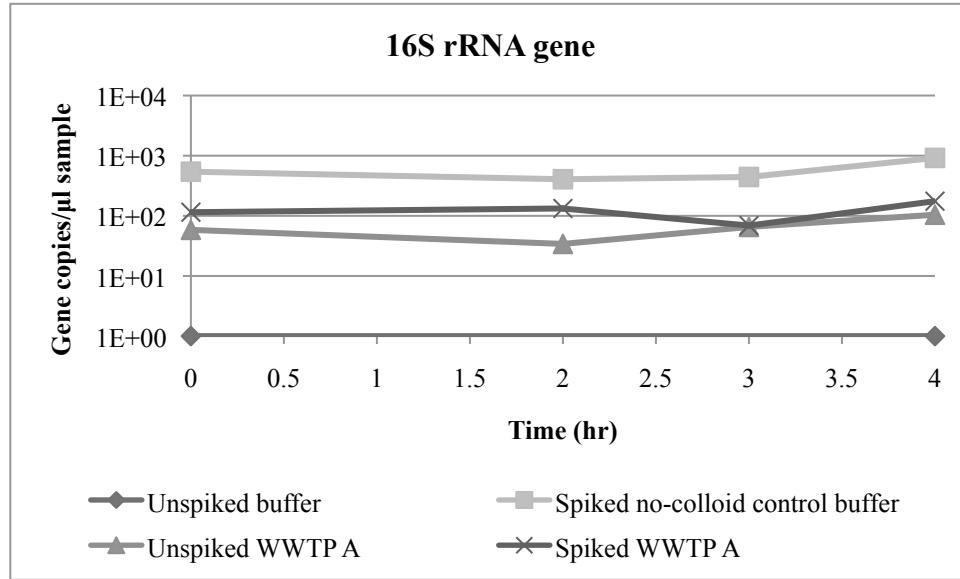


Figure 4.6. DNA degradation test results obtained for WWTP A (2nd trial) 16S rRNA genes. 16S rRNA genes in samples collected for each time step during 4 hours were quantified in qPCR triplicate reactions.

4.1.3. WWTP B

DNA degradation results for *bla*_{TEM}, *vanA*, and 16S rRNA genes are shown in Figure 4.7 - Figure 4.9. Negligible degradation was observed in the spiked samples. Unspiked WWTP B effluent contained average *bla*_{TEM}, *vanA*, and 16S rRNA gene concentrations of 3.1×10^1 , 7.4, and 4.1×10^2 gene copies/ μl .

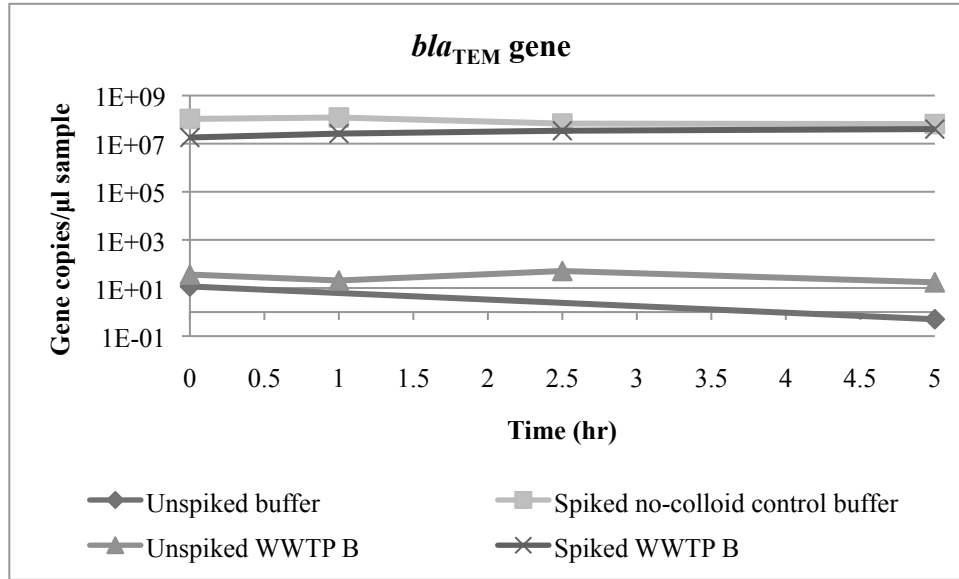


Figure 4.7. DNA degradation test results obtained for WWTP B *bla*_{TEM} genes. *bla*_{TEM} genes in samples collected for each time step during 5 hours were quantified in qPCR triplicate reactions.

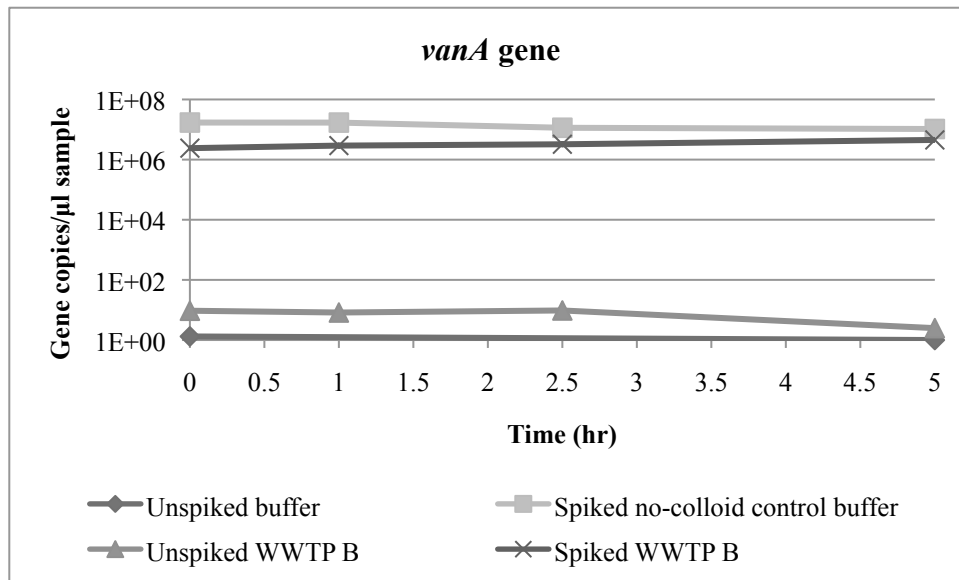


Figure 4.8. DNA degradation test results obtained for WWTP B *vanA* genes. *vanA* genes in samples collected for each time step during 5 hours were quantified in qPCR triplicate reactions.

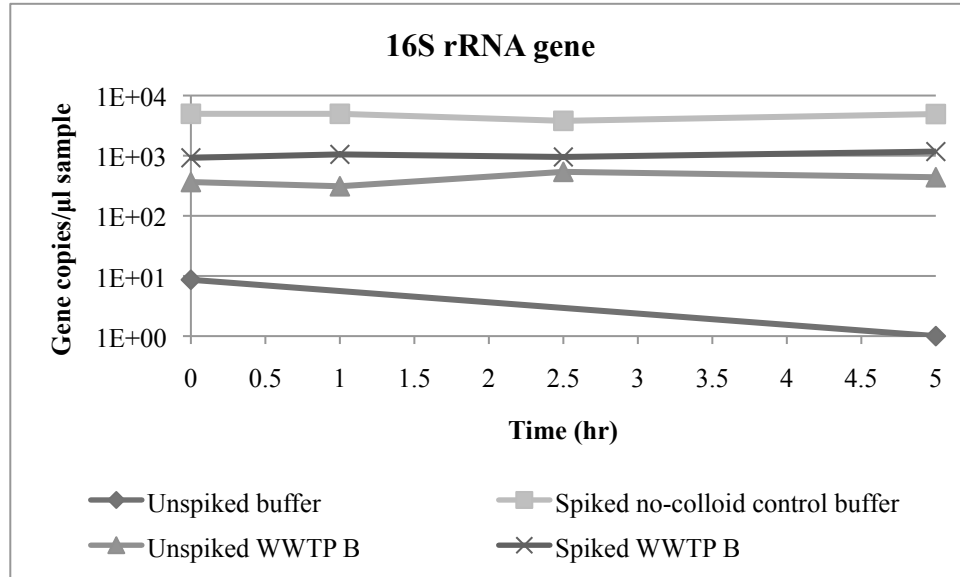


Figure 4.9. DNA degradation test results obtained for WWTP B 16S rRNA genes. 16S rRNA genes in samples collected for each time step during 5 hours were quantified in qPCR triplicate reactions.

4.1.4. WWTP C

DNA degradation results for *bla*_{TEM}, *vanA*, and 16S rRNA genes are shown in Figure 4.10 - Figure 4.12. Negligible degradation was observed in the spiked samples.

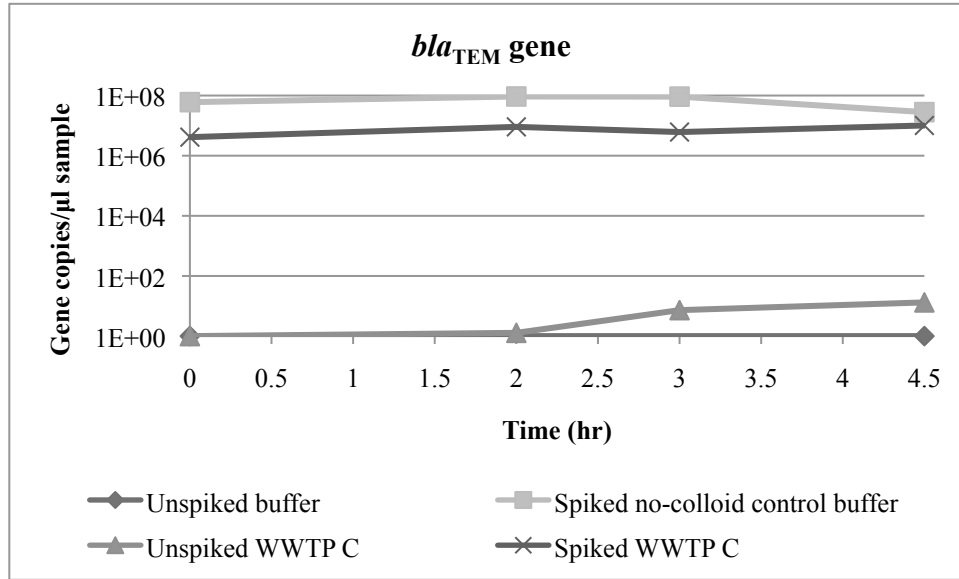


Figure 4.10. DNA degradation test results obtained for WWTP C *bla*_{TEM} genes. *bla*_{TEM} genes in samples collected for each time step during 4.5 hours were quantified in qPCR triplicate reactions.

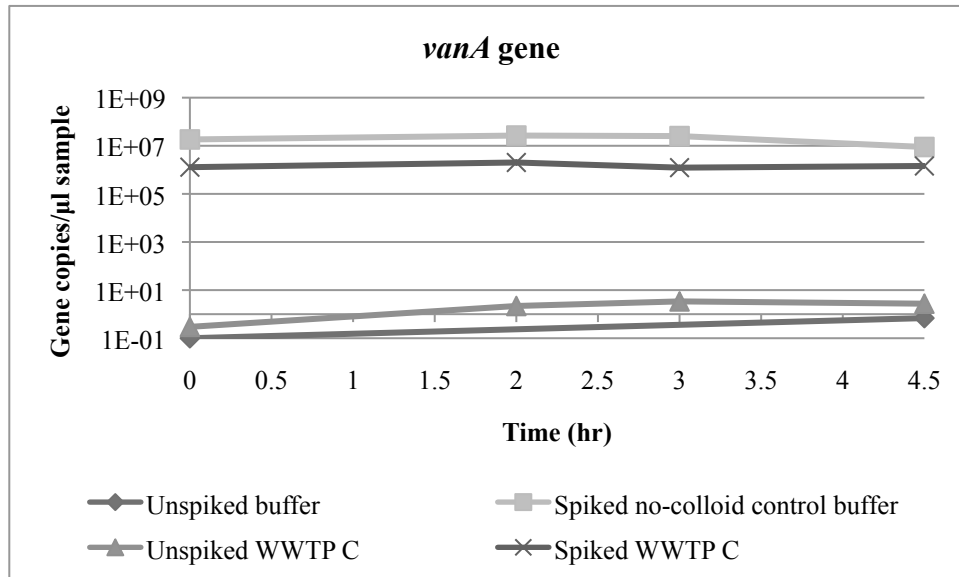


Figure 4.11. DNA degradation test results obtained for WWTP C *vanA* genes. *vanA* genes in samples collected for each time step during 4.5 hours were quantified in qPCR triplicate reactions.

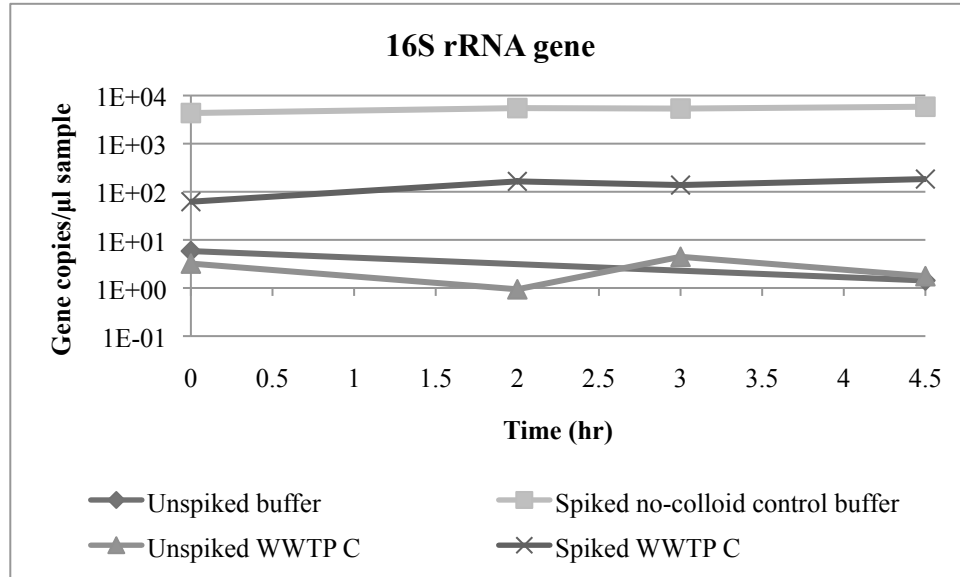


Figure 4.12. DNA degradation test results obtained for WWTP C 16S rRNA genes. 16S rRNA genes in samples collected for each time step during 4.5 hours were quantified in qPCR triplicate reactions.

4.2. POST-FILTRATION DNA QUANTIFICATION

Post-filtration qPCR DNA quantification yielded the *bla*_{TEM}, *vanA*, and 16S rRNA gene concentrations provided in Appendix A, Table A 10 - Table A 13. These values were used to calculate the filtrate fractions shown in Table A 9, and compared in Figure 4.15 - Figure 4.26. The filtrate fractions were calculated by dividing the filtrate concentration by the averaged concentration of the samples collected for the degradation test. Statistical analyses were done using the R statistics software. Based on the two-way ANOVA test, significantly higher spiked DNA removal was achieved in the presence of colloidal material than in its absence. The presence of colloidal material in the water was to have a significant effect in the removal of *bla*_{TEM} and *vanA* genes, with p values equal to 0.011 and 0.003, respectively. There was no significant difference in the removal of 16S rRNA genes ($p = 0.666$). Not surprisingly, the membrane pore size was confirmed to have a significant effect in the removal of all three genes in the presence and absence of colloidal material ($p < 0.01$).

Gene concentrations in the unspiked WWTP effluent samples are reported in Figure 4.13 - Figure 4.14 for WWTP A (1st trial) and WWTP B, respectively. Concentrations were below the LOQ for WWTP A (2nd trial) and WWTP C samples.

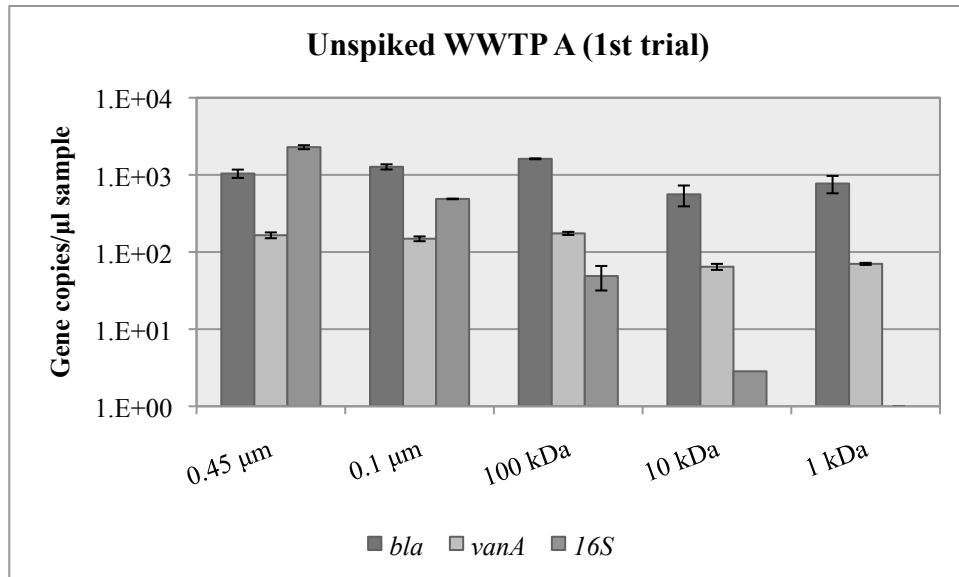


Figure 4.13. Gene concentrations in unspiked WWTP A (1st trial) filtrates. Samples were qPCR quantified in triplicate reactions. Error bars represent analytical error and are larger than measurement where absent.

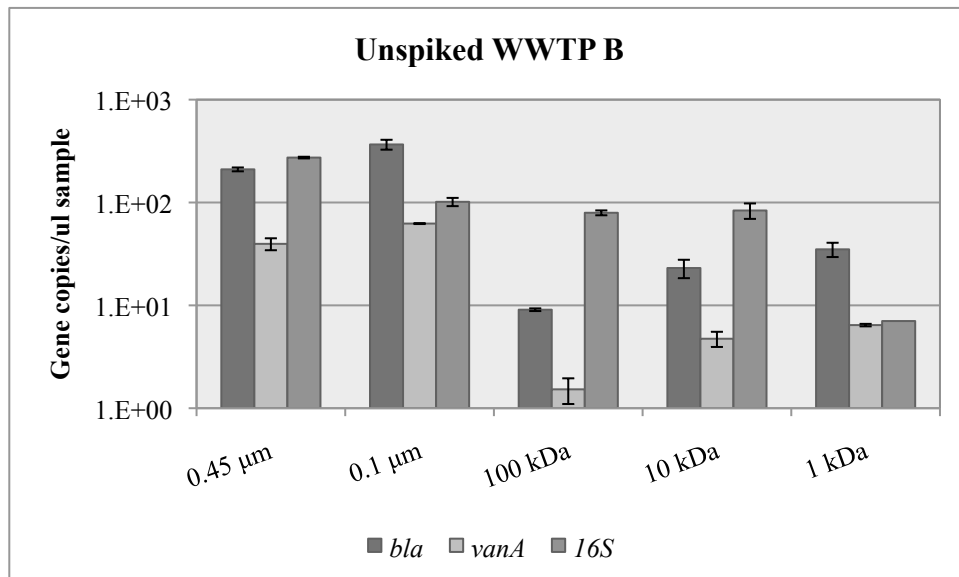


Figure 4.14. Gene concentrations in unspiked WWTP B filtrates. Samples were qPCR quantified in triplicate reactions. Error bars represent analytical error and are larger than measurement where absent.

4.2.1. WWTP A (1ST TRIAL)

An estimated 1×10^8 plasmid copies/ μl was added to the spiked buffer and WWTP effluent samples based on *bla*_{TEM} gene concentration; however, initial *bla*_{TEM} and *vanA* gene concentrations were measured to be 1.6×10^8 and 2.8×10^7 gene copies/ μl in the WWTP effluent sample, while the 1kDa filtrate concentrations were measured to be 1.0×10^3 and 9.3×10^1 gene copies/ μl , respectively. For the spiked buffer sample, the initial *bla*_{TEM} and *vanA* gene concentrations were measured to be 1.5×10^8 and 3.4×10^7 gene copies/ μl , and the 1 kDa membrane effluent concentrations were measured to be 1.7×10^2 and 4.4×10^1 gene copies/ μl . A graphical comparison between the post-filtration *bla*_{TEM}, *vanA*, and 16S rRNA gene fractions in the spiked buffer and WWTP A (1st trial) filtrates is shown in Figure 4.15 - Figure 4.17. Although the presence of colloids appeared to have no effect on the membrane-removal of the *bla*_{TEM} and *vanA* genes, an effect was observed on the removal of 16S rRNA genes. The results for the next three experiments, which included a 2nd trial of WWTP A, yielded opposite results showing an effect on the removal of *bla*_{TEM} and *vanA* genes, but no effect in the removal of 16S rRNA genes. Although the trend was opposite, the values obtained from the WWTP A 1st trial were also included in the overall statistical analyses, which still confirmed a significant effect of wastewater colloids on DNA removal.

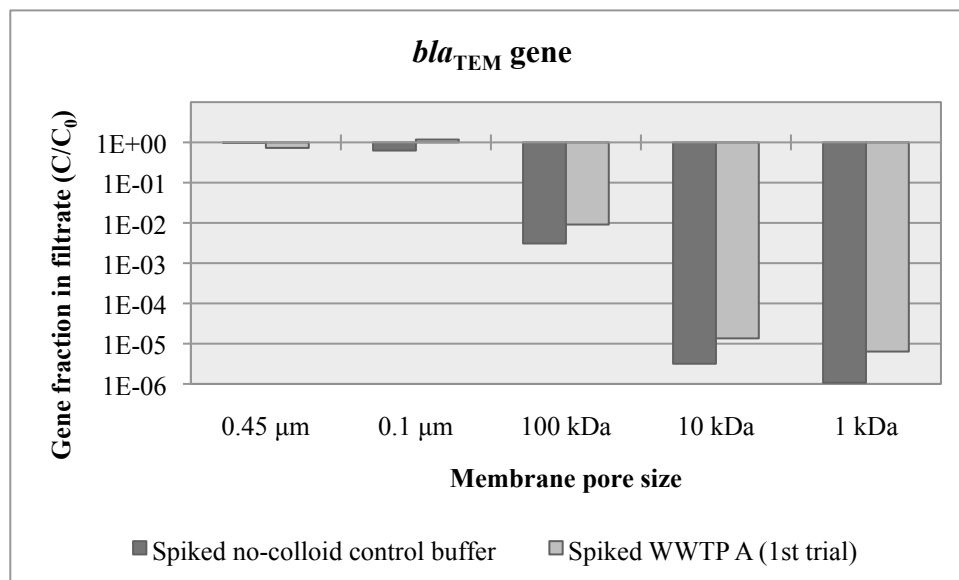


Figure 4.15. *bla*_{TEM} gene fraction in spiked buffer and WWTP A (1st trial) filtrates. Numerical values provided in Appendix A, **Table A 9**.

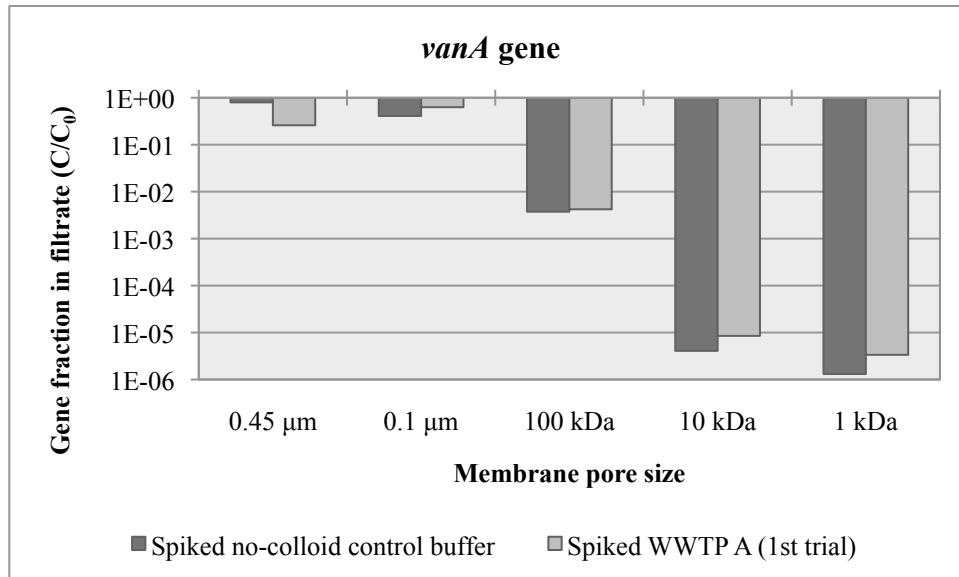


Figure 4.16. *vanA* gene fraction in spiked buffer and WWTP A (1st trial) filtrates. Numerical values provided in Appendix A, **Table A 9**.

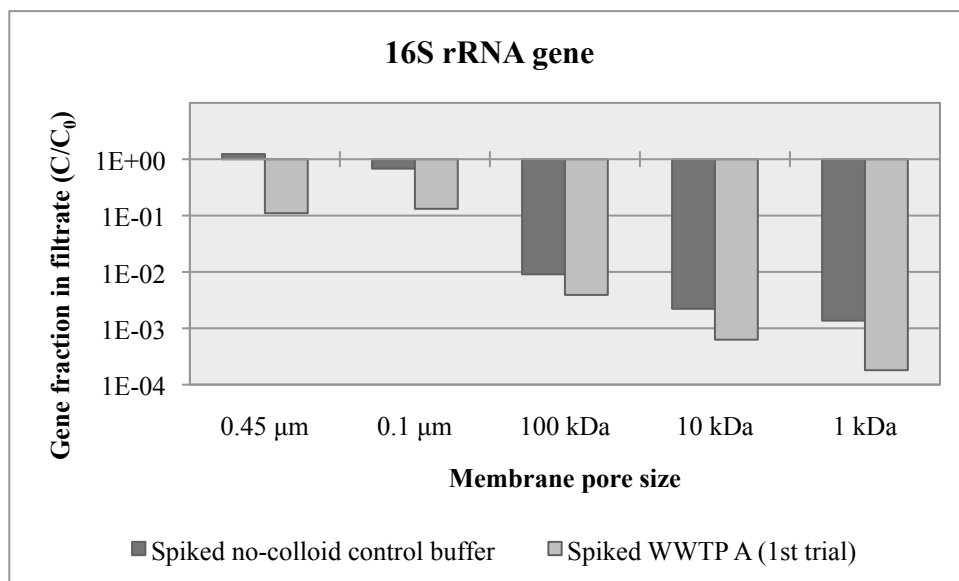


Figure 4.17. 16S rRNA gene fraction in spiked buffer and WWTP A (1st trial) filtrates. Numerical values provided in Appendix A, **Table A 9**.

4.2.2. WWTP A (2ND TRIAL)

The spiked buffer and WWTP effluent samples were spiked to a predicted concentration of 1×10^7 gene copies/ μl . The measured initial bla_{TEM} and $vanA$ gene concentrations, measured from the samples collected for the degradation test, were 9.0×10^6 and 1.1×10^6 in the spiked buffer sample, and 1.4×10^6 and 2.0×10^5 in the spiked wastewater sample. The bla_{TEM} and $vanA$ gene concentrations in the 1 kDa filtrate were measured to be 1.5×10^3 and 2.9×10^2 , respectively, for the spiked buffer; and 2.1 and 0.2, respectively, for the spiked wastewater. Figure 4.18 - Figure 4.20 compare filtrate gene concentrations of spiked no-colloid buffer samples vs. WWTP A (2nd trial) effluent samples.

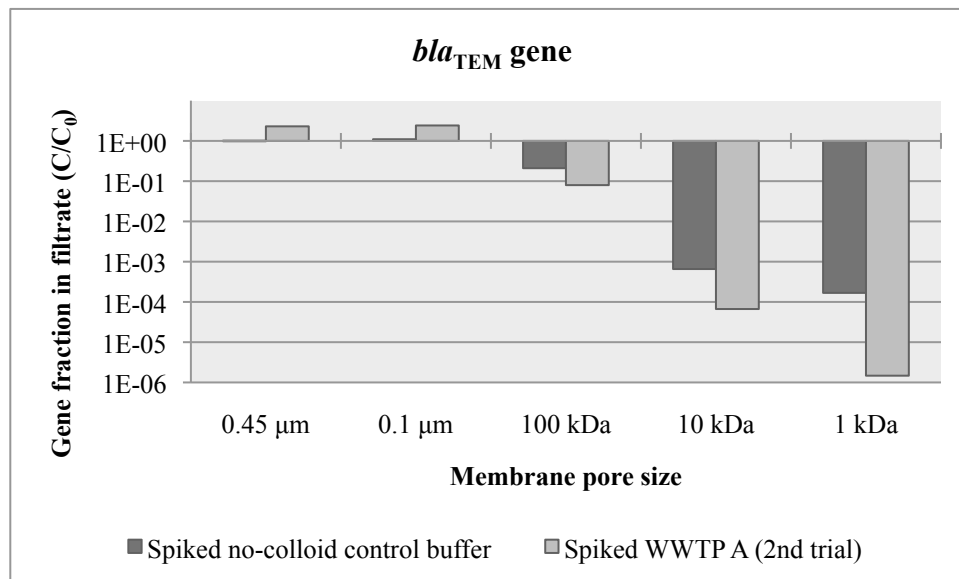


Figure 4.18. bla_{TEM} gene fraction in spiked buffer and WWTP A (2nd trial) filtrates. Numerical values provided in Appendix A, **Table A 9**.

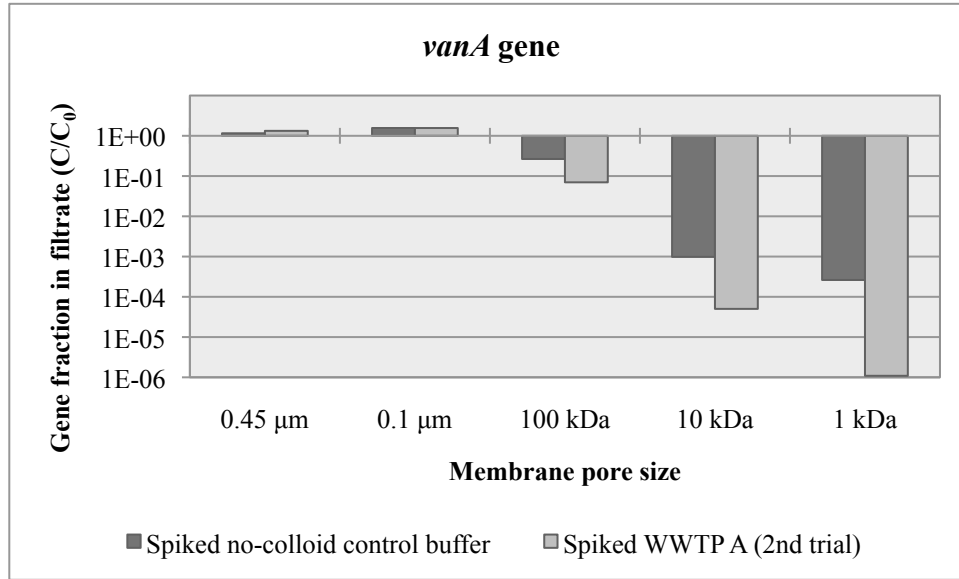


Figure 4.19. *vanA* gene fraction in spiked buffer and WWTP A (2nd trial) filtrates. Numerical values provided in Appendix A, **Table A 9**.

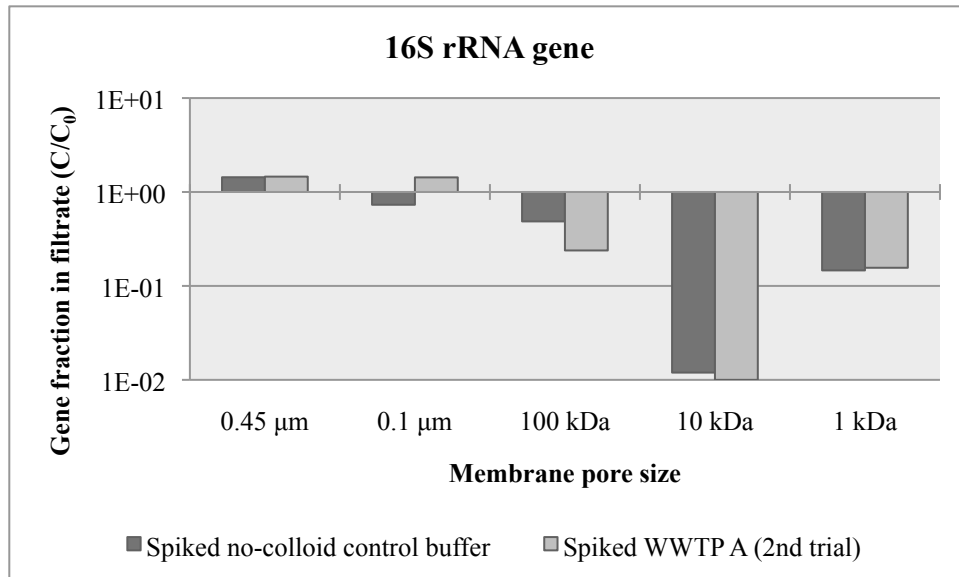


Figure 4.20. 16S rRNA gene fraction in spiked buffer and WWTP A (2nd trial) filtrates. Numerical values provided in Appendix A, **Table A 9**.

4.2.3. WWTP B

An estimated 1×10^8 plasmid copies/ μl were added to the spiked buffer and WWTP B effluent samples. The measured initial bla_{TEM} and $vanA$ gene concentrations in each of the samples were 9.1×10^7 and 1.4×10^7 , respectively, for the spiked buffer; and 3.0×10^7 and 3.3×10^6 , respectively, for the spiked WWTP effluent. The 1 kDa filtrate bla_{TEM} and $vanA$ gene concentrations were measured to be 5.8×10^3 and 6.4×10^2 , respectively, for the spiked buffer; and 3.0 and 0.1, respectively, for the spiked wastewater. Figure 4.21 - Figure 4.23 compare filtrate gene concentrations of spiked no-colloid buffer samples vs. WWTP B effluent samples.

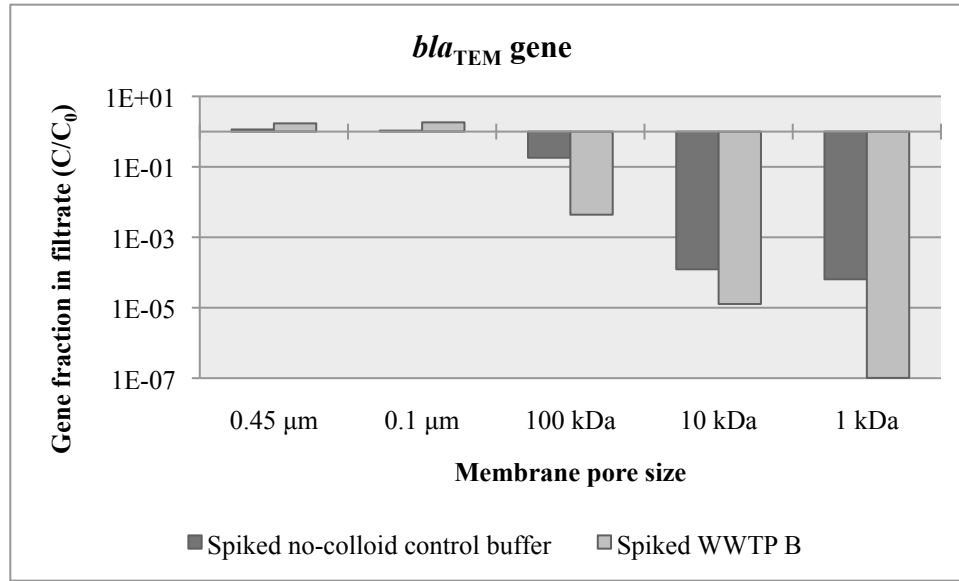


Figure 4.21. bla_{TEM} gene fraction in spiked buffer and WWTP B filtrates. Numerical values provided in Appendix A, Table A 9.

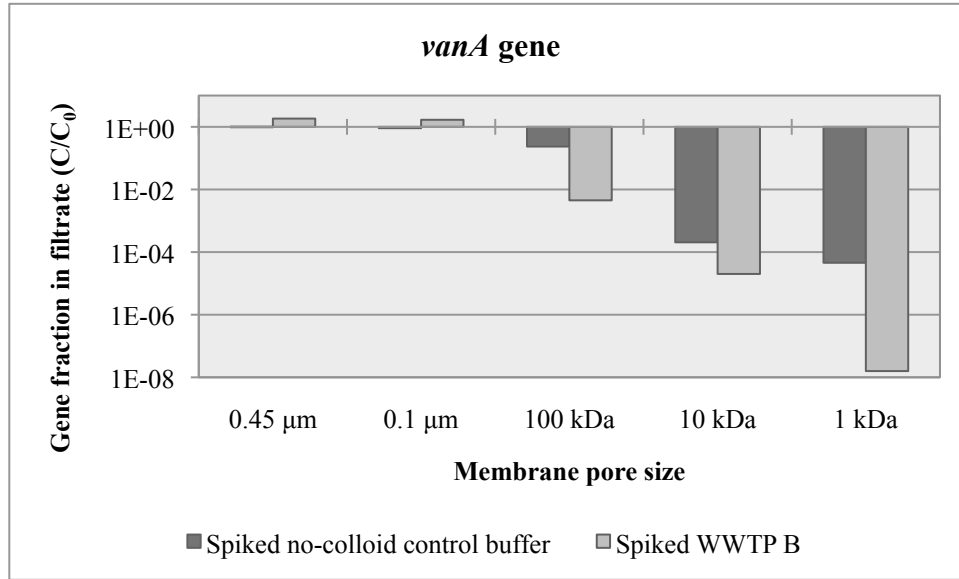


Figure 4.22. *vanA* gene fraction in spiked buffer and WWTP B filtrates. Numerical values provided in Appendix A, **Table A 9**.

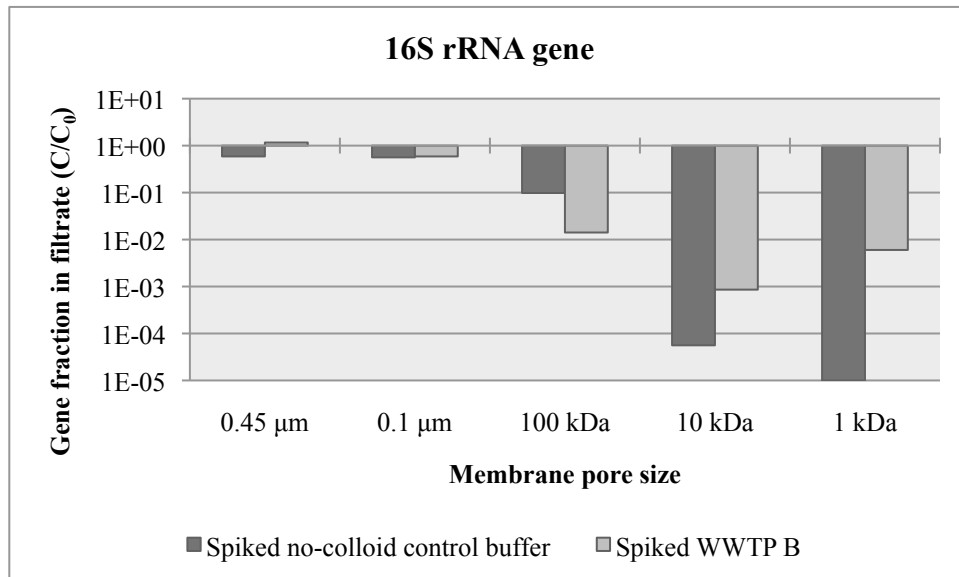


Figure 4.23. 16S rRNA gene fraction in spiked buffer and WWTP B filtrates. Numerical values provided in Appendix A, **Table A 9**.

4.2.4. WWTP C

A predicted 1×10^8 plasmid copies/ μl was spiked into the buffer and WWTP C effluent based on bla_{TEM} gene concentration. An initial 6.8×10^7 and 2.0×10^7 gene copies/ μl were measured in the spiked buffer for the bla_{TEM} and $vanA$ genes, respectively; while 7.4×10^6 and 1.5×10^6 gene copies/ μl were measured in the spiked wastewater for the respective genes. The 1 kDa filtrate bla_{TEM} and $vanA$ gene concentrations were measured to be 1.3×10^3 and 5.7×10^2 gene copies/ μl , respectively, for the spiked buffer; and 3.0 and 1.7 gene copies/ μl for the spiked wastewater. Figure 4.24 - Figure 4.26 compare filtrate gene concentrations of spiked no-colloid buffer samples vs. WWTP C effluent samples.

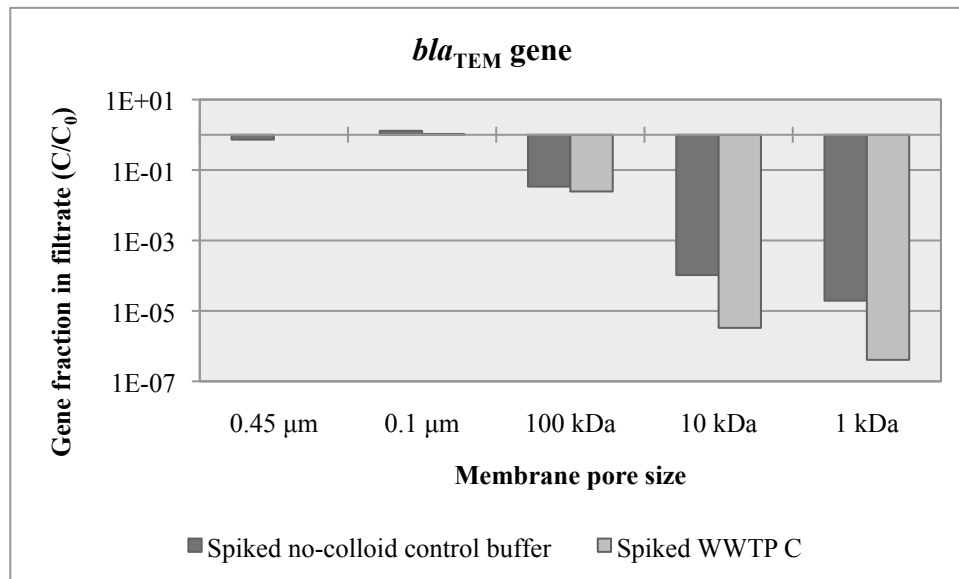


Figure 4.24. bla_{TEM} gene fraction in spiked buffer and WWTP C filtrates. Numerical values provided in Appendix A, **Table A 9**.

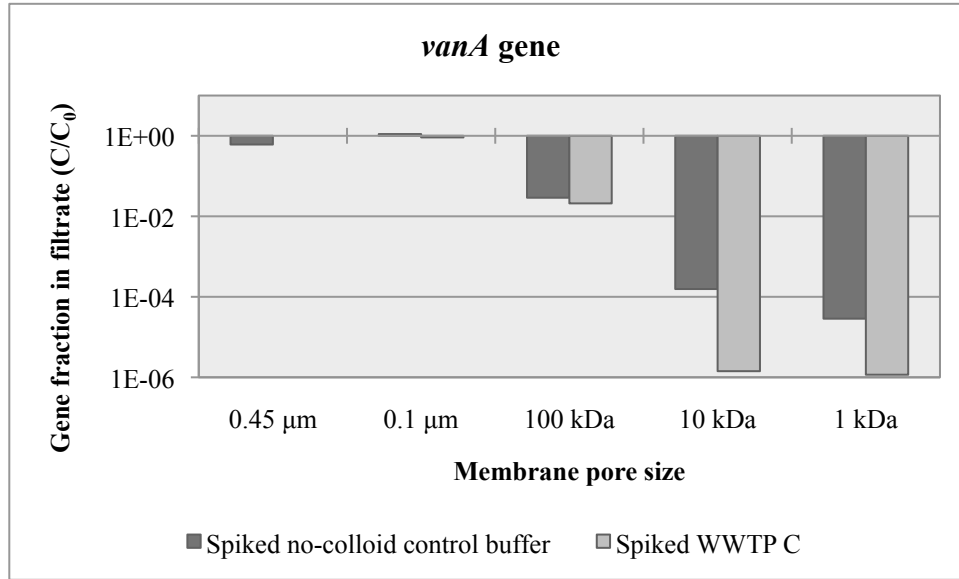


Figure 4.25. *vanA* gene fraction in spiked buffer and WWTP C filtrates. Numerical values provided in Appendix A, **Table A 9**.

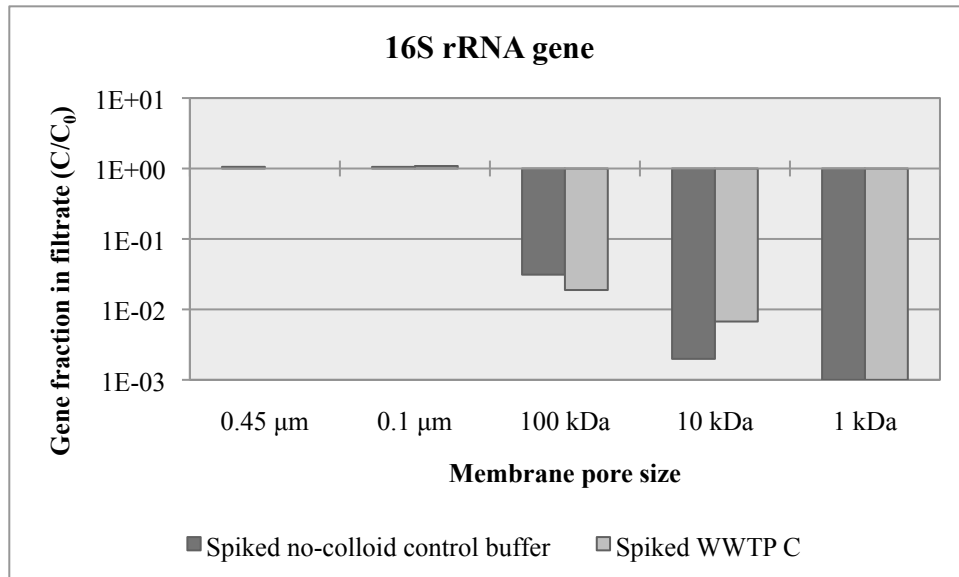


Figure 4.26. 16S rRNA gene fraction in spiked buffer and WWTP C filtrates. Numerical values provided in Appendix A, **Table A 9**.

4.3. COLLOID CHARACTERIZATION

The colloidal components present in the WWTP effluents were characterized in terms of TOC, proteins, and polysaccharides. A correlation test between the filtrate fraction of each of the colloidal components and the logarithm of the filtrate gene fraction was done in the R statistical software, applying a one-sided Pearson correlation test. The results of the TOC, protein, and polysaccharide tests are shown in Sections 4.3.1 – 4.3.3, respectively. Pearson correlation (r) values, and p -values are shown in Table 4.1. Numerical results for all genes and colloidal components and WWTP are provided in Appendix A, Table A 14.

4.3.1. TOTAL ORGANIC CARBON (TOC)

The post-filtration TOC concentrations for all WWTPs are shown in Figure 4.27. The Pearson correlation coefficient, r , for both the *bla*_{TEM} and *vanA* genes was determined to be 0.62 ($p < 0.01$). Correlation graphs are shown in Figure 4.28 and Figure 4.29.

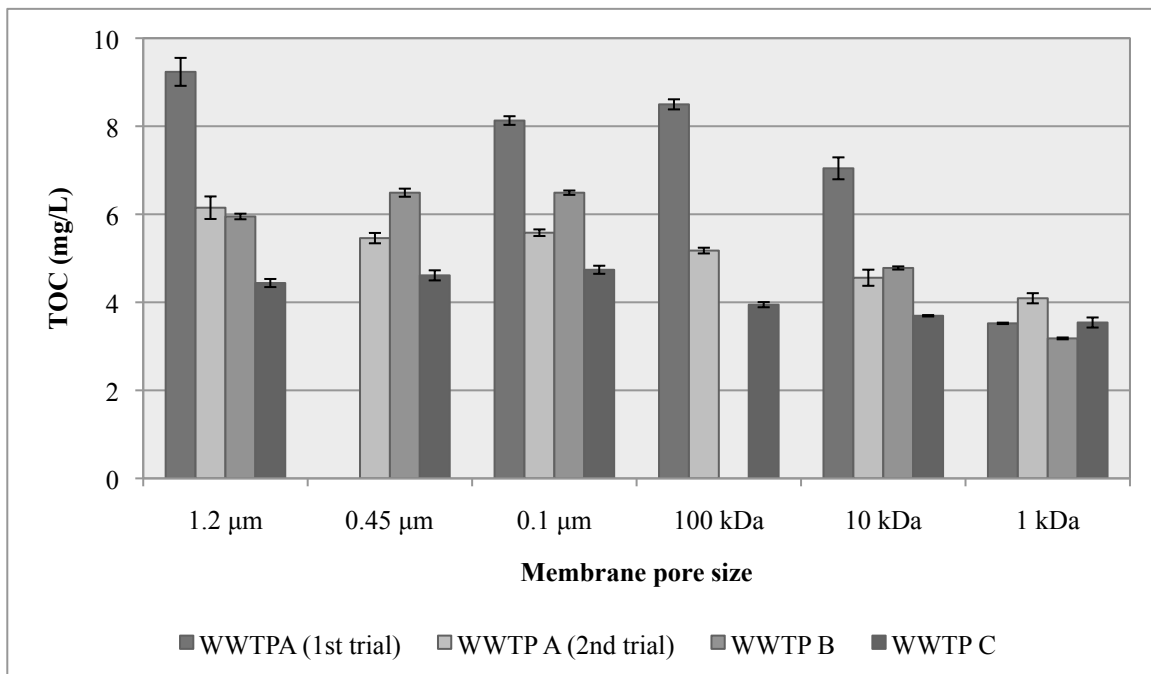


Figure 4.27. TOC concentrations in serially filtered unspiked WWTP A (1st trial) samples.

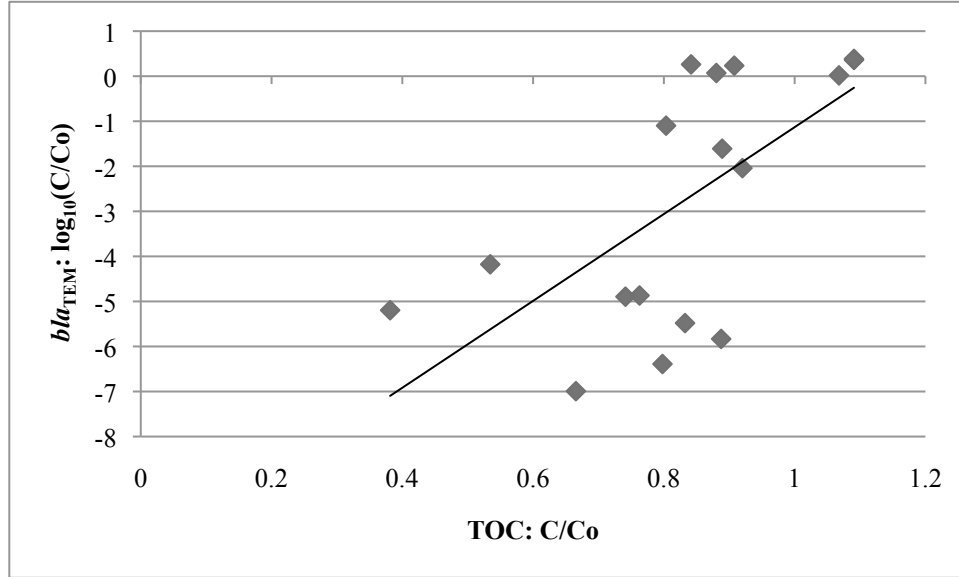


Figure 4.28. Correlation between membrane removal of *bla*_{TEM} genes and TOC. One-sided Pearson correlation coefficient, *r*, is 0.62 (*p* < 0.01).

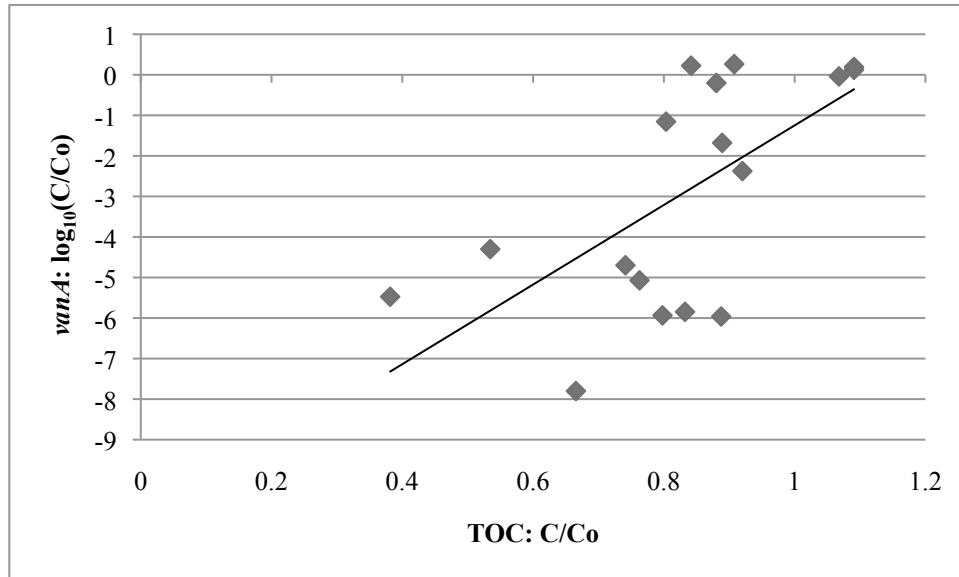


Figure 4.29. Correlation between membrane removal of *vanA* genes and TOC. One-sided Pearson correlation coefficient, *r*, is 0.62 (*p* < 0.01).

4.3.2. PROTEINS AND POLYSACCHARIDES

Protein concentrations of the filtered unspiked WWTP effluents are shown in Figure 4.30. Correlation plots are also provided (Figure 4.31 - Figure 4.32). The one-sided Pearson correlation coefficients were determined to be 0.80 and 0.83 for the *bla*_{TEM} and *vanA* gene-correlations to protein removal ($p < 0.01$), respectively.

Post-filtration polysaccharide concentrations for each of the WWTP are shown in Figure 4.33. In addition, correlation graphs are provided in Figure 4.34 - Figure 4.35 for the *bla*_{TEM}- and *vanA*-gene removal correlations to polysaccharide removal. The one-sided Pearson correlation coefficients were determined to be 0.60 and 0.62 for the *bla*_{TEM} and *vanA* genes ($p < 0.01$), respectively.

Additional correlation graphs showing the relationship between gene removal and the removal of the added protein and polysaccharide concentrations are shown in Figure 4.36 - Figure 4.37. One-sided Pearson correlation coefficients were determined to be 0.82 and 0.83 for the *bla*_{TEM} and *vanA* genes ($p < 0.01$), respectively.

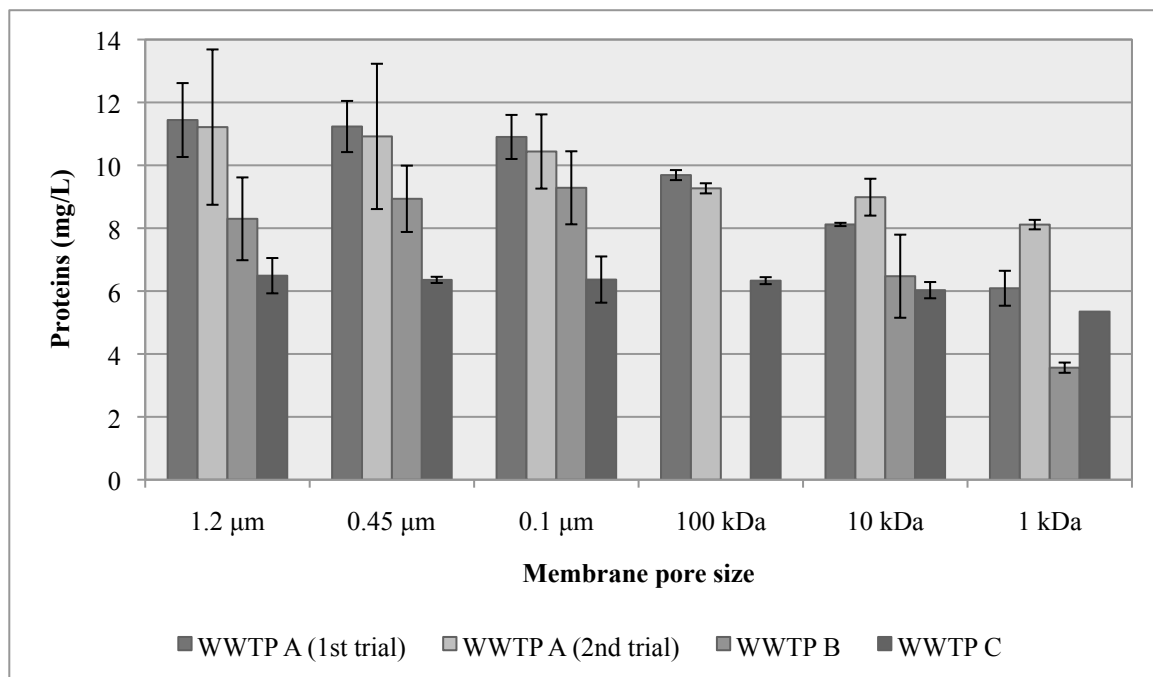


Figure 4.30. Protein concentrations in serially filtered unspiked WWTP A (1st trial) samples.

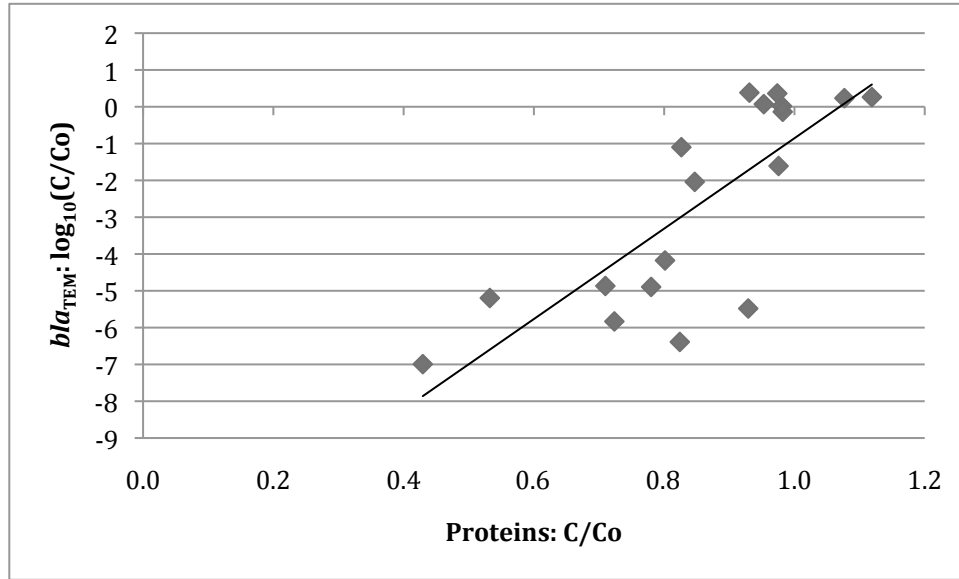


Figure 4.31. Correlation between membrane removal of *bla*_{TEM} genes and proteins. One-sided Pearson correlation coefficient, *r*, is 0.80 (*p* < 0.01).

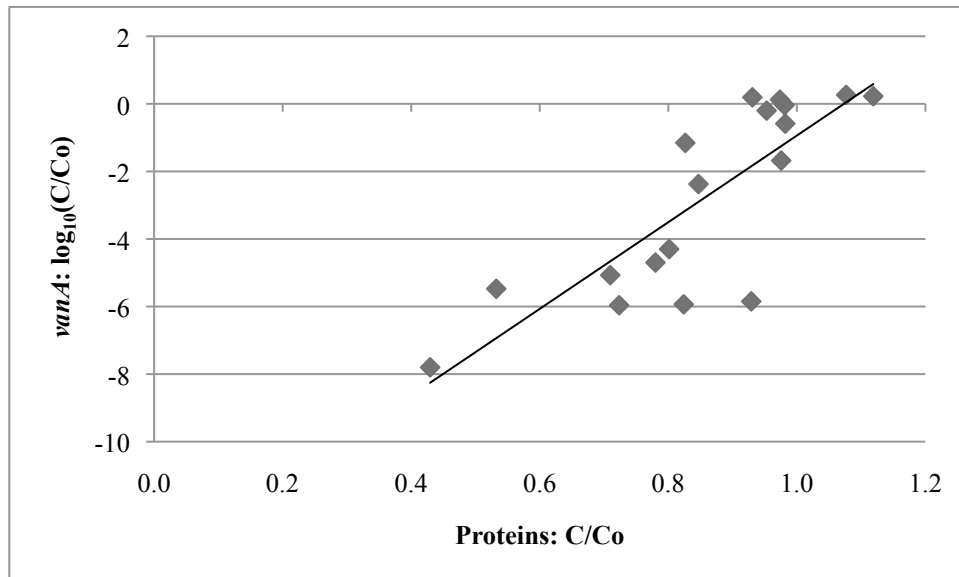


Figure 4.32. Correlation between membrane removal of *vanA* genes and proteins. One-sided Pearson correlation coefficient, *r*, is 0.83 (*p* < 0.01).

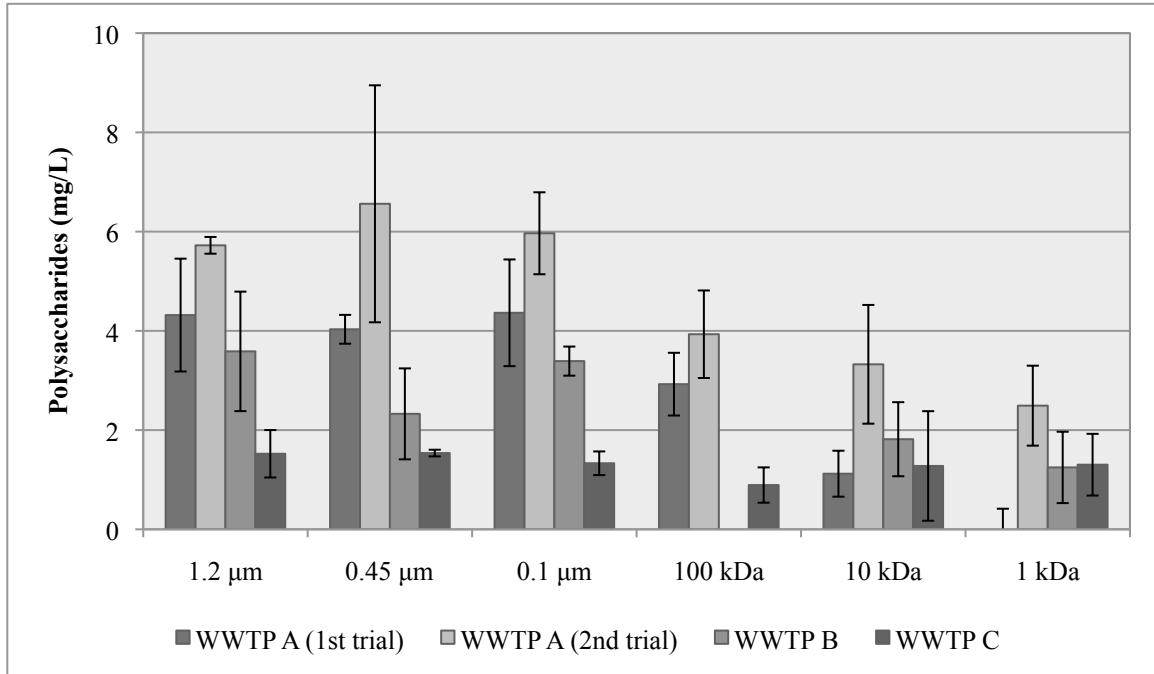


Figure 4.33. Polysaccharide concentrations in serially filtered unspiked WWTP A (1st trial) samples.

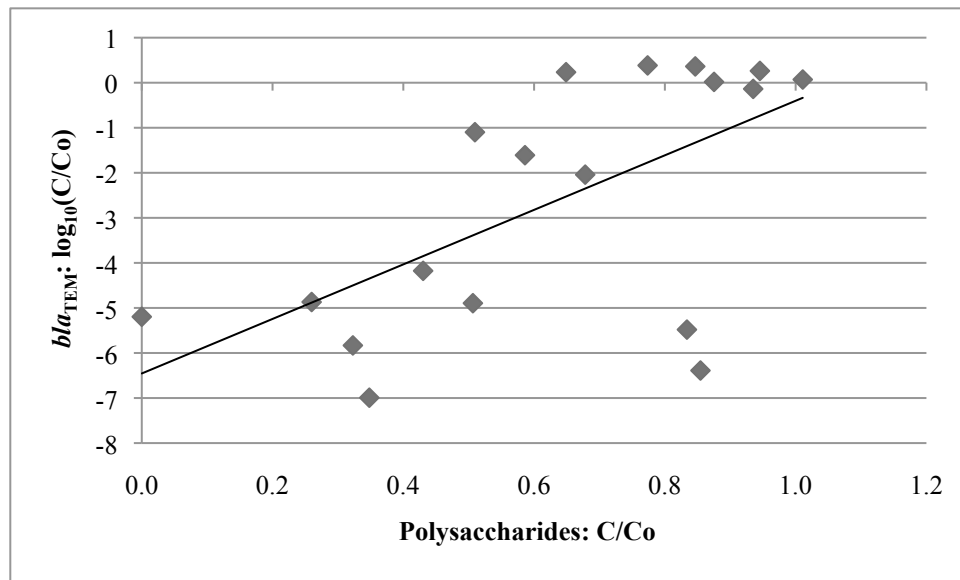


Figure 4.34. Correlation between membrane removal of *bla*_{TEM} genes and polysaccharides. One-sided Pearson correlation coefficient, *r*, is 0.60 (*p* < 0.01).

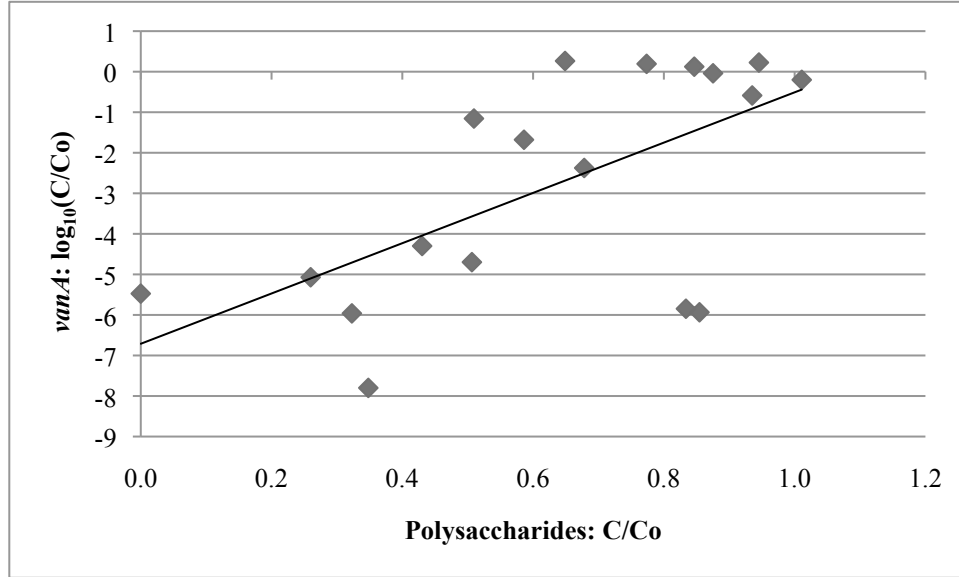


Figure 4.35. Correlation between membrane removal of *vanA* genes and polysaccharides. One-sided Pearson correlation coefficient, r , is 0.62 ($p < 0.01$).

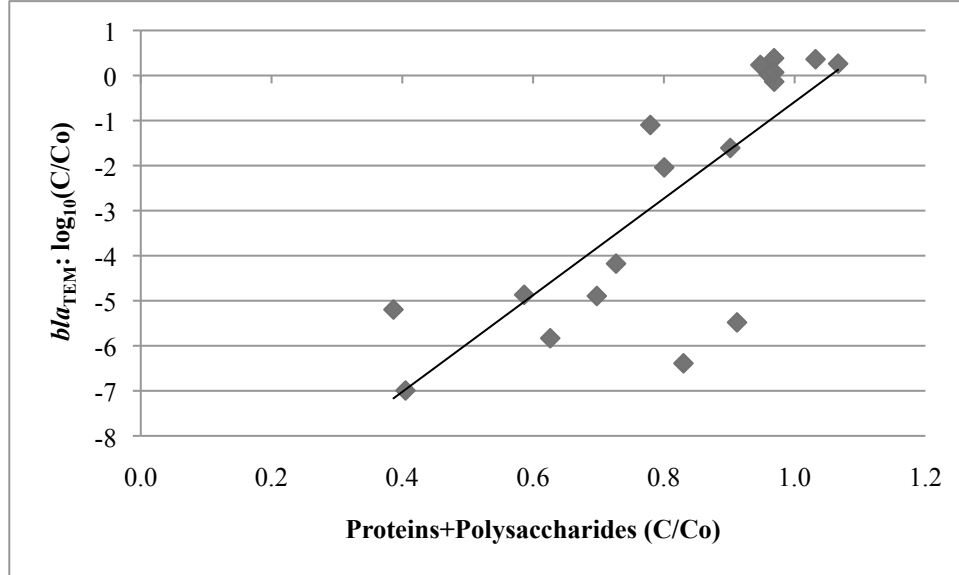


Figure 4.36. Correlation between membrane removal of *bla_{TEM}* genes and the added protein and polysaccharide concentrations. One-sided Pearson correlation coefficient, r , is 0.82 ($p < 0.01$).

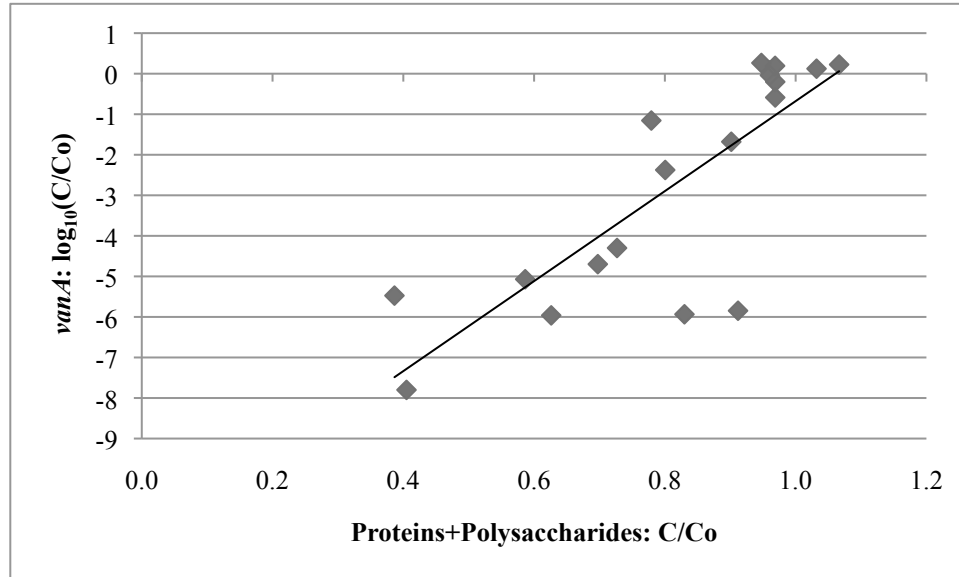


Figure 4.37. Correlation between membrane removal of *vanA* genes and the added protein and polysaccharide concentrations. One-sided Pearson correlation coefficient, r , is 0.83 ($p < 0.01$).

Table 4.1. Pearson correlation coefficients and their corresponding p-values associated with the correlation between colloidal component- and gene-membrane removal.

Gene	TOC		Proteins		Polysaccharides		Proteins+ Polysaccharides	
	r	p	r	p	r	p	r	p
<i>bla</i> _{TEM}	0.62	3.91×10^{-3}	0.80	3.68×10^{-5}	0.60	4.04×10^{-3}	0.82	1.78×10^{-5}
<i>vanA</i>	0.62	4.05×10^{-3}	0.83	1.25×10^{-5}	0.62	3.18×10^{-3}	0.83	8.79×10^{-6}
16S rRNA	0.65	2.19×10^{-3}	0.42	4.25×10^{-2}	0.27	0.14	0.45	0.03

Note: p-values calculated using R for the correlation between $\log_{10}(C/C_0)$ of each gene versus C/C_0 of TOC, proteins, or polysaccharides.

4.3.4. SCANNING ELECTRON MICROSCOPY (SEM)

SEM images of freeze dried filtered WWTP effluent samples were captured with the purpose of characterizing the particle size distribution of each of the colloidal fractions. Unfortunately, a particle size characterization was not possible as originally intended due to the occurrence of particle agglomeration during sample preparation. However, other important conclusions were drawn from these images and will be further discussed in Chapter 5. Selected images are shown in Figure 4.38 - Figure 4.54.

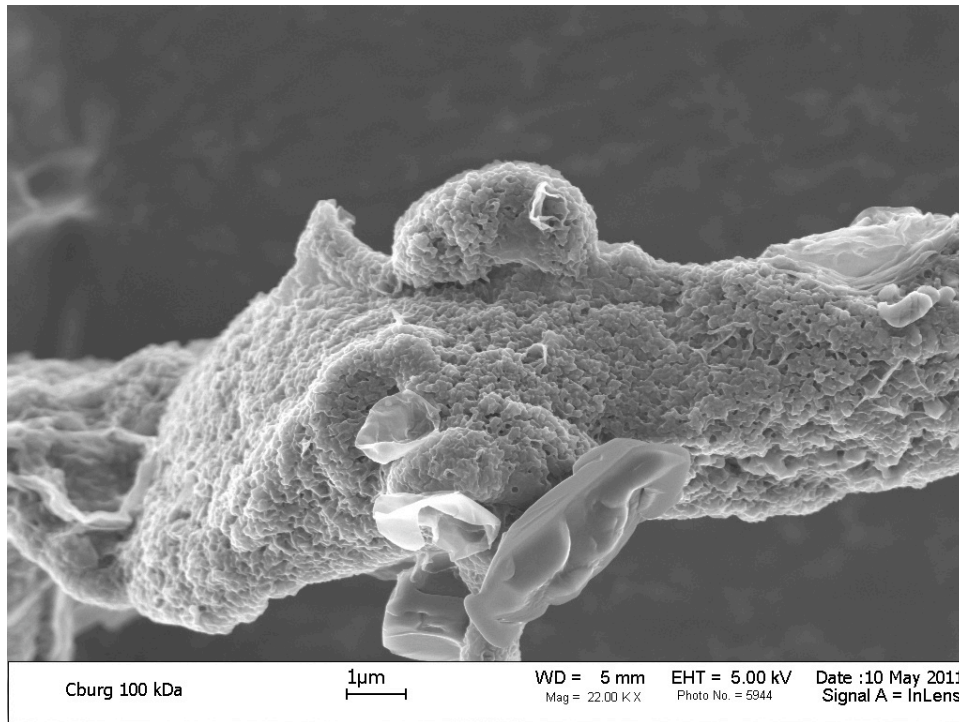


Figure 4.38. SEM image of freeze-dried WWTP A effluent filtered through a 100 kDa-pore size membrane. Reference bar = 1 μm . Magnification = 20,000 X.

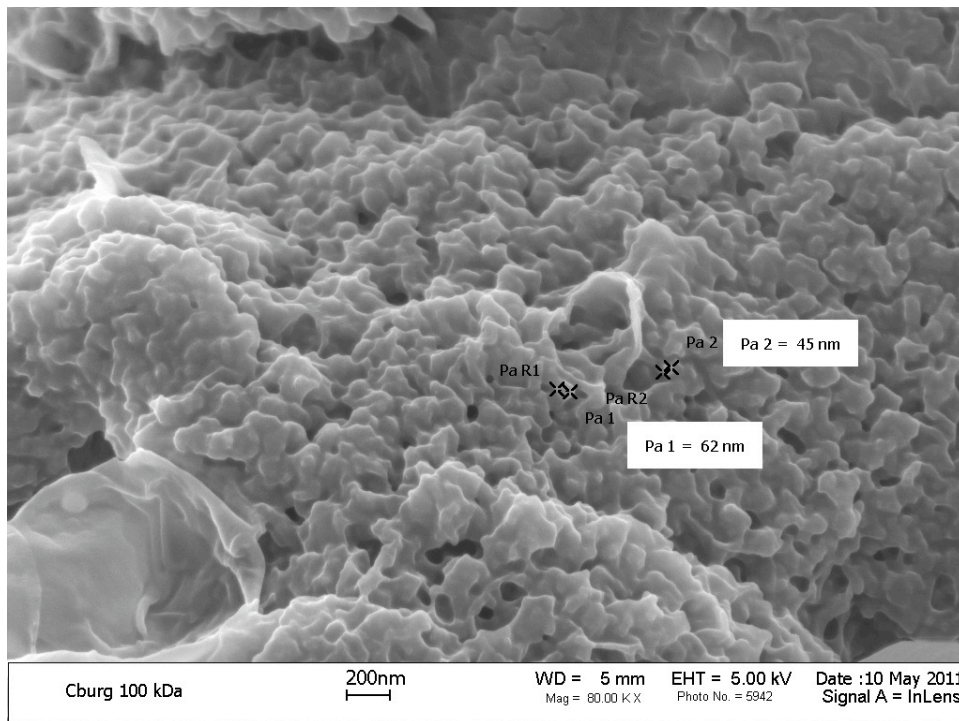


Figure 4.39. SEM image of freeze-dried WWTP A effluent filtered through a 100 kDa-pore size membrane. Reference bar = 200 nm. Magnification = 80,000 X.

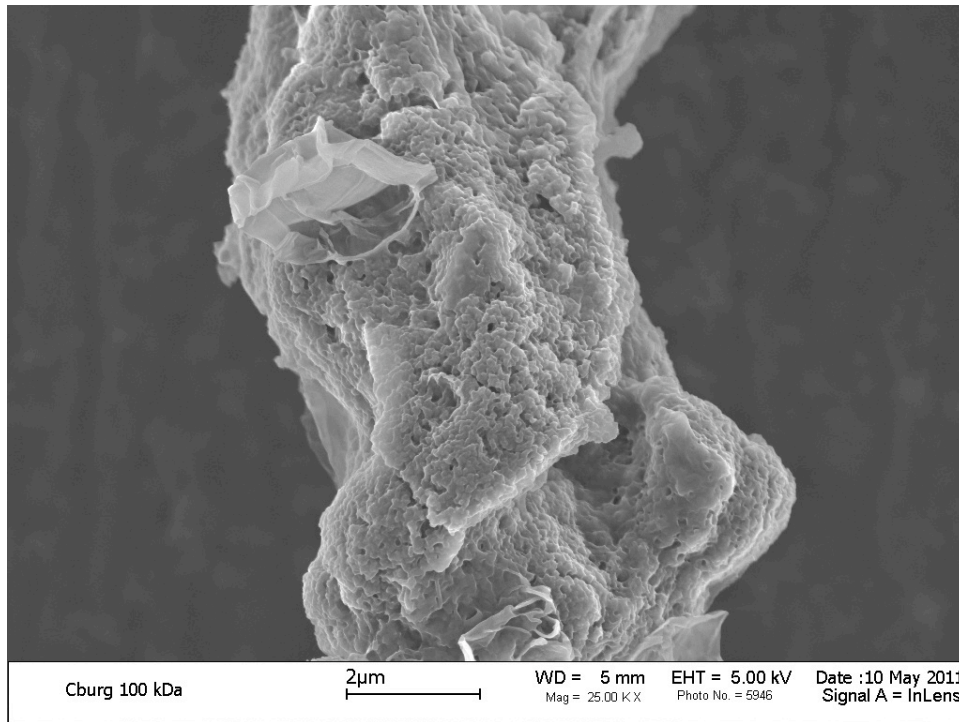


Figure 4.40. SEM image of freeze-dried WWTP A effluent filtered through a 100 kDa-pore size membrane. Reference bar = 2 μm . Magnification = 25,000 X.

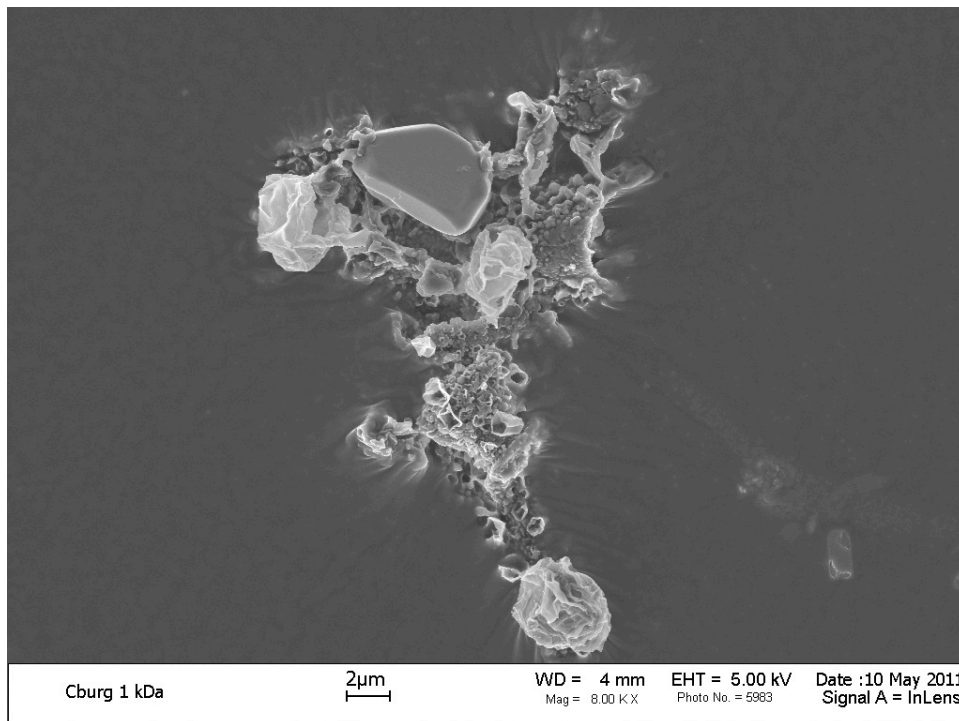


Figure 4.41. SEM image of freeze-dried WWTP A effluent filtered through a 1 kDa-pore size membrane. Reference bar = 2 μm . Magnification = 8,000 X.

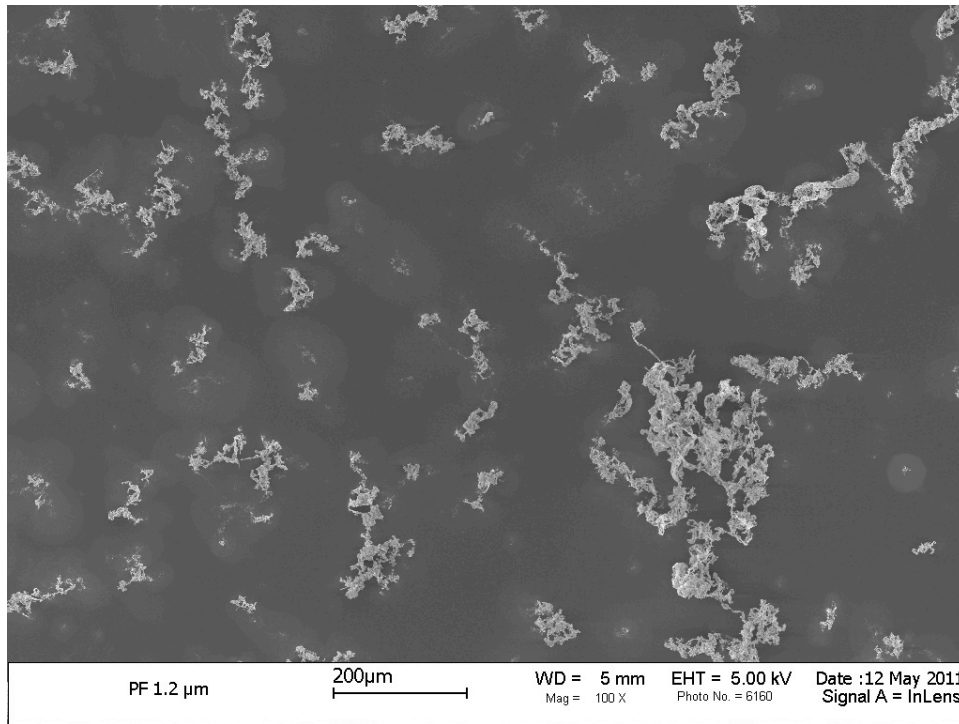


Figure 4.42. SEM image of freeze-dried WWTP C effluent filtered through a 1.2 μm -pore size membrane. Reference bar = 200 μm . Magnification = 100 X.

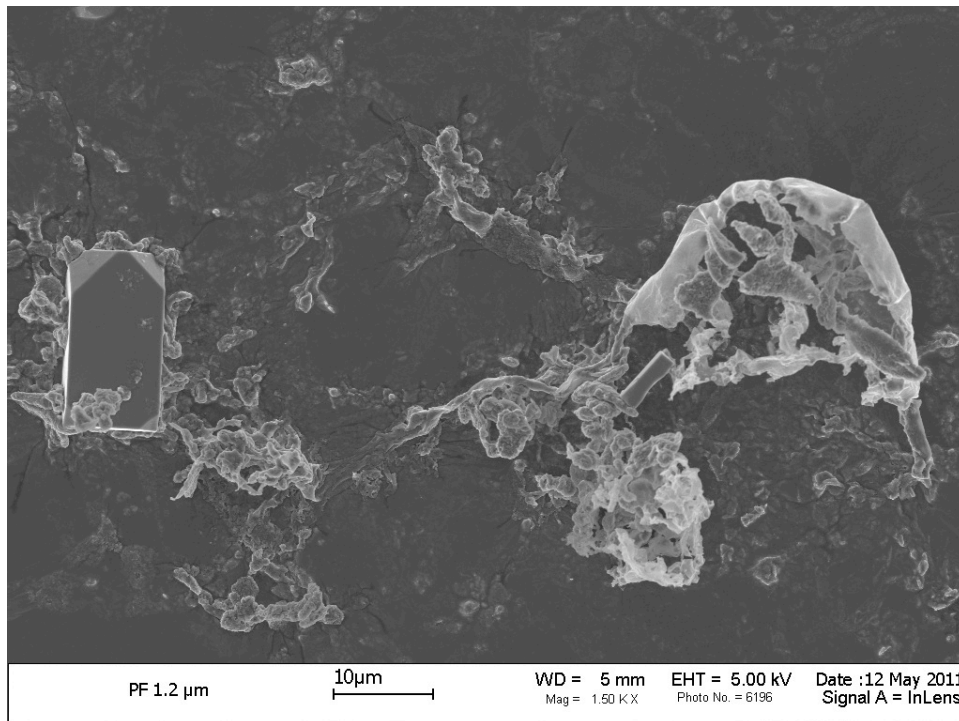


Figure 4.43. SEM image of freeze-dried WWTP C effluent filtered through a 1.2 μm -pore size membrane. Reference bar = 10 μm . Magnification = 1,500 X.

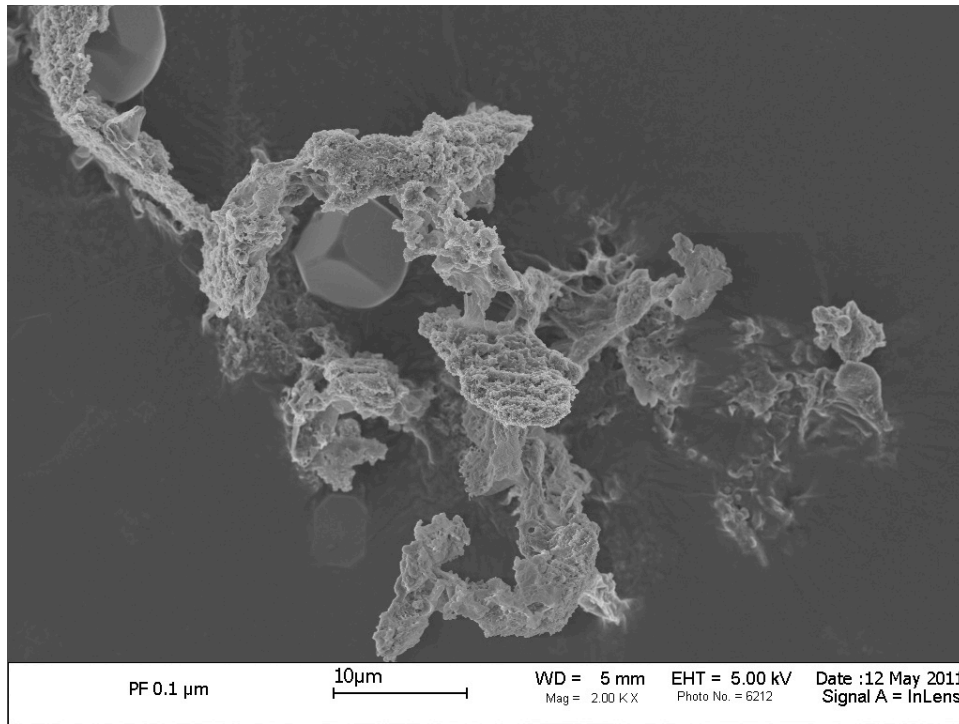


Figure 4.44. SEM image of freeze-dried WWTP C effluent filtered through a 0.1 μm -pore size membrane. Reference bar = 10 μm . Magnification = 2,000 X.

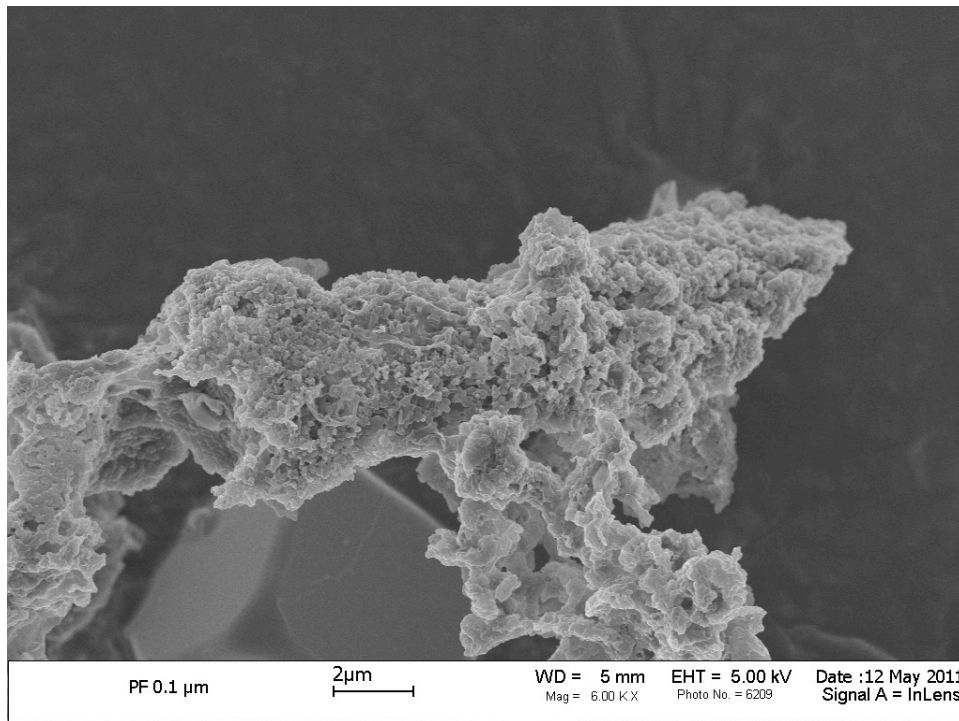


Figure 4.45. SEM image of freeze-dried WWTP C effluent filtered through a 0.1 μm -pore size membrane. Reference bar = 2 μm . Magnification = 6,000 X.

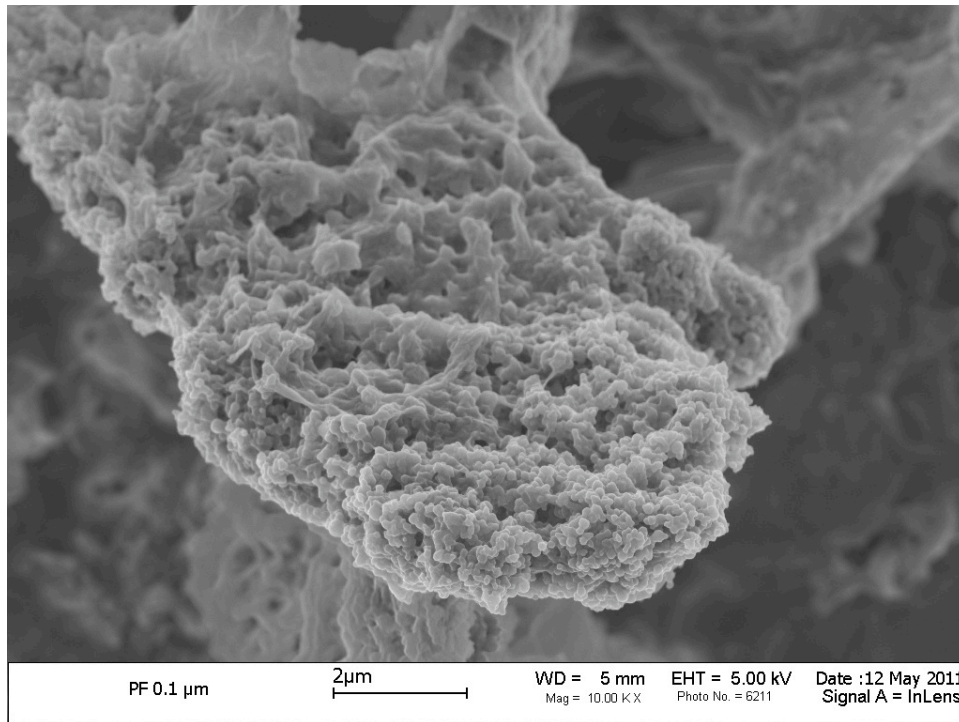


Figure 4.46. SEM image of freeze-dried WWTP C effluent filtered through a 0.1 μm -pore size membrane. Reference bar = 2 μm . Magnification = 10,000 X.

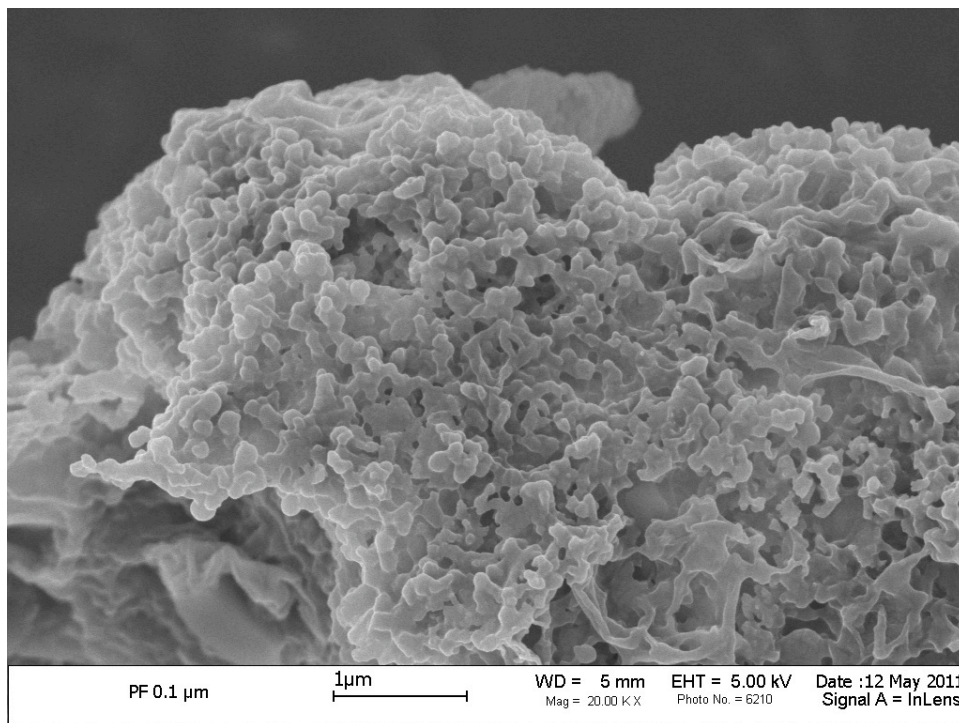


Figure 4.47. SEM image of freeze-dried WWTP C effluent filtered through a 0.1 μm -pore size membrane. Reference bar = 1 μm . Magnification = 20,000 X.

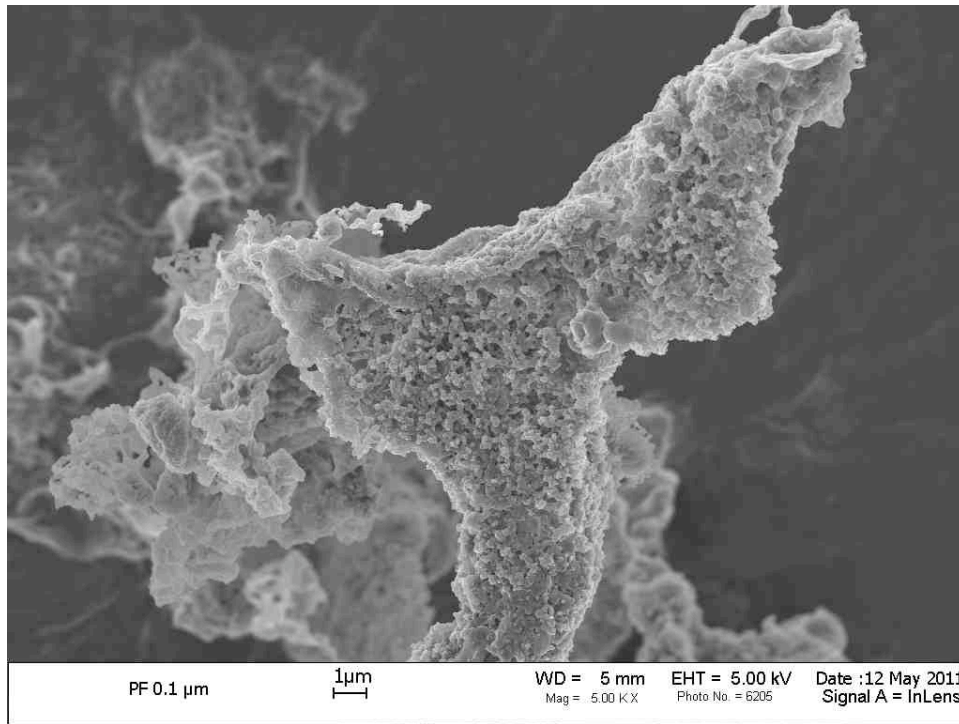


Figure 4.48. SEM image of freeze-dried WWTP C effluent filtered through a 0.1 μm -pore size membrane. Reference bar = 1 μm . Magnification = 5,000 X.

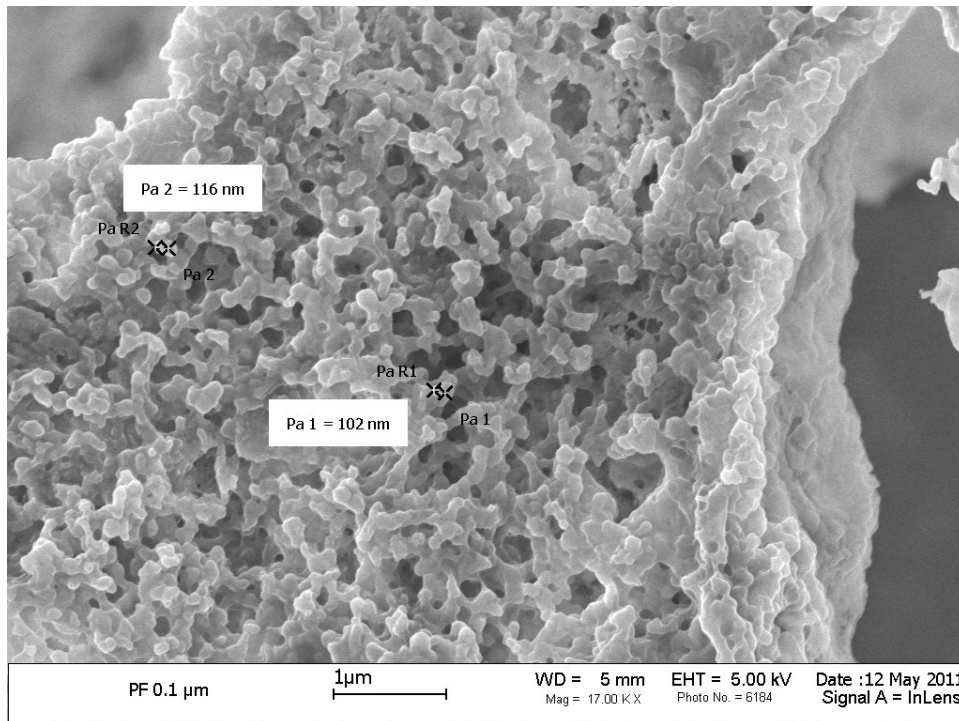


Figure 4.49. SEM image of freeze-dried WWTP C effluent filtered through a 0.1 μm -pore size membrane. Reference bar = 1 μm . Magnification = 17,000 X.

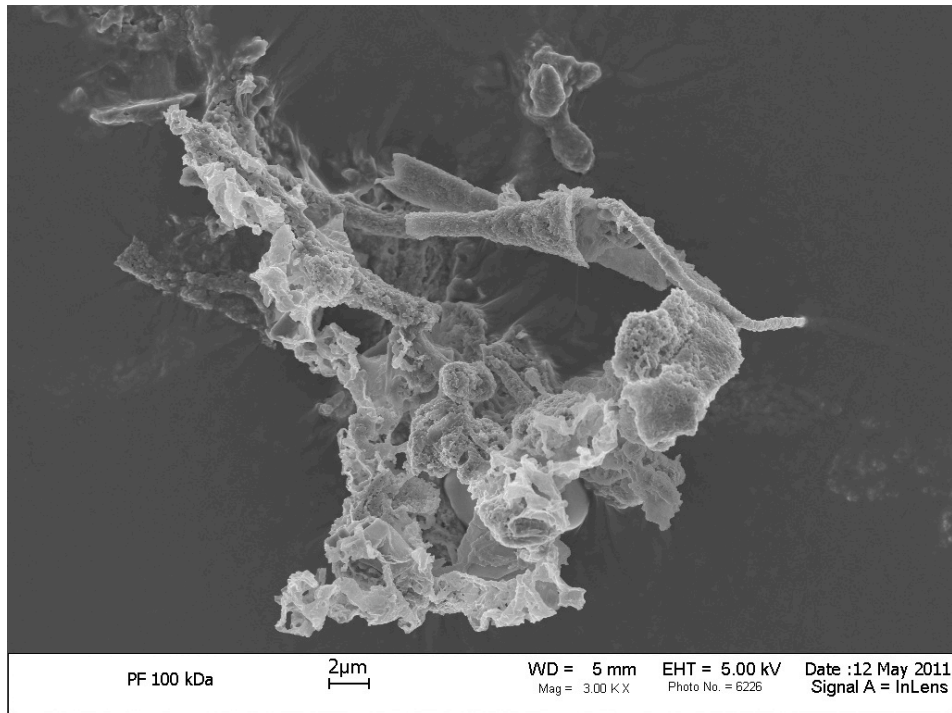


Figure 4.50. SEM image of freeze-dried WWTP C effluent filtered through a 100 kDa-pore size membrane. Reference bar = 2 μm . Magnification = 3,000 X.

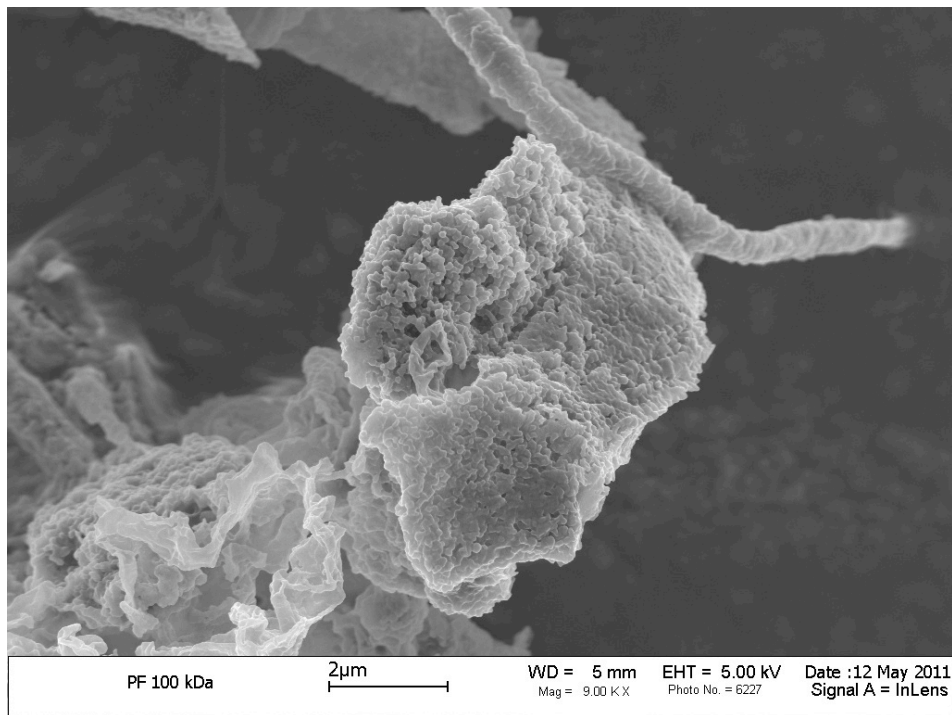


Figure 4.51. SEM image of freeze-dried WWTP C effluent filtered through a 100 kDa-pore size membrane. Reference bar = 2 μm . Magnification = 9,000 X.

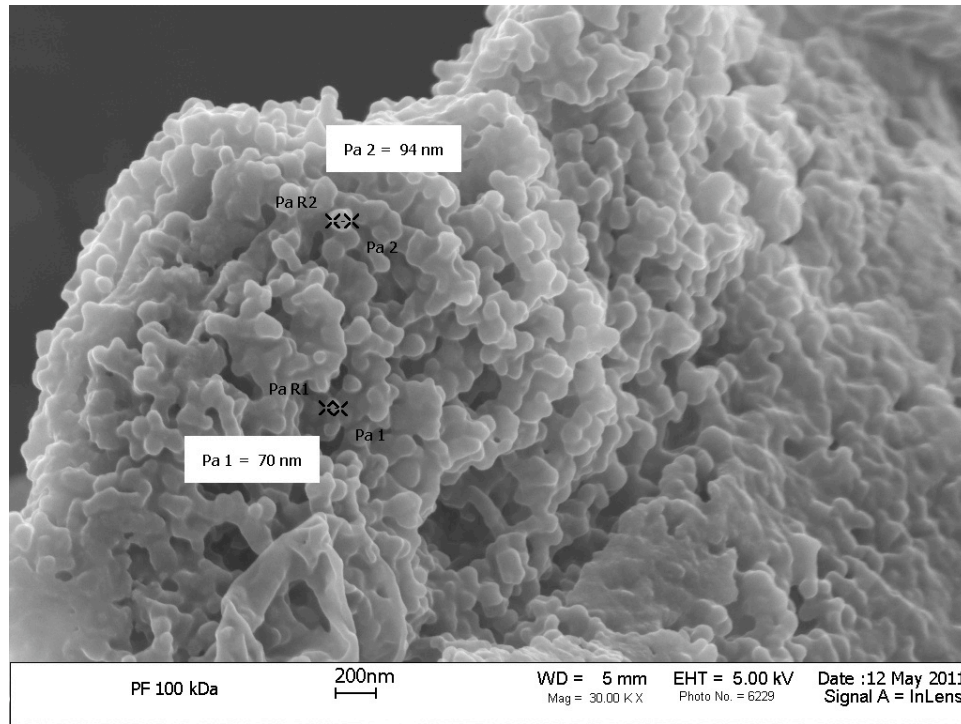


Figure 4.52. SEM image of freeze-dried WWTP C effluent filtered through a 100 kDa-pore size membrane. Reference bar = 200 nm. Magnification = 30,000 X.

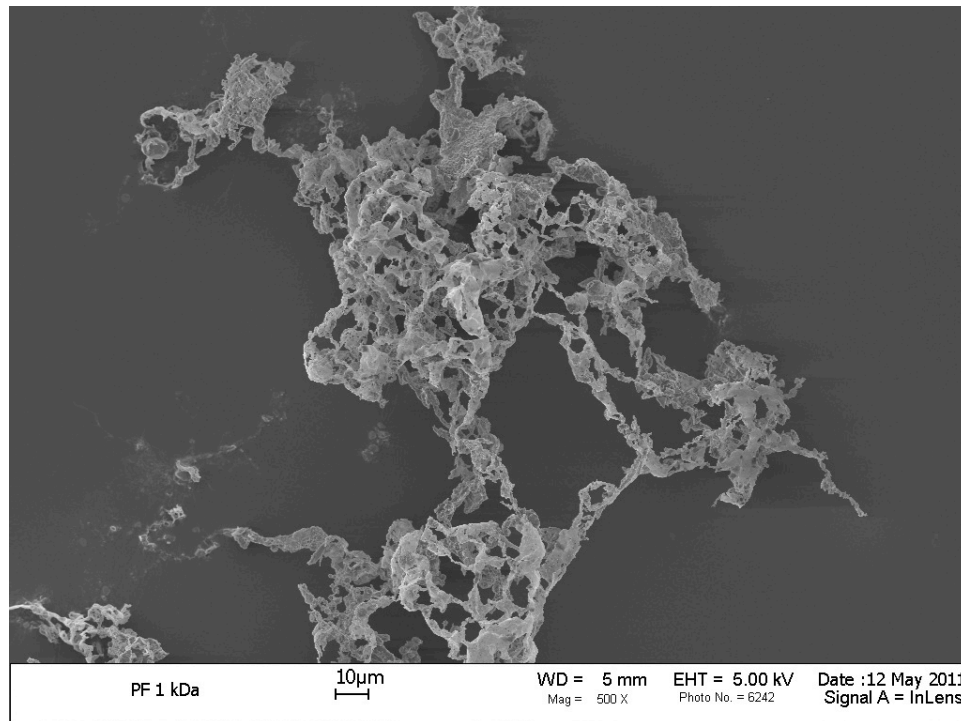


Figure 4.53. SEM image of freeze-dried WWTP C effluent filtered through a 1 kDa-pore size membrane. Reference bar = 10 µm. Magnification = 500 X.

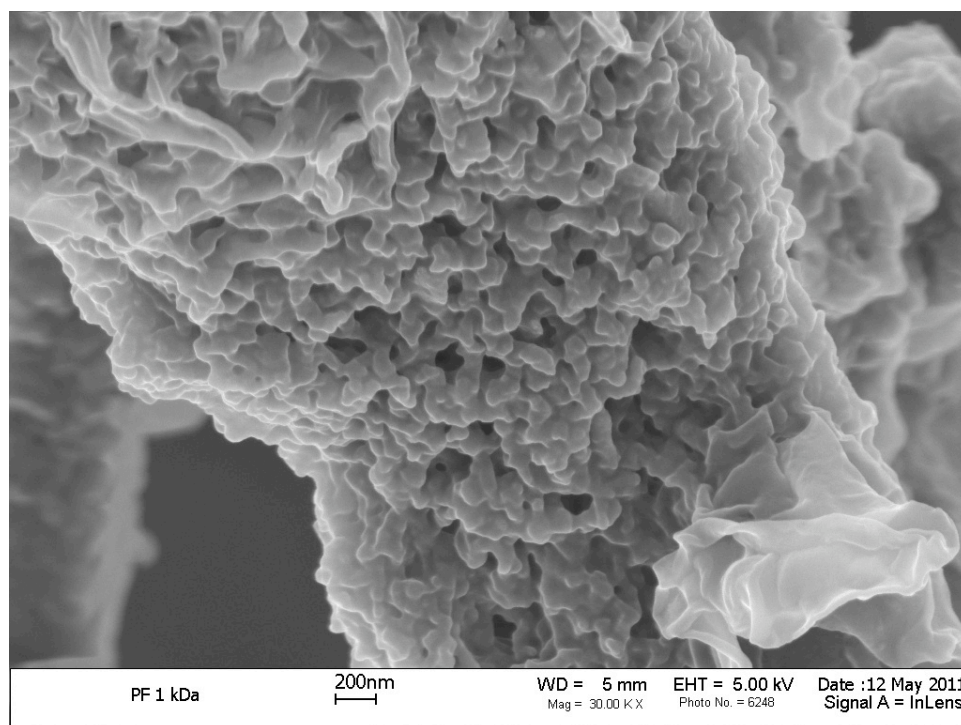


Figure 4.54. SEM image of freeze-dried WWTP C effluent filtered through a 1 kDa-pore size membrane. Reference bar = 200 nm. Magnification = 30,000 X.

4.4. COMPARISON BETWEEN PVDF AND ALUMINA MEMBRANES

A comparison between the MF (0.1 μm -pore size) hydrophilic PVDF Durapore[®] (Millipore, Billerica, MA) and alumina Anodisc 47[®] (Whatman GmbH, Germany) was carried out for all of the WWTP effluents. The alumina Anodisc 47[®] membrane was found to remove significantly higher amounts of ARGs ($p = 0.01$) than the Durapore PVDF membrane. Colloids were also found to have a significant effect in the DNA removal ($p < 0.05$). Although higher TOC, protein, and polysaccharide removal was also observed for the alumina membrane, there was no significant difference in the removal between the two membrane types ($p > 0.05$) for these colloidal components. Figure 4.55 - Figure 4.57 compare the removal of the *bla*_{TEM}, *vanA*, and 16S rRNA genes from the spiked WWTP. In addition, a comparison between the DNA removal from spiked buffer by both membranes is shown in Figure 4.58.

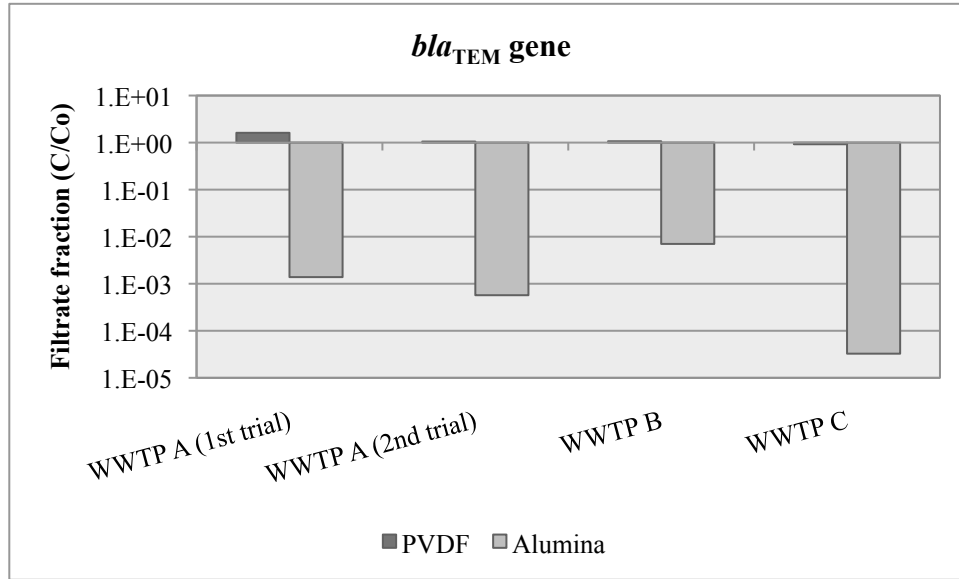


Figure 4.55. Comparison between 0.1 μm pore size PVDF and alumina membranes for the removal of *bla*_{TEM} genes. Numerical values provided in Appendix A, **Table A 15**.

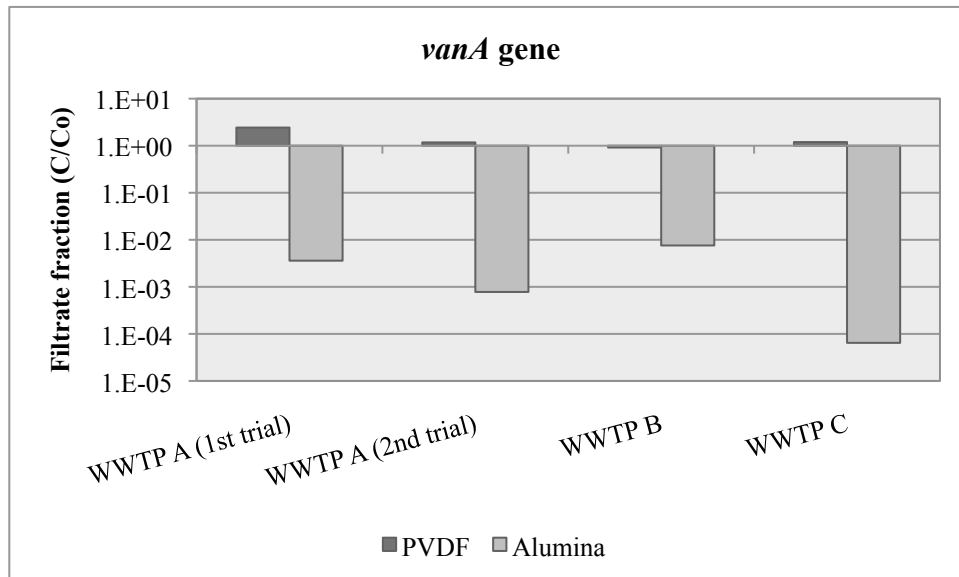


Figure 4.56. Comparison between 0.1 μm pore size PVDF and alumina membranes for the removal of *vanA* genes. Numerical values provided in Appendix A, **Table A 15**.

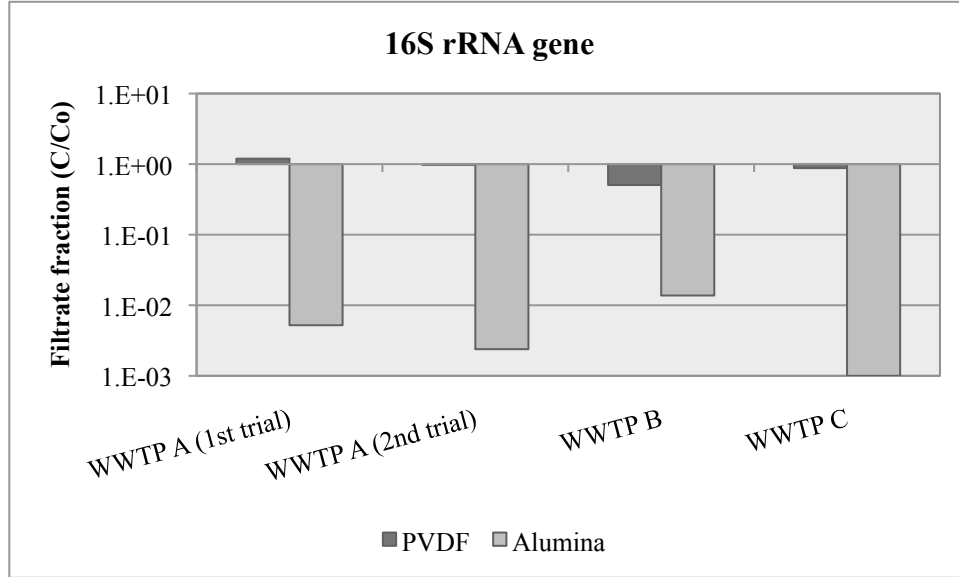


Figure 4.57. Comparison between 0.1 μm pore size PVDF and alumina membranes for the removal of 16S rRNA genes. Numerical values provided in Appendix A, **Table A 15**.

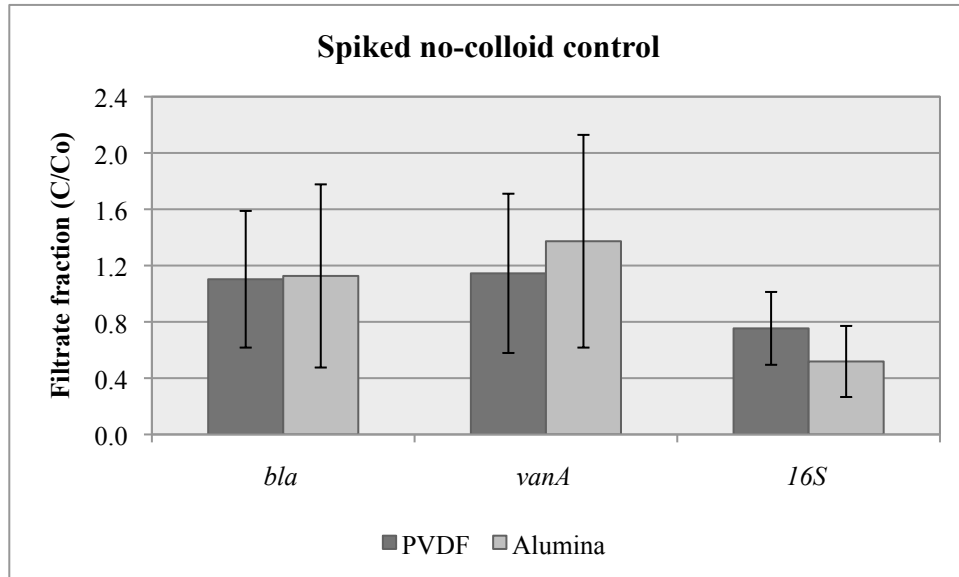


Figure 4.58. Filtrate fraction of spiked buffer after 0.1 μm PVDF or Alumina membrane filtration. Measurements obtained from spiked control buffer during the four filtration experiments were compiled and averaged. Numerical values are provided in **Table A 16**.

5. EFFECT OF WASTEWATER COLLOIDS ON MEMBRANE REMOVAL OF MICROCONSTITUENT ARGs: DISCUSSION AND CONCLUSIONS

As Environmental Engineers, it is our moral responsibility to devise treatment technologies that will not only meet current regulations, but that will also protect the public and the environment from anthropogenically generated emerging contaminants. In this matter, developing a treatment process to limit the dissemination of anthropogenic sources of ARGs requires much deeper knowledge than the fundamental fact that DNA can range from hundreds to millions of Daltons in molecular weight. In fact, the effective size of DNA for membrane retention is much smaller than it would be predicted based only on its molecular weight. This is because DNA is a flexible molecule that could easily squeeze through a membrane pore presumed to be smaller than the molecule itself. In spite of this, DNA conformation and behavior can widely vary depending on water chemistry and composition. Some of these changes and interactions could be advantageous in the membrane retention of ARGs.

Previous reports provide evidence of interactions between DNA and organic and inorganic materials that are likely present in wastewaters and also in natural waters. These naturally occurring interactions could be used to our advantage in the design of energy efficient ARG-retaining systems. The purpose of this project, therefore, was to study the effect of wastewater colloids on the membrane removal of ARGs. Available studies regarding the sorption of DNA to colloids have been done in simplified artificial systems, and for this reason, it is difficult to predict how DNA would behave in a more complex medium such as WWTP effluent. This task was undertaken through this project by attempting to answer basic questions regarding the degradability of DNA in WWTP effluent, and the effect of colloidal material on its removal by membrane filtration.

Effluent from three WWTPs was collected and used as natural colloid-containing medium in our tests. Two key points necessary for the experimental design of this and future experiments were DNA sorption time and plasmid spike concentration. According to the literature, DNA has been found to bind to a variety of organic and inorganic materials including

different soil colloidal particles, different types of clay, and NOM (13-15, 18, 39-41). However, DNA sorption behavior not only varies with type of sorbent, but also with pH, ionic strength, type of cations present and DNA conformation (14, 36, 39, 41, 51). For this reason, it is not possible to generate sorption isotherms that would be consistent across effluents. Even within one WWTP effluent, the composition would likely change daily. Based on sorption times reported in the literature (36) and on traditional WWTP retention times, a 4-hour sorption time was chosen to allow the DNA to interact with colloidal material in the wastewater effluent.

5.1. DNA DEGRADATION

Because it is possible that DNA could be degraded in the wastewater after plasmid spiking, it was necessary to perform a degradation test to account for alternative sources of DNA loss. These degradation tests were applied to all of the WWTP effluents to account for the possibility of changing wastewater characteristics and, thus, varying DNA degradability. The degradation test results showed consistently negligible DNA degradation in all of the WWTP effluents, and for this reason, the following conclusions were drawn:

- DNA readily associated with colloidal material in the wastewater, which protected it from degradation by nucleases and other potential stressors.
- Because there is negligible DNA degradation, any ARG removal after filtration can be attributed to either direct size exclusion of the DNA by the membrane, retention of the colloid-sorbed DNA, or interactions with the membrane itself.

A higher concentration of native DNA was observed in WWTP A (1st trial) effluent than in all other effluents tested. Interestingly, high ARG concentrations were also observed as presented in Figure 4.1 - Figure 4.2. However, as the 16S rRNA gene concentrations decreased with each filtration step, *bla*_{TEM} and *vanA* gene concentration remained relatively constant (See Figure 4.13). This suggests that cross-contamination occurred during this experiment, even though the experimental blank remained uncontaminated. If contamination occurred during this experiment, it most likely happened during freeze-drying. Membrane-caused contamination is unlikely because the membranes were thoroughly cleaned between uses.

5.2. POST-FILTRATION DNA QUANTIFICATION

Recent studies have showed trends of DNA transmission through UF membranes at different ionic strengths, pH, and pressure (3, 29). For this reason, the ionic strength of the no-colloid control, as well as the working pressure for all UF membranes were kept constant throughout the experiments of this study.

Filtration experiment results showed a statistically positive effect of the presence of colloids on the removal of the *bla*_{TEM} and *vanA* genes that were present in the spiked plasmids. Size exclusion of free DNA by a 1 kDa pore size membrane was expected but not observed for the spiked plasmids as shown in Figure 4.18, Figure 4.19, Figure 4.21, Figure 4.22, Figure 4.24, and Figure 4.25. However, greater removal of colloid-associated DNA was observed by the same pore size membrane. These results support the previous conclusion regarding DNA interactions with wastewater colloids and support the possibility less energy intense WWTP polishing step capable of removing low molecular weight ARGs and, likely, other emerging contaminants. Although the results of the 1st trial WWTP A filtration experiment indicated a contrasting effect in the presence of colloidal material, two possibilities can be considered:

- Partial DNA degradation was observed in the no-colloid control buffer associated with this experiment. It is possible that the DNA in the no-colloid control buffer further degraded during filtration, thus giving the appearance of a higher membrane removal than actual.
- A higher concentration of native DNA was already present in the WWTP effluent (1 – 2 orders of magnitude higher 16S rRNA genes compared to the other three effluents), and the DNA sorption sites had already become saturated, so the spiked DNA did not significantly interact with the colloids and remained free.

The latter possibility can be supported by the fact that the 16S rRNA genes were observed to be removed more efficiently in the WWTP effluent than in the spiked buffer as shown in Figure 4.17. A second trial using effluent from the same WWTP (WWTP A 2nd trial) showed results consistent to those obtained from the remaining two WWTPs (WWTP B and WWTP C), though the effluents used for the last three experiments also contained lower native DNA concentrations.

Although it was originally preferred to spike plasmid DNA alone, it was not possible to remove a small fraction (3×10^{-4} 16S rRNA to *bla*_{TEM} gene ratio) of genomic competent *E. coli* DNA from the plasmid DNA extract as determined by qPCR measurements (See Figure 2.3). This chromosomal DNA fraction was inevitably spiked along with the plasmid DNA. Except for the case of WWTP A (1st trial), the presence of colloidal material was not observed to have an effect on the removal of spiked 16S rRNA genes. Based on statistical analyses, the effect of colloids on ARG membrane-removal was not significant. It is possible that the plasmid DNA became preferentially bound to the colloidal material while the chromosomal DNA remained supercoiled and free. However, it is also likely that the spiked genomic DNA concentration was too low and close to the limit of quantification (5×10^2 gene copies/ μ l for 16S rRNA genes) for the rest of the WWTPs, and thus it was difficult to detect significant differences in DNA removal. In general, the limit of quantification is higher for 16S rRNA genes than for other, less commonly occurring genes such as ARGs, because background sources can be easily amplified and mask low 16S rRNA gene concentrations.

An additional observation regarding the removal of genomic DNA in the presence versus the absence of colloids is shown in Figure 4.23 and Figure 4.26, where the 16S rRNA genes appeared to be removed more effectively from buffer samples than from WWTP effluent samples by 10 and 1 kDa membranes. This could be due to differences in DNA size and conformation. In other words, it is likely that the spiked DNA was relatively intact and unfragmented, while native wastewater DNA may have been subjected to fragmenting weathering and enzymatic cleavage. This could have caused the spiked DNA to be retained more effectively by UF membranes that otherwise allowed smaller DNA fractions to pass through.

In addition to the results obtained from this study supporting the positive effect of wastewater colloids on the removal of ARGs, a recent study also showed significantly higher ARB and ARG removals from wastewater after treatment with a membrane bioreactor when compared to conventional treatment (37). This further substantiates the idea of DNA-colloid interactions, because based purely on molecular weight, a conventional MBR system would not be expected to significantly remove extracellular ARGs from wastewaters.

5.3. COLLOID CHARACTERIZATION AND CORRELATION ANALYSES

The characterization of the colloidal components of the wastewater was done in terms of the TOC, protein, and polysaccharide composition. In addition, correlation tests were done in order to quantify the relationship between ARG removal and the removal of each of the mentioned colloidal components. Two particularly key points can be made regarding the colloidal composition: First, the highest TOC and protein concentrations were associated with the WWTP effluent containing the highest native DNA concentrations (WWTP A 1st trial). This is in agreement with the fact that DNA is an important structural component of the EPS holding biofilms together; high concentrations of which should be expected to be present in WWTP waters. This suggests that the interactions taking place in the wastewater are complex and involve the agglomeration of different materials, rather than the simple interaction between DNA and individual particles. Lower native DNA concentrations were found in the remaining WWTP effluents, including the effluent collected for the 2nd trial of the WWTP A experiment. Second, there was a statistically significant correlation between the removal of the colloidal components and the removal of ARGs (See Table 4.1 for Pearson correlation coefficients and their associated p-values). The similarities among these correlations are in agreement with the previous statement that agglomerations between different materials are taking place, and that DNA is not interacting with one specific material in the wastewater.

A particle size distribution characterization of the different filtrate fractions was attempted by taking SEM images of the filtrate samples; however, it was not possible to achieve a sample preparation in which the wastewater components did not aggregate. Dynamic light scattering (DLS) was also attempted for the same purpose; however, poor results were obtained for two reasons: First, the filtered WWTP effluent samples were too dilute for detection using this methodology; and second, the particle size distribution in each of the fractions was too broad for DLS requirements.

A few conclusions were made from the SEM images presented in Chapter 4: First, the freeze-dried 1 kDa filtrate is characterized by a higher proportion of polymeric substances compared to the larger membrane pore-size filtrates. This is likely due to the more flexible nature of these polymeric substances and, therefore, their higher transmission through UF membranes. In this regard, if the DNA interacts with highly flexible polymeric substances in the wastewater,

its removal may not necessarily become enhanced by membrane filtration. Second, particles that appear to be larger than expected based on membrane pore sizes can be seen in ultra-membrane filtrates. This effect could either be due to the particles becoming coated by salts or polymeric substances during sample preparation, or to larger particles actually passing through the membranes due to their high flexibility.

When devising a membrane filtration process for the removal of molecular contaminants such as ARGs, it is not enough to consider the size or molecular weight of these contaminants only, but also their response to environment characteristics such as temperature, pH, ionic strength, etc. For example, as mentioned previously the conformation of DNA, its degradability, and its sorption behavior can change dramatically depending on what cations, if any, are present in the medium. It is also essential to consider the presence and effect of other materials, such as colloids, in the wastewater, and their interaction with the contaminant. In the presence of divalent cations, for example, DNA sorbs more strongly to a variety of materials (39, 41).

5.4. COMPARISON BETWEEN PVDF AND ALUMINA MEMBRANES

A comparison was made between two different membrane types, alumina and PVDF, of the same reported pore size. It was interesting to find that the removal of ARGs was significantly enhanced both in the presence of colloids and by the use of the alumina membrane. Although DNA has been previously reported to interact with alumina and aluminum species at intermediate pHs (26, 33), the removal of DNA in the absence of colloidal material was negligible as shown in Figure 4.58. This suggests that DNA-alumina interactions may not be a significant factor affecting the enhanced DNA removal by alumina membranes. Although an enhanced colloid-component removal by the alumina membrane was observed, this effect was not found to be significant ($p > 0.05$). It is possible, however, that the observed decreased transmission of TOC, proteins, and polysaccharides was due to interactions between alumina and these materials, and was therefore responsible for the enhanced ARG removal.

One of the reported attributes of the Anodisc alumina membrane is that it is made of a non-deformable material with no crossover between individual pores. It is possible that although the reported pore size of the PVDF membrane was the same as that of the alumina membrane (0.1 μm), either the variability of the pore size was higher and reached pore sizes above 0.1 μm ,

or there were crossovers among the pores. It is also possible that the PVDF membrane was slightly deformable, thus allowing the transmission of larger particles.

5.5. SUMMARY AND CONCLUSIONS

This research represents an important stepping-stone in the understanding of naturally occurring interactions between DNA and colloidal material present in WWTP effluents. Previous reports of DNA-colloid interactions, DNA protection against degradation, and the role of eDNA as a structural component of EPS, were supported by our experiments. Evidence obtained from this study supporting DNA-colloid interactions included a significant correlation between the removal of DNA and the removal of ARGs, the significant effect of colloids on the removal of ARGs, and the low degradability of DNA in the WWTP effluent. A graphical representation of these DNA-colloid interactions is shown in Figure 5.1.

The most direct solution for the problem of antibiotic resistance would be the discontinued use of antibiotics; however, the use of these “miraculous” drugs is necessary for saving lives and will most likely continue to exist in our futures. For this reason, it is not enough to practice the responsible use of antibiotics and hospital hygiene; but it is necessary and essential to develop enhanced treatment processes for limiting the dissemination of anthropogenic sources of ARGs into the environment. The reducing rate of new antibiotic discovery further underscores the need to investigate alternative strategies to contain resistance.

The application of a membrane filtration polishing step in wastewater treatment would not only help alleviate the problem of the spread of ARGs, but would also extend to the potential removal of other colloid associated environmental pollutants such as pharmaceuticals (e.g. antibiotics, estrogenic compounds, etc.) and their metabolites, other DNA contaminants such as virulence genes and viruses, nanomaterials, etc. In addition, the physical removal of bacterial cells would eliminate the potential for DNA protection and downstream gene transfer, and of the amplification of resistant or pathogenic microorganisms in the environment.

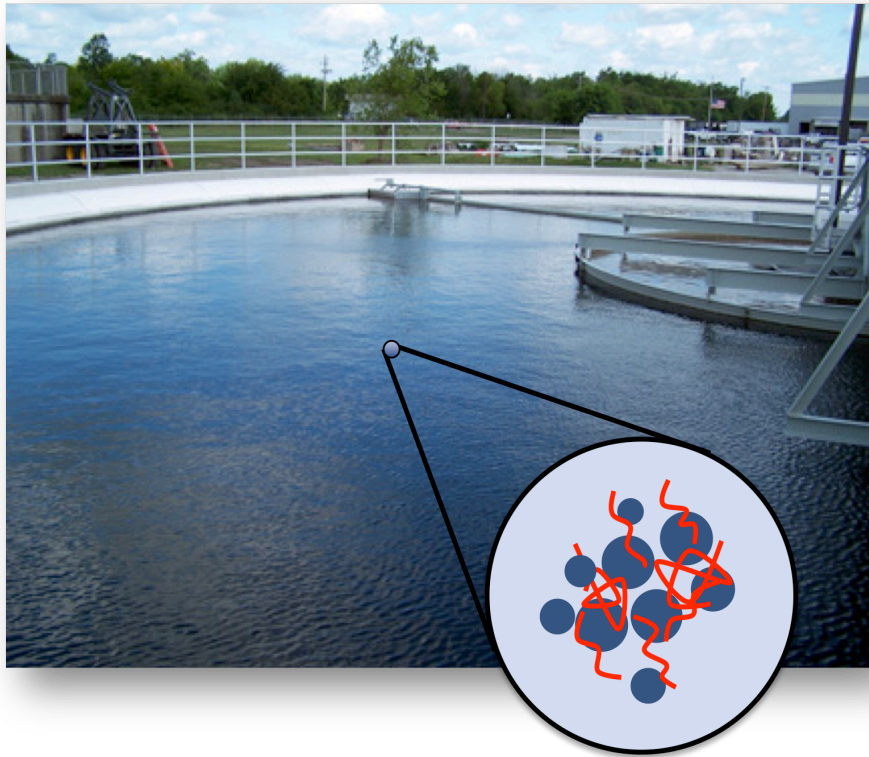


Figure 5.1. Graphical representation of DNA-colloid interactions in wastewater. Blue circles represent colloidal material in the wastewater. Red lines represent eDNA in a stable sorbed state. WWTP clarifier image obtained from the St. Peters, MO website on August 2011 and used under fair use, 2011 (<http://www.stpetersmo.net/wastewater.aspx>) (16).

5.6. UNANSWERED QUESTIONS

A few points raised during this study require further attention. Most of these have been a long-lasting question for many scientists and are currently under investigation:

- Discriminating between extracellular and intracellular DNA in a dilute medium; and, accordingly, estimating the extent of eDNA in wastewater effluents.
- Characterizing the colloid size distribution in the WWTP effluent
- Better understanding the differences between chromosomal DNA sorption and plasmid DNA interactions with colloids.

REFERENCES

1. **Alanis, A. J.** 2005. Resistance to antibiotics: Are we in the post-antibiotic era? *Archives of Medical Research* **36**:697-705.
2. **Aminov, R. I., and R. I. Mackie.** 2007. Evolution and ecology of antibiotic resistance genes. *Fems Microbiology Letters* **271**:147-161.
3. **Arkhangelsky, E., B. Steubing, E. Ben-Dov, A. Kushmaro, and V. Gitis.** 2008. Influence of pH and ionic strength on transmission of plasmid DNA through ultrafiltration membranes. *Desalination* **227**:111-119.
4. **Armstrong, J. L., J. J. Calomiris, and R. J. Seidler.** 1982. Selection of antibiotic-resistant standard plate-count bacteria during water treatment. *Applied and Environmental Microbiology* **44**:308-316.
5. **Auerbach, E. A., E. E. Seyfried, and K. D. McMahon.** 2007. Tetracycline resistance genes in activated sludge wastewater treatment plants. *Water Research* **41**:1143-1151.
6. **AWWA.** 2005. Microfiltration and ultrafiltration membranes for drinking water. Glacier Publishing Services.
7. **Baquero, F., J. L. Martinez, and R. Canton.** 2008. Antibiotics and antibiotic resistance in water environments. *Current Opinion in Biotechnology* **19**:260-265.
8. **Bennett, P. M.** 2008. Plasmid encoded antibiotic resistance: Acquisition and transfer of antibiotic resistance genes in bacteria. *British Journal of Pharmacology* **153**:S347-S357.
9. **Bibbal, D., V. Dupouy, J. P. Ferre, P. L. Toutain, O. Fayet, M. F. Prere, and A. Bousquet-Melou.** 2007. Impact of three ampicillin dosage regimens on selection of ampicillin resistance in *Enterobacteriaceae* and excretion of *bla*_{TEM} genes in swine feces. *Applied and Environmental Microbiology* **73**:4785-4790.
10. **Bockelmann, U., H. H. Dorries, M. N. Ayuso-Gabella, M. S. de Marçay, V. Tandoi, C. Levantesi, C. Masciopinto, E. Van Houtte, U. Szewzyk, T. Wintgens, and E. Grohmann.** 2009. Quantitative PCR monitoring of antibiotic resistance genes and bacterial pathogens in three European artificial groundwater recharge systems. *Applied and Environmental Microbiology* **75**:154-163.
11. **Borjesson, S., A. Matussek, S. Melin, S. Lofgren, and P. E. Lindgren.** 2010. Methicillin-resistant *Staphylococcus aureus* (MRSA) in municipal wastewater: An uncharted threat? *Journal of Applied Microbiology* **108**:1244-1251.
12. **Boto, L.** 2010. Horizontal gene transfer in evolution: Facts and challenges. *Proceedings of the Royal Society B-Biological Sciences* **277**:819-827.
13. **Cai, P., Q. Huang, W. Chen, D. Zhang, K. Wang, D. Jiang, and W. Liang.** 2007. Soil colloids-bound plasmid DNA: Effect on transformation of *E. coli* and resistance to DNase I degradation. *Soil Biology & Biochemistry* **39**:1007-1013.
14. **Cai, P., Q. Huang, X. Zhang, and H. Chen.** 2006. Sorption of DNA on clay minerals and various colloidal particles from an Alfisol. *Soil Biology & Biochemistry* **38**:471-476.

15. **Cai, P., Q. Y. Huang, and X. W. Zhang.** 2006. Interactions of DNA with clay minerals and soil colloidal particles and protection against degradation by DNase. *Environmental Science & Technology* **40**:2971-2976.
16. **City of St. Peters, MO.** 2010, posting date. City of St. Peters wastewater treatment plant. [Online.]
17. **Corinaldesi, C., R. Danovaro, and A. Dell'Anno.** 2005. Simultaneous recovery of extracellular and intracellular DNA suitable for molecular studies from marine sediments. *Applied and Environmental Microbiology* **71**:46-50.
18. **Crecchio, C., and G. Stotzky.** 1998. Binding of DNA on humic acids: Effect on transformation of *Bacillus subtilis* and resistance to DNase. *Soil Biology and Biochemistry* **30**:1061-1067.
19. **Das, T., P. K. Sharma, H. J. Busscher, H. C. van der Mei, and B. P. Krom.** 2010. Role of extracellular DNA in initial bacterial adhesion and surface aggregation. *Applied and Environmental Microbiology* **76**:3405-3408.
20. **Dubois, M., K. A. Gilles, J. K. Hamilton, P. A. Rebers, and F. Smith.** 1956. Colorimetric Method for Determination of Sugars and Related Substances. *Analytical Chemistry* **28**:350-356.
21. **Dutka-Malen, S., S. Evers, and P. Courvalin.** 1995. Detection of glycopeptide resistance genotypes and identification to the species level of clinically relevant *Enterococci* by PCR. *Journal of Clinical Microbiology* **33**:24-27.
22. **Engleberg, N. C., DiRita, V., and Dermody, T.S.** 2007. Schaechter's mechanisms of microbial disease, 4th ed. Lippincott Williams and Wilkins.
23. **Gogarten, J. P., W. F. Doolittle, and J. G. Lawrence.** 2002. Prokaryotic evolution in light of gene transfer. *Molecular Biology and Evolution* **19**:2226-2238.
24. **Huang, C.-H., J. E. Renew, K. L. Smeby, K. Pinkston, and D. L. Sedlak.** 2011. Assessment of potential antibiotic contaminants in water and preliminary occurrence analysis. *Journal of Contemporary Water Research and Education* **120**.
25. **Jayaraman, R.** 2009. Antibiotic resistance: An overview of mechanisms and a paradigm shift. *Current Science* **96**:1475-1484.
26. **Karlik, S. J., G. L. Eichhorn, P. N. Lewis, and D. R. Crapper.** 1980. Interaction of aluminum species with deoxyribonucleic-acid. *Biochemistry* **19**:5991-5998.
27. **Khanna, M., and G. Stotzky.** 1992. Transformation of *Bacillus subtilis* by DNA bound on montmorillonite and effect of DNase on the transforming ability of bound DNA. *Applied and Environmental Microbiology* **58**:1930-1939.
28. **Koonin, E. V., K. S. Makarova, and L. Aravind.** 2001. Horizontal gene transfer in prokaryotes: Quantification and classification. *Annual Review of Microbiology* **55**:709-742.
29. **Latulippe, D. R., and A. L. Zydney.** 2008. Salt-induced changes in plasmid DNA transmission through ultrafiltration membranes. *Biotechnology and Bioengineering* **99**:390-398.
30. **Linz, S., A. Radtke, and A. von Haeseler.** 2007. A likelihood framework to measure horizontal gene transfer. *Molecular Biology and Evolution* **24**:1312-1319.
31. **Lorenz, M. G., and W. Wackernagel.** 1987. Sorption of DNA to sand and variable degradation rates of sorbed DNA. *Applied and Environmental Microbiology* **53**:2948-2952.

32. **Lowry, O. H., N. J. Rosebrough, A. L. Farr, and R. J. Randall.** 1977. Protein measurement with folin phenol reagent. *Current Contents*:7-7.
33. **Ma, C. B., and E. S. Yeung.** 2010. Entrapment of individual DNA molecules and nanoparticles in porous alumina membranes. *Analytical Chemistry* **82**:654-657.
34. **Masters, G. M., and W. P. Ella.** 2008. *Introduction to Environmental Engineering and Science*, Third ed. Pearson Education.
35. **Mathew, A. G., R. Cissell, and S. Liamthong.** 2007. Antibiotic resistance in bacteria associated with food animals: A United States perspective of livestock production. *Foodborne Pathogens and Disease* **4**:115-133.
36. **Mitra, A., P. Chakraborty, and D. K. Chattoraj.** 2001. Kinetics of sorption of DNA at solid-liquid interfaces. *Journal of the Indian Chemical Society* **78**:689-696.
37. **Munir, M., K. Wong, and I. Xagorarakis.** 2011. Release of antibiotic resistant bacteria and genes in the effluent and biosolids of five wastewater utilities in Michigan. *Water Research* **45**:681-693.
38. **Murray, G. E., R. S. Tobin, B. Junkins, and D. J. Kushner.** 1984. Effect of chlorination on antibiotic-resistance profiles of sewage-related bacteria. *Applied and Environmental Microbiology* **48**:73-77.
39. **Nguyen, T. H., K. L. Chen, and M. Elimelech.** 2010. Sorption kinetics and reversibility of linear plasmid DNA on silica surfaces: Influence of alkaline earth and transition metal ions. *Biomacromolecules* **11**:1225-1230.
40. **Nguyen, T. H., and M. Elimelech.** 2007. Sorption of plasmid DNA to a natural organic matter-coated silica surface: Kinetics, conformation, and reversibility. *Langmuir* **23**:3273-3279.
41. **Nguyen, T. H., and M. Elimelech.** 2007. Plasmid DNA sorption on silica: Kinetics and conformational changes in monovalent and divalent salts. *Biomacromolecules* **8**:24-32.
42. **Ochman, H., J. G. Lawrence, and E. A. Groisman.** 2000. Lateral gene transfer and the nature of bacterial innovation. *Nature* **405**:299-304.
43. **Ogeer-Gyles, J. S., K. A. Mathews, and P. Boerlin.** 2006. Nosocomial infections and antimicrobial resistance in critical care medicine. *Journal of Veterinary Emergency and Critical Care* **16**:1-18.
44. **Pal, C., B. Papp, and M. J. Lercher.** 2005. Adaptive evolution of bacterial metabolic networks by horizontal gene transfer. *Nature Genetics* **37**:1372-1375.
45. **Pei, R. T., S. C. Kim, K. H. Carlson, and A. Pruden.** 2006. Effect of river landscape on the sediment concentrations of antibiotics and corresponding antibiotic resistance genes (ARG). *Water Research* **40**:2427-2435.
46. **Philpott, J.** 2011. *Antibiotresist*. The Science Creative Quarterly.
47. **Pietramellara, G., J. Ascher, F. Borgogni, M. T. Ceccherini, G. Guerri, and P. Nannipieri.** 2009. Extracellular DNA in soil and sediment: Fate and ecological relevance. *Biology and Fertility of Soils* **45**:219-235.
48. **Pote, J., P. Mavingui, E. Navarro, W. Rosselli, W. Wildi, P. Simonet, and T. M. Vogel.** 2009. Extracellular plant DNA in Geneva groundwater and traditional artesian drinking water fountains. *Chemosphere* **75**:498-504.
49. **Pruden, A., R. T. Pei, H. Storteboom, and K. H. Carlson.** 2006. Antibiotic resistance genes as emerging contaminants: Studies in northern Colorado. *Environmental Science & Technology* **40**:7445-7450.

50. **Romanowski, G., M. G. Lorenz, and W. Wackernagel.** 1991. Sorption of plasmid DNA to mineral surfaces and protection against DNaseI. *Applied and Environmental Microbiology* **57**:1057-1061.
51. **Saeki, K., T. Kunito, and M. Sakai.** 2010. Effects of pH, ionic strength, and solutes on DNA sorption by andosols. *Biology and Fertility of Soils* **46**:531-535.
52. **Schwartz, T., W. Kohnen, B. Jansen, and U. Obst.** 2003. Detection of antibiotic-resistant bacteria and their resistance genes in wastewater, surface water, and drinking water biofilms. *Fems Microbiology Ecology* **43**:325-335.
53. **Seveno, N. A., D. Kallifidas, K. Smalla, J. D. van Elsas, J. M. Collard, A. D. Karagouni, and E. M. H. Wellington.** 2002. Occurrence and reservoirs of antibiotic resistance genes in the environment. *Reviews in Medical Microbiology* **13**:15-27.
54. **Shrivastava, R., R. K. Upreti, S. R. Jain, K. N. Prasad, P. K. Seth, and U. C. Chaturvedi.** 2004. Suboptimal chlorine treatment of drinking water leads to selection of multidrug-resistant *Pseudomonas aeruginosa*. *Ecotoxicology and Environmental Safety* **58**:277-283.
55. **Snyder, L., and W. Champness.** 2007. *Molecular genetics of bacteria*, Third ed. ASM Press.
56. **Sostarich, A. M., D. Zolldann, H. Haefner, R. Luetticken, R. Schulze-Roebecke, and S. W. Lemmen.** 2008. Impact of multiresistance of gram-negative bacteria in bloodstream infection on mortality rates and length of stay. *Infection* **36**:31-35.
57. **Spellberg, B.** 2010. Antibiotic resistance: Promoting critically needed antibiotic research and development and appropriate use ("stewardship") of these precious drugs, Testimony of the Infectious Diseases Society of America (IDSA).
58. **Storteboom, H., M. Arabi, J. G. Davis, B. Crimi, and A. Pruden.** 2010. Identification of antibiotic-resistance-gene molecular signatures suitable as tracers of pristine river, urban, and agricultural sources. *Environmental Science & Technology* **44**:1947-1953.
59. **Summers, A. O.** 2002. Generally overlooked fundamentals of bacterial genetics and ecology. *Clinical Infectious Diseases* **34**:S85-S92.
60. **Suzuki, M. T., L. T. Taylor, and E. F. DeLong.** 2000. Quantitative analysis of small-subunit rRNA genes in mixed microbial populations via 5'-nuclease assays. *Applied and Environmental Microbiology* **66**:4605-4614.
61. **Tetz, V. V., and G. V. Tetz.** 2010. Effect of extracellular DNA destruction by DNase I on characteristics of forming biofilms. *DNA and Cell Biology* **29**:399-405.
62. **USEPA.** 2005. Membrane filtration guidance manual. *In* U. E. P. A. O. o. Water (ed.), Cincinnati.
63. **Viola, C., and S. J. DeVincent.** 2006. Overview of issues pertaining to the manufacture, distribution, and use of antimicrobials in animals and other information relevant to animal antimicrobial use data collection in the United States. *Preventive Veterinary Medicine* **73**:111-131.
64. **Volkman, H., T. Schwartz, P. Bischoff, S. Kirchen, and U. Obst.** 2004. Detection of clinically relevant antibiotic-resistance genes in municipal wastewater using real-time PCR (TaqMan). *Journal of Microbiological Methods* **56**:277-286.
65. **WEF.** 2006. *Membrane systems for wastewater treatment*. McGraw-Hill

66. **Wu, J. F., and C. W. Xi.** 2009. Evaluation of different methods for extracting extracellular DNA from the biofilm matrix. *Applied and Environmental Microbiology* **75**:5390-5395.
67. **Xi, C. W., Y. L. Zhang, C. F. Marrs, W. Ye, C. Simon, B. Foxman, and J. Nriagu.** 2009. Prevalence of antibiotic resistance in drinking water treatment and distribution systems. *Applied and Environmental Microbiology* **75**:5714-5718.
68. **Zeman, L. J., and A. L. Zydney.** 1996. *Microfiltration and ultrafiltration: Principles and applications.* Marcel Dekker, INC.
69. **Zhang, Y. L., C. F. Marrs, C. Simon, and C. W. Xi.** 2009. Wastewater treatment contributes to selective increase of antibiotic resistance among *Acinetobacter* spp. *Science of the Total Environment* **407**:3702-3706.

APPENDIX A

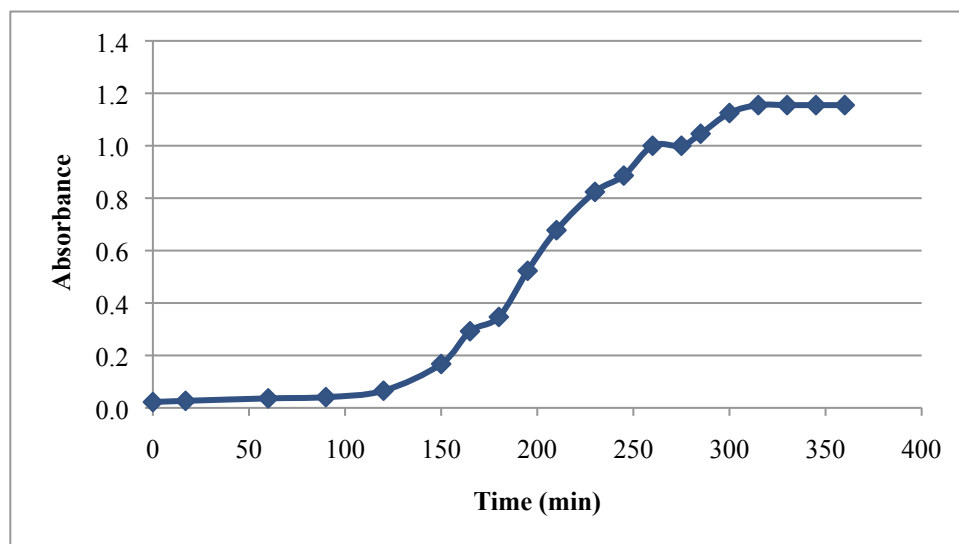


Figure A 1. *E. coli* growth curve.

Table A 1. Gene concentrations reported in Figure 2.3.

Plasmid extraction product	Gene copies/ μ l plasmid extraction product		
	<i>bla</i> _{TEM}	<i>vanA</i>	16S rRNA
Mini 1	3.94E+10	4.44E+10	4.54E+05
Mini 2	4.23E+10	3.94E+10	2.93E+05
Mini 3	8.94E+10	7.38E+10	5.55E+05
Mini 4	4.20E+10	3.80E+10	6.49E+05
Mini 5	1.79E+10	*	9.28E+06
Mini 6	3.43E+10	*	6.43E+07
Mini 7	9.03E+10	*	1.27E+09
Mini 8	4.15E+11	2.80E+11	7.23E+07
Mini 9	5.01E+11	3.42E+11	9.55E+07
Mini 10	4.91E+11	3.53E+11	7.54E+07
Mini 11	1.12E+12	4.99E+11	9.92E+07
Mini 12	4.54E+11	2.50E+11	3.02E+07
Mini 13	2.92E+11	1.87E+11	4.45E+07
Mega 1	4.00E+11	1.08E+11	1.19E+08

* Data not available

Table A 2. Degradation values reported in **Figure 2.4 - Figure 2.6.**

Sample	Time (hr)	Gene copies/ μ l sample		
		<i>bla</i> _{TEM}	<i>vanA</i>	16S rRNA
PBS + Plasmids	1	1.57E+06	3.16E+05	9.90E+01
PBS + Plasmids	2.5	2.07E+06	4.73E+05	2.34E+02
PBS + Plasmids	4	4.07E+06	6.97E+05	2.03E+02
PBS + Plasmids + Cells	1	3.21E+07	7.19E+06	1.47E+07
PBS + Plasmids + Cells	2.5	6.00E+07	1.11E+07	1.58E+07
PBS + Plasmids + Cells	4	4.67E+07	8.80E+06	1.17E+07
WWTP effluent + Plasmids	1	1.01E+07	7.96E+05	1.06E+03
WWTP effluent + Plasmids	2.5	2.41E+07	7.58E+05	2.82E+03
WWTP effluent + Plasmids	4	1.19E+07	2.44E+05	3.08E+03

Table A 3. Numerical values used to create **Figure 2.7 - Figure 2.11.**

Concentration method	Sample	Gene copies/ μ l sample		
		<i>bla</i> _{TEM}	<i>vanA</i>	16S rRNA
Silica sorption + Centrifugation	PBS	7.34E+01	0.00E+00	0.00E+00
	PBS+plasmid	5.41E+02	9.17E+01	0.00E+00
	PBS+cells+plasmid	4.47E+04	9.02E+03	9.83E+03
	Wastewater	4.79E+02	0.00E+00	0.00E+00
	WW+plasmid	1.37E+04	2.32E+02	4.37E+01
Filtration	PBS	1.41E+02	1.08E+01	0.00E+00
	PBS+plasmid	3.97E+04	8.86E+03	0.00E+00
	PBS+cells+plasmid	1.42E+05	3.40E+04	9.87E+05
	Wastewater	8.53E+01	1.19E+01	0.00E+00
	WW+plasmid	1.60E+04	1.13E+03	2.07E+02
Silica sorption + Filtration	PBS	4.42E+01	1.28E+01	0.00E+00
	PBS+plasmid	1.14E+05	2.15E+04	0.00E+00
	PBS+cells+plasmid	9.22E+06	1.79E+06	1.95E+06
	Wastewater	4.55E+02	1.07E+02	2.43E+01
	WW+plasmid	4.30E+05	1.32E+04	5.13E+01
Freeze drying	PBS	1.05E+02	2.18E+01	1.91E+01
	PBS+plasmid	4.07E+06	6.97E+05	2.03E+02
	PBS+cells+plasmid	4.67E+07	8.80E+06	1.17E+07
	Wastewater	1.87E+02	3.86E+01	2.05E+03
	WW+plasmid	1.19E+07	2.44E+05	3.08E+03

Table A 4. qPCR quantification results shown in **Figure 2.12**.

Sample	Gene copies/ μ l sample	
	<i>bla</i> _{TEM}	<i>vanA</i>
Spk buffer: Resuspended	2.17E+06	1.73E+05
Spk buffer: Extracted	8.73E+03	6.82E+02
Spk buffer: Purified	5.85E+05	4.75E+04
Spk WWTP A: Extracted	1.38E+06	1.10E+05
Spk WWTP A: Purified	1.94E+04	1.08E+03

Table A 5. qPCR quantification results shown in **Figure 4.1 - Figure 4.3**.

Sample	Time (hr)	Gene copies/ μ l sample		
		<i>bla</i> _{TEM}	<i>vanA</i>	16S rRNA
Unspiked buffer	0	6.84E+02	0.00E+00	0.00E+00
	4	1.27E+00	0.00E+00	9.11E+00
Spiked no-colloid control buffer	0	5.13E+07	1.24E+07	9.06E+03
	1	2.93E+08	6.23E+07	1.24E+04
	2.5	2.11E+08	4.61E+07	8.49E+03
	4	6.58E+07	1.42E+07	9.47E+03
Unspiked WWTP A (1st trial)	0	1.72E+03	3.39E+02	1.13E+04
	1	1.48E+03	2.25E+02	1.07E+04
	2.5	1.58E+03	1.77E+02	1.23E+04
	4	4.15E+03	5.06E+02	1.23E+04
Spiked WWTP A (1st trial)	0	1.31E+08	2.82E+07	1.26E+04
	1	1.44E+08	2.69E+07	1.30E+04
	2.5	2.05E+08	3.02E+07	1.73E+04
	4	1.75E+08	2.59E+07	1.24E+04
	10	1.30E+08	1.26E+07	9.88E+03

Table A 6. qPCR quantification results shown in **Figure 4.4 - Figure 4.6.**

Sample	Time (hr)	Gene copies/ μ l sample		
		<i>bla</i> _{TEM}	<i>vanA</i>	16S rRNA
Unspiked buffer	0	0.00E+00	0.00E+00	0.00E+00
	4	0.00E+00	6.60E-01	0.00E+00
Spiked no-colloid control buffer	0	6.88E+06	8.00E+05	5.42E+02
	2	9.32E+06	1.20E+06	4.06E+02
	3	9.26E+06	1.01E+06	4.42E+02
	4	1.05E+07	1.38E+06	9.18E+02
Unspiked WWTP A (1st trial)	0	1.49E+00	3.28E+00	5.85E+01
	2	0.00E+00	3.89E-01	3.41E+01
	3	0.00E+00	3.25E-01	6.54E+01
	4	3.11E+00	5.47E-01	1.04E+02
Spiked WWTP A (1st trial)	0	6.38E+05	1.46E+05	1.15E+02
	2	1.63E+06	2.29E+05	1.33E+02
	3	1.68E+06	2.39E+05	6.89E+01
	4	1.77E+06	2.03E+05	1.75E+02
	8	1.72E+06	1.20E+05	1.53E+02

Table A 7. qPCR quantification results shown in **Figure 4.7 - Figure 4.9.**

Sample	Time (hr)	Gene copies/ μ l sample		
		<i>bla</i> _{TEM}	<i>vanA</i>	16S rRNA
Unspiked buffer	0	1.16E+01	1.32E+00	8.64E+00
	5	5.02E-01	0.00E+00	0.00E+00
Spiked no-colloid control buffer	0	1.07E+08	1.71E+07	4.97E+03
	1	1.22E+08	1.70E+07	4.97E+03
	2.5	6.83E+07	1.14E+07	3.80E+03
	5	6.52E+07	1.04E+07	4.93E+03
Unspiked WWTP B	0	3.62E+01	9.42E+00	3.65E+02
	1	2.05E+01	8.22E+00	3.10E+02
	2.5	5.09E+01	9.62E+00	5.39E+02
	5	1.72E+01	2.49E+00	4.38E+02
Spiked WWTP B	0	1.80E+07	2.40E+06	9.23E+02
	1	2.62E+07	2.92E+06	1.05E+03
	2.5	3.45E+07	3.23E+06	9.52E+02
	5	4.04E+07	4.51E+06	1.17E+03

Table A 8. qPCR quantification results shown in **Figure 4.10 - Figure 4.12.**

Sample	Time (hr)	Gene copies/ μ l sample		
		<i>bla</i> _{TEM}	<i>vanA</i>	16S rRNA
Unspiked buffer	0	0.00E+00	0.00E+00	5.85E+00
	4.5	0.00E+00	6.86E-01	1.43E+00
Spiked no-colloid control buffer	0	6.03E+07	1.83E+07	4.33E+03
	2	9.30E+07	2.66E+07	5.48E+03
	3	9.20E+07	2.53E+07	5.36E+03
	4.5	2.81E+07	8.90E+06	5.85E+03
Unspiked WWTP C	0	0.00E+00	2.97E-01	3.22E+00
	2	1.28E+00	2.19E+00	9.39E-01
	3	7.30E+00	3.40E+00	4.45E+00
	4.5	1.32E+01	2.73E+00	1.76E+00
Spiked WWTP C	0	4.13E+06	1.29E+06	6.21E+01
	2	9.09E+06	2.02E+06	1.64E+02
	3	6.10E+06	1.23E+06	1.38E+02
	4.5	1.01E+07	1.45E+06	1.84E+02
	10	3.51E+06	6.05E+05	6.83E+01

Table A 9. qPCR results and calculated values shown in **Figure 4.15 - Figure 4.26.**

WWTP ID	ID	Membrane pore size	C ₀ = Gene copies/μl before filtration			C = Filtrate concentration (gene copies/μl)			Fraction in filtrate (C/C ₀)		
			<i>bla</i> _{TEM}	<i>vanA</i>	16S rRNA	<i>bla</i> _{TEM}	<i>vanA</i>	16S rRNA	<i>bla</i> _{TEM}	<i>vanA</i>	16S rRNA
WWTP A (1st trial)	ST	0.45 μm	1.6E+08	3.4E+07	9.9E+03	1.6E+08	2.7E+07	1.2E+04	1.0E+00	8.0E-01	1.2E+00
WWTP A (1st trial)	ST	0.1 μm				9.7E+07	1.4E+07	6.7E+03	6.3E-01	4.1E-01	6.8E-01
WWTP A (1st trial)	ST	100 kDa				4.8E+05	1.3E+05	8.9E+01	3.1E-03	3.7E-03	9.1E-03
WWTP A (1st trial)	ST	10 kDa				4.9E+02	1.4E+02	2.2E+01	3.2E-06	4.1E-06	2.2E-03
WWTP A (1st trial)	ST	1 kDa				1.7E+02	4.4E+01	1.3E+01	1.1E-06	1.3E-06	1.4E-03
WWTP A (1st trial)	SW	0.45 μm	1.6E+08	2.8E+07	1.4E+04	1.2E+08	7.2E+06	1.5E+03	7.3E-01	2.6E-01	1.1E-01
WWTP A (1st trial)	SW	0.1 μm				1.9E+08	1.8E+07	1.8E+03	1.2E+00	6.3E-01	1.3E-01
WWTP A (1st trial)	SW	100 kDa				1.5E+06	1.2E+05	5.4E+01	9.1E-03	4.2E-03	3.9E-03
WWTP A (1st trial)	SW	10 kDa				2.2E+03	2.4E+02	8.7E+00	1.4E-05	8.5E-06	6.3E-04
WWTP A (1st trial)	SW	1 kDa				1.0E+03	9.3E+01	2.5E+00	6.4E-06	3.4E-06	1.8E-04
WWTP A (2nd trial)	ST	0.45 μm	9.0E+06	1.1E+06	5.8E+02	9.1E+06	1.3E+06	8.3E+02	1.0E+00	1.2E+00	1.4E+00
WWTP A (2nd trial)	ST	0.1 μm				9.9E+06	1.7E+06	4.2E+02	1.1E+00	1.6E+00	7.3E-01
WWTP A (2nd trial)	ST	100 kDa				1.9E+06	2.9E+05	2.8E+02	2.1E-01	2.7E-01	4.9E-01
WWTP A (2nd trial)	ST	10 kDa				5.9E+03	1.1E+03	6.9E+00	6.6E-04	9.8E-04	1.2E-02
WWTP A (2nd trial)	ST	1 kDa				1.5E+03	2.9E+02	8.4E+01	1.7E-04	2.6E-04	1.5E-01
WWTP A (2nd trial)	SW	0.45 μm	1.4E+06	2.0E+05	1.2E+02	3.3E+06	2.7E+05	1.8E+02	2.3E+00	1.3E+00	1.5E+00
WWTP A (2nd trial)	SW	0.1 μm				3.5E+06	3.2E+05	1.8E+02	2.4E+00	1.6E+00	1.4E+00
WWTP A (2nd trial)	SW	100 kDa				1.1E+05	1.4E+04	2.9E+01	8.0E-02	7.0E-02	2.4E-01
WWTP A (2nd trial)	SW	10 kDa				9.5E+01	1.0E+01	0.0E+00	6.7E-05	5.0E-05	0.0E+00
WWTP A (2nd trial)	SW	1 kDa				2.1E+00	2.2E-01	1.9E+01	1.5E-06	1.1E-06	1.6E-01
WWTP B	ST	0.45 μm	9.1E+07	1.4E+07	4.7E+03	1.0E+08	1.4E+07	2.7E+03	1.2E+00	1.0E+00	5.9E-01
WWTP B	ST	0.1 μm				9.7E+07	1.3E+07	2.6E+03	1.1E+00	9.1E-01	5.6E-01
WWTP B	ST	100 kDa				1.6E+07	3.3E+06	4.6E+02	1.8E-01	2.4E-01	9.8E-02
WWTP B	ST	10 kDa				1.1E+04	2.9E+03	2.6E-01	1.2E-04	2.1E-04	5.6E-05
WWTP B	ST	1 kDa				5.8E+03	6.4E+02	0.0E+00	6.4E-05	4.6E-05	0.0E+00
WWTP B	SW	0.45 μm	3.0E+07	3.3E+06	1.0E+03	5.1E+07	6.0E+06	1.2E+03	1.7E+00	1.8E+00	1.2E+00
WWTP B	SW	0.1 μm				5.4E+07	5.5E+06	6.0E+02	1.8E+00	1.7E+00	5.9E-01
WWTP B	SW	100 kDa				1.3E+05	1.5E+04	1.4E+01	4.4E-03	4.5E-03	1.4E-02

WWTP B	SW	10 kDa				3.8E+02	6.5E+01	8.8E-01	1.3E-05	2.0E-05	8.6E-04
WWTP B	SW	1 kDa				3.0E+00	5.2E-02	6.2E+00	1.0E-07	1.6E-08	6.0E-03
WWTP C	ST	0.45 μ m	6.8E+07	2.0E+07	5.3E+03	5.0E+07	1.2E+07	5.6E+03	7.3E-01	6.1E-01	1.1E+00
WWTP C	ST	0.1 μ m				8.9E+07	2.2E+07	5.5E+03	1.3E+00	1.1E+00	1.1E+00
WWTP C	ST	100 kDa				2.3E+06	5.7E+05	1.6E+02	3.4E-02	2.9E-02	3.1E-02
WWTP C	ST	10 kDa				7.1E+03	3.1E+03	1.0E+01	1.0E-04	1.6E-04	2.0E-03
WWTP C	ST	1 kDa				1.3E+03	5.7E+02	0.0E+00	2.0E-05	2.9E-05	0.0E+00
WWTP C	SW	0.45 μ m	7.4E+06	1.5E+06	1.4E+02						
WWTP C	SW	0.1 μ m				7.7E+06	1.4E+06	1.5E+02	1.0E+00	9.1E-01	1.1E+00
WWTP C	SW	100 kDa				1.8E+05	3.1E+04	2.6E+00	2.5E-02	2.1E-02	1.9E-02
WWTP C	SW	10 kDa				2.4E+01	2.1E+00	9.2E-01	3.3E-06	1.4E-06	6.7E-03
WWTP C	SW	1 kDa				3.0E+00	1.7E+00	0.0E+00	4.1E-07	1.2E-06	0.0E+00

ST = Spiked no-colloid Tris buffer

SW= Spiked WWTP effluent

Table A 10. qPCR quantified post-filtration gene concentrations in spiked and unspiked WWTPA (1st trial) and buffer samples.

Sample	Membrane pore size	Gene concentration (gene copies/ μ l)		
		<i>bla</i> _{TEM}	<i>vanA</i>	16S rRNA
Buffer blank	0.45 μ m	6.52E+00	0.00E+00	0.00E+00
	0.1 μ m	1.67E+01	0.00E+00	0.00E+00
	100 kDa	1.81E+01	1.25E+00	0.00E+00
	10 kDa	8.16E+00	0.00E+00	2.87E+00
	1 kDa	2.93E+00	1.49E+00	5.79E+00
Spiked no-colloid control buffer	0.45 μ m	1.56E+08	2.69E+07	1.22E+04
	0.1 μ m	9.74E+07	1.38E+07	6.71E+03
	100 kDa	4.78E+05	1.27E+05	8.94E+01
	10 kDa	4.93E+02	1.38E+02	2.18E+01
	1 kDa	1.66E+02	4.42E+01	1.35E+01
Unspiked WWTP A (1st trial)	0.45 μ m	1.04E+03	1.65E+02	2.29E+03
	0.1 μ m	1.27E+03	1.49E+02	4.88E+02
	100 kDa	1.61E+03	1.74E+02	4.88E+01
	10 kDa	5.60E+02	6.44E+01	2.84E+00
	1 kDa	7.73E+02	7.02E+01	0.00E+00
Spiked WWTP A (1st trial)	0.45 μ m	1.20E+08	7.20E+06	1.53E+03
	0.1 μ m	1.93E+08	1.75E+07	1.82E+03
	100 kDa	1.49E+06	1.17E+05	5.41E+01
	10 kDa	2.22E+03	2.36E+02	8.69E+00
	1 kDa	1.04E+03	9.34E+01	2.50E+00

Table A 11. qPCR quantified post-filtration gene concentrations in spiked and unspiked WWTPA (2nd trial) and buffer samples.

Sample	Membrane pore size	Gene concentration (gene copies/ μ l)		
		<i>bla</i> _{TEM}	<i>vanA</i>	16S rRNA
Unspiked buffer	0.45 μ m	0.00E+00	0.00E+00	6.79E+01
	0.1 μ m	2.04E+00	0.00E+00	0.00E+00
	100 kDa	1.33E+01	0.00E+00	1.95E+01
	10 kDa	3.93E+00	0.00E+00	9.20E+01
	1 kDa	3.91E+01	0.00E+00	4.36E+01
Spiked no-colloid control buffer	0.45 μ m	9.14E+06	1.27E+06	8.28E+02
	0.1 μ m	9.90E+06	1.71E+06	4.22E+02
	100 kDa	1.89E+06	2.91E+05	2.80E+02
	10 kDa	5.90E+03	1.08E+03	6.89E+00
	1 kDa	1.51E+03	2.87E+02	8.44E+01
Unspiked WWTP A (2nd trial)	0.45 μ m	6.71E+00	1.85E+00	1.52E+02
	0.1 μ m	9.15E+00	4.63E-01	7.62E+01
	100 kDa	3.05E-01	0.00E+00	6.87E+00
	10 kDa	4.45E+00	4.47E-01	2.68E+01
	1 kDa	5.22E+00	0.00E+00	9.67E+00
Spiked WWTP A (2nd trial)	0.45 μ m	3.28E+06	2.71E+05	1.79E+02
	0.1 μ m	3.45E+06	3.19E+05	1.76E+02
	100 kDa	1.14E+05	1.43E+04	2.93E+01
	10 kDa	9.51E+01	1.03E+01	0.00E+00
	1 kDa	2.10E+00	2.23E-01	1.92E+01

Table A 12. qPCR quantified post-filtration gene concentrations in spiked and unspiked WWTP B and buffer samples.

Sample	Membrane pore size	Gene concentration (gene copies/ μ l)		
		<i>bla</i> _{TEM}	<i>vanA</i>	16S rRNA
Unspiked buffer	0.45 μ m	0.00E+00	0.00E+00	5.38E+00
	0.1 μ m	0.00E+00	0.00E+00	1.35E+01
	100 kDa	2.20E+00	0.00E+00	2.42E+00
	10 kDa	0.00E+00	0.00E+00	2.78E+00
	1 kDa	7.01E+04	6.62E+03	1.96E+00
Spiked no-colloid control buffer	0.45 μ m	1.04E+08	1.42E+07	2.75E+03
	0.1 μ m	9.67E+07	1.27E+07	2.62E+03
	100 kDa	1.64E+07	3.29E+06	4.58E+02
	10 kDa	1.12E+04	2.87E+03	2.61E-01
	1 kDa	5.81E+03	6.37E+02	0.00E+00
Unspiked WWTP B	0.45 μ m	2.10E+02	3.96E+01	2.73E+02
	0.1 μ m	3.67E+02	6.24E+01	1.02E+02
	100 kDa	9.07E+00	1.53E+00	7.95E+01
	10 kDa	2.31E+01	4.74E+00	8.36E+01
	1 kDa	3.50E+01	6.43E+00	7.04E+00
Spiked WWTP B	0.45 μ m	5.10E+07	6.00E+06	1.19E+03
	0.1 μ m	5.44E+07	5.49E+06	6.03E+02
	100 kDa	1.30E+05	1.47E+04	1.45E+01
	10 kDa	3.79E+02	6.54E+01	8.80E-01
	1 kDa	3.03E+00	5.18E-02	6.15E+00

Table A 13. qPCR quantified post-filtration gene concentrations in spiked and unspiked WWTP C and buffer samples.

Sample	Membrane pore size	Gene concentration (gene copies/ μ l)		
		<i>bla</i> _{TEM}	<i>vanA</i>	16S rRNA
Unspiked buffer	0.45 μ m	0.00E+00	0.00E+00	8.97E+00
	0.1 μ m	1.01E+00	0.00E+00	0.00E+00
	100 kDa	0.00E+00	0.00E+00	2.44E+00
	10 kDa	5.98E+01	6.67E+00	0.00E+00
	1 kDa	2.44E+01	4.77E+00	2.57E+01
Spiked no-colloid control buffer	0.45 μ m	5.00E+07	1.20E+07	5.55E+03
	0.1 μ m	8.86E+07	2.18E+07	5.55E+03
	100 kDa	2.31E+06	5.72E+05	1.64E+02
	10 kDa	7.12E+03	3.09E+03	1.04E+01
	1 kDa	1.33E+03	5.66E+02	0.00E+00
Unspiked WWTP C	0.45 μ m	3.77E+00	1.31E+00	1.03E+00
	0.1 μ m	7.79E+00	1.49E+00	4.46E+00
	100 kDa	4.90E-01	6.90E-01	3.10E-01
	10 kDa	2.81E+00	1.30E+00	0.00E+00
	1 kDa	1.14E+01	1.32E+00	3.01E-01
Spiked WWTP C	0.45 μ m	1.24E+06	2.14E+05	3.11E+01
	0.1 μ m	7.67E+06	1.37E+06	1.49E+02
	100 kDa	1.81E+05	3.13E+04	2.58E+00
	10 kDa	2.43E+01	2.13E+00	9.22E-01
	1 kDa	3.00E+00	1.74E+00	0.00E+00

Table A 14. Total non-purgeable organic carbon, protein, and polysaccharide values graphed in Sections 4.3.1 – 4.3.3.

WWTP ID	Membrane pore size	TOC (mg/L)	Proteins (mg/L)	Polysaccharides (mg/L)	Proteins + Polysaccharides (mg/L)
WWTP A (1st trial)	1.2 µm	9.24	11.44	4.32	15.76
WWTP A (1st trial)	0.45 µm	*	11.23	4.03	15.27
WWTP A (1st trial)	0.1 µm	8.13	10.90	4.36	15.27
WWTP A (1st trial)	100 kDa	8.50	9.69	2.93	12.61
WWTP A (1st trial)	10 kDa	7.04	8.12	1.12	9.24
WWTP A (1st trial)	1 kDa	3.52	6.09	0.00	6.09
WWTP A (2nd trial)	1.2	6.15	11.21	5.72	16.94
WWTP A (2nd trial)	0.45 µm	5.46	10.92	6.56	17.48
WWTP A (2nd trial)	0.1 µm	5.58	10.44	5.97	16.41
WWTP A (2nd trial)	100 kDa	5.18	9.27	3.93	13.20
WWTP A (2nd trial)	10 kDa	4.56	8.99	3.33	12.31
WWTP A (2nd trial)	1 kDa	4.09	8.11	2.49	10.61
WWTP B	1.2	5.95	8.30	3.59	11.88
WWTP B	0.45 µm	6.49	8.93	2.33	11.26
WWTP B	0.1 µm	6.49	9.28	3.39	12.68
WWTP B	100 kDa	*	*	*	*
WWTP B	10 kDa	4.78	6.47	1.82	8.29
WWTP B	1 kDa	3.18	3.56	1.25	4.81
WWTP C	1.2	4.44	6.49	1.52	8.01
WWTP C	0.45 µm	4.61	6.36	1.54	7.89
WWTP C	0.1 µm	4.74	6.37	1.33	7.70
WWTP C	100 kDa	3.95	6.33	0.89	7.22
WWTP C	10 kDa	3.69	6.03	1.28	7.31
WWTP C	1 kDa	3.54	5.35	1.30	6.65

* Data not available

Table A 15. Gene and colloidal component fractions used to compare PVDF and alumina membranes in Figure 4.55 - Figure 4.57 (Section 4.4).

WWTP	Membrane	Filtrate fraction (C/Co)					proteins	polysaccharides
		bla _{TEM}	vanA	16S rRNA	TOC			
WWTP A	PVDF	1.614E+00	2.431E+00	1.195E+00	*	0.953	1.011	
(1st trial)	Alumina	1.383E-03	3.600E-03	5.212E-03	*	0.903	0.935	
WWTP A	PVDF	1.052E+00	1.175E+00	9.816E-01	0.908	0.931	0.774	
(2nd trial)	Alumina	5.702E-04	7.790E-04	2.385E-03	0.774	0.928	0.49	
	PVDF	1.068E+00	9.150E-01	5.058E-01	1.091	1.119	0.945	
WWTP B	Alumina	7.018E-03	7.580E-03	1.374E-02	0.958	0.957	0.738	
	PVDF	9.216E-01	1.196E+00	8.783E-01	1.068	0.981	0.875	
WWTP C	Alumina	3.262E-05	6.451E-05	0.000E+00	0.945	0.971	0.854	

* Data not available

Table A 16. Spiked buffer filtrate fractions associated with the 0.1 μm pore size PVDF and Alumina membranes compared in **Figure 4.58**.

0.1 μm pore size membrane filtrate gene fraction (C/Co)				
Blank used with WWTP	Membrane	<i>bla</i>_{TEM}	<i>vanA</i>	16S rRNA
A (1st trial)	PVDF	0.63	0.51	0.55
A (1st trial)	Alumina	1.17	1.11	0.52
A (2nd trial)	PVDF	1.08	1.35	0.51
A (2nd trial)	Alumina	0.87	0.96	0.16
B	PVDF	0.93	0.89	0.95
B	Alumina	0.47	0.92	0.67
C	PVDF	1.77	1.82	1.00
C	Alumina	2.00	2.50	0.72